12-1-2013

Anti-Cancer Effects Of Garcinol In Pancreatic Cancer Transgenic Mouse Model

Nadia Saadat
Wayne State University,

ANTI-CANCER EFFECTS OF GARCINOL IN PANCREATIC CANCER TRANSGENIC MOUSE MODEL

by

NADIA SAADAT

DISSERTATION

Submitted to the Graduate School

of Wayne State University,

Detroit, Michigan

in partial fulfillment of the requirements

for the degree of

DOCTOR OF PHILOSOPHY

2013

MAJOR: NUTRITION AND FOOD SCIENCE

Approved by:

_____

Advisor Date

_____

_____

_____

ACKNOWLEDGMENTS

First I would like to express my deepest gratitude to my advisor Dr. Smiti Gupta for her help and support throughout my PhD project. Her guidance and well-timed advice has helped me accomplish major goals in my life and academic career. She provided me the opportunity to work as a lead researcher during my PhD project, which I feel has resulted in my educational and research growth. She was always there to support me when I wanted to include new techniques and untraditional approaches to my project. Thank you so much for everything.

I would like to thank my dissertation committee. First I would like to thank Dr. Doina David for her valuable suggestions which guided me in the histology part of my project. I highly appreciate her commitment to accommodate my research queries in her busy schedule. I would like to express my gratitude to Dr. Pramod Khosla and Dr. Ahmad Heydari for their time, encouragement and their valuable comments. Also, I would like to thank Dr. Gail Bentley for her expert advice in the hematology of mice.

I would like to acknowledge my colleagues Arvind Goja and Andreea Geamanu for their continuous help since I first joined the lab. We worked on multiple projects together as a great team. I would like to acknowledge Nurul Huda Razali, Sarah Akhtar, Aminder Gill and Fadi Abdulahad for their help in my PhD project. I also thank my fellow lab members, Lichchavee Rajasinghe and Yan Wu, for their help, encouraging comments and useful discussion points.

Finally, I would like to thank my family: My husband Saadat Hameed--whom without I would have never completed my PhD--and my sons Sohaib Saadat, Affaan Saadat, Ammaar Saadat and Muhammad Sobaan Saadat. I thank them all for their

continuous love, support, prayers and understanding. I really appreciate comments and support from my brother Jahanzeb Baqai and his wife Arifa Baqai. Their supportive texts before my exams and presentations meant a lot to me and gave me the strength I needed. Last but not least, I would like to thank my mom Neelofar Baqai for her encouragement and guidance throughout my life. What I am now is because of her upbringing, motivation, devotion and love. She was always beside me whenever I felt weak and held me up when strong. Her prayers have kept me going throughout my life.

TABLE OF CONTENTS

LIST OF TABLES

LIST OF FIGURES

CHAPTER 1: Introduction

1.1 Pancreatic Cancer:

Pancreatic Cancer is one of the most aggressive cancer types with < 6% survival rate. According to the National cancer Institute it is expected that 45,220 men and women will be diagnosed with pancreatic cancer and 38,460 men and women will die of cancer of the pancreas in 2013. While the death rate for other cancer types has decreased, the upward trend for pancreatic cancer is alarming and calls for biomarker research, diagnosis and drug discovery for this complicated disease.

The most common type of pancreatic cancer is pancreatic ductal adenocarcinoma, which accounts for 95 percent of all pancreatic cancer cases. The remaining 5 percent include other tumors of the exocrine pancreas, acinar cell, and pancreatic neuroendocrine cells which generally have a much different diagnostic and therapeutic profile and a more favorable prognosis. Several studies have shown that the risk of developing pancreatic cancers increases with age, smoking, type2 diabetes and obesity. The symptoms of pancreatic ductal adenocarcinoma are primarily caused by mass effect rather than disruption of exocrine or endocrine function [1]. These include jaundice, loss of appetite, abdominal pain, nausea and unexplained weight loss. Since these symptoms are non-specific, pancreatic cancer often goes undetected. At present since there is no specific diagnostic procedure for early detection of pancreatic cancers, most cases when diagnosed are in advanced stages. Tumors of head of pancreas are more common as compared to tumors of the body and tail and cause more problems like biliary duct obstruction and Jaundice. Presently, surgical resection with adjuvant

chemotherapy is the only curative procedure for patients with pancreatic cancer. However, this is only possible for 20% of diagnosed cases of pancreatic cancer [1]. Many drugs and chemotherapeutic regimens, both single and multi-agent are being studied; but with no survival or clinical benefit. Gemcitabine, fluorouracil monotherapy and leucovorin are being used for treatment with little benefit in advanced cases of pancreatic cancer[2]. Intra-operative radiation therapy has shown to decrease progression of locally advanced disease, but have no effects on metastasized cancer, or survival rate. On the bright side a combination of both radiation therapy and fluorouracil-based chemotherapy has shown significant improvement in survival rate, around 40 percent for combination compared to 10 percent for radiation alone after one year [1]. Research advances into the pathogenesis of pancreatic cancer have led to a better understanding of the types of pathways involved. Drugs or agents that may target one or more of the mechanisms underlying the development and progression of this disease may be beneficial.

1.2 Bioactive food components and Pancreatic cancer:

Recent interest is shifting towards natural compounds present in botanicals and herbs. Natural extracts and compounds have been shown to have medicinal properties since centuries. Bioactive food components and nutraceuticals comprise of large groups of food, or parts of foods that have shown therapeutic health benefits for many diseases. Recently, some of the natural extracts and functional compounds have shown promising results in pancreatic cancer research without added side effects [3]. The range of bioactive food components with potential anti-cancer benefits is numerous. These agents possess antioxidant, anti-inflammatory, pro-apoptotic and anti-angiogenic

effects which can inhibit the initiation, promotion and metastatic phases of pancreatic cancer respectively.

Based on various clinical trials, the efficacy of these compounds has been proven both invitro and invivo. It is important to mention that most bioactive food components are pleotropic in nature, capable of acting at different stages of cancer progression and are not limited to a single mechanism. A number of these components like lycopene, vitamin A, vitamin C and selenium have antioxidant effects and can help in arresting pancreatic cancer at the initiation phase of pancreatic carcinogenesis [4]. Anti-apoptotic and inflammatory properties of curcumin, Garcinol and resveratrol can provide a good line of defense during the promotion phase as well as inhibit angiogenic factors, preventing metastasis and invasion. Once the cancer is metastasized, these agents such as omega 3 in fish oil and aged garlic extract can prolong survival, decrease cachexia and improve the quality of life in patients with advanced cases of pancreatic cancer. Some of these bioactive food components such as curcumin, isoflavones and lycopene have passed the phase I clinical trials and are in phase II with different cancer types, including pancreatic cancer phase ll trial with curcumin [5, 6].

The synergistic effects of these components, among themselves and with pharmaceutical drugs have opened new doors for cancer management. Studies have shown some beneficial interaction of two of more of food components on the incidence of pancreatic carcinomas. The synergistic interaction of curcumin and isoflavone showed significant inhibition of cell proliferation, apoptosis, and levels of NFkB than compared to single agents alone [7]. Other studies showed that the combination of vitamin C, vitamin E, β-carotene and selenium significantly reduced pancreatic cancer

incidence[4]. Combination of gemcitabine (the current chemotherapeutic drug for pancreatic cancer) curcumin [8] and resveratrol [9]showed a significant reduction in cell proliferation, increased apoptosis, reduced angiogenesis and invasion. Synergistic effects of curcumin and Garcinol on pancreatic cancer cell lines, have been documented by our lab [10]. In addition it was reported that Garcinol showed synergism with drug of choice gemcitabine in pancreatic cancer cell lines and these results were more pronounce in Panc 1 kras mutated cell line[11].

1.3 Garcinol a potential anticancer agent:

Garcinol or camboginol is extracted from the rind of fruit of *Garcinia indica (*Kokum or Mangosteen). It has been used in the Indian subcontinent, far-east Asia and Africa for centuries. Garcinol is known for its medicinal properties in home remedies and Ayurvedic system of medicine [12]. Garcinol and isogarcinol are the benzophenone derivatives of the fruit extract. Citric acid, Hydroxycitric acid (HCA), hydroxycitric acid lactone and oxalic acid are also active components of the extract.[12]. Garcinol and isogarcinol have shown to have antioxidant properties attributed to its structure. The fruit extract also has hypocholesterolemic and anti-obesity effects due to its HCA component.

Chemically Garcinol ($C_{38}H_{50}O_6$) is a yellow crystalline compound with molecular weight 602. Its antioxidant properties are due to both hydroxyl groups and β-diketone moiety[13]. This structure is similar to some antioxidants, Rao et al. determined the location of terminal alkene in and the presence of a β-diketone in Garcinol [13]. Isogarcinol or cambogin is formed after the terminal alkene undergo cyclization in acidic conditions[14]. The oxidized isomer isogarcinol is related to its properties as

antibacterial, antiulcer antiviral and anti-obesity agent [15]. Structure of Garcinol is similar to many naturally occurring phytochemicals like curcumin, chalcones and oblogifolins reported to have anti-carcinogenic activity [16, 17].

Garcinol is known for its microbial properties due to its use in traditional medicine. Garcinol has shown to affect negatively a whole spectrum of microbiota growth including fungi [18]. Antioxidant properties of Garcinol have been evaluated in various research studies, Garcinol retarded same amount of superoxide ion as DL-alpha-tocopherol in hypoxanthine/xanthine oxidase system. In an indometacin induced acute ulcer rat model oral Garcinol prevented formation of ulcers [19]. Neuroprotective properties of Garcinol in rat cortical neuron cultures via preventing nitric oxide (NO) accumulation in astrocytes have been reported [20].

In recent studies potential role of Garcinol as anticancer agent has been elucidated. It has shown its efficacy due to its pleotropic nature. As an antioxidant and anti-inflammatory agent it has shown an increase in liver detoxifying enzymes, glutathione S-transferase (GST) and quinone reductase (QR) levels, after feeding Garcinol in azoxymethane (AOM) induced colon cancer rat model, with reduction in colonic aberrant crypt foci (ACF) [21, 22]. Additionally it has inhibited O_2^-, Nitric Oxide (NO), iNOS, and COX2 at comparable or better than epigallocatechingallate (EGCG), a green tea polyphenol [21]. COX-2 levels were also reduced in male F344 rats in 4-nitroquinoline 1-oxide (4-NQO) induced tongue lesions, with dietary Garcinol administration [23]. Another study has shown reduction of arachidonic acid and its metabolites in the intestinal and macrophage cell lines investigated. They also reported reduction in NFκB and COX-2 expressions [24].

Apoptotic pathways were also reported to be target of Garcinol in some *invitro* studies. There was up-regulation of proapototic Bax and Bad proteins with subsequent down-regulation of proapototic Bcl2 along with activation of caspase-3,in human leukemia HL-60 cells resulting in release of cytochrome C from mitochondria [25]. Increase in activity of Caspase-3 is also explained in colon and breast cancer cell lines [26, 27]. Garcinol has also shown induction of death receptors DR4 and DR5 in various cancer cell lines [28]. Molecular targets of Garcinol are highlighted in Figure 1

Garcinol is established as a potent histone acetyl-transferase (HAT) inhibitor. It has been reported to inhibit HATs p300 and PCAF, and can therefore cause epigenetic suppression to gene transcription [29]. Post transcriptional regulation of genes by miRNA can effect cancer cell growth and proliferation at different levels. In a recent study done on human pancreatic cancer cell lines, (BxPC-3 and Panc-1) in our lab, Garcinol has shown modulation of microRNA molecules in favorable manner[11].

Invitro studies have shown positive effects of Garcinol on most of the cancer cell lines tested, but there are very few animal studies using this bioactive food component *invivo*. The physiological barriers, bioavailability and metabolism of the compound tested complicate the translation of similar effects *invivo*. In this study we investigated the effects of Garcinol in Pancreatic cancer transgenic mouse model (KPC).

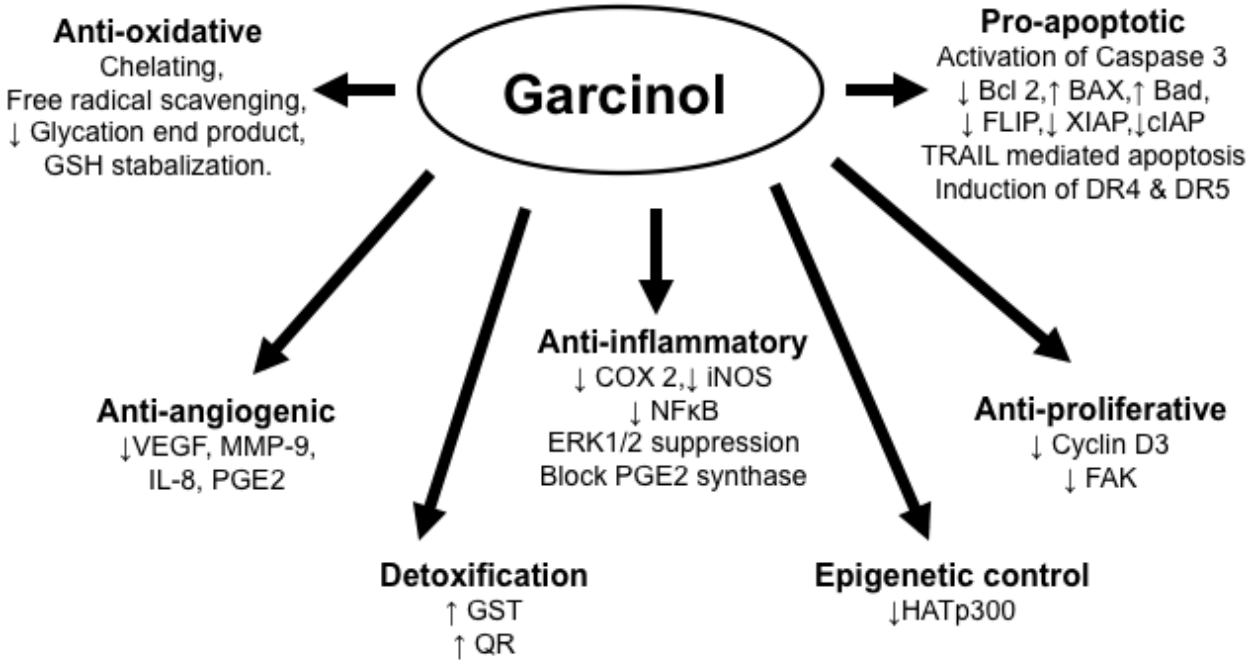

Figure 1: Molecular targets of Garcinol [30]

Hypothesis

Dietary Garcinol treatment will slow down the progression of Pancreatic Cancer in Kras and p53 transgenic Pancreatic Cancer mouse model.

Specific Aim 1:

To investigate the invivo response of dietary Garcinol on PaCa in mouse model.

1a, To monitor tumor progression with MRI.

1b, To evaluate possibility of toxicity of dietary Garcinol by blood smears and fore -stomach Hematoxylin and eosin slides (H&E).

1c, Histological evaluation of formalin fixed pancreatic tissue.

The purpose of this aim was to study the development and advancement of Pancreatic cancer in this mouse model and to investigate the favorable or unfavorable effects of dietary Garcinol. Pancreatic cancer transgenic mice were fed Garcinol diet or Isocaloric diet. MRI is a technique used to monitor cancer progression at different time points in this study. Basement membrane and the lining of fore stomach is normally hypertrophied with the ingestion of toxic substances and blood smears can provide us the insight of RBC and WBC changes in control and treatment groups. RBC changes including basophilic stippling and Heinz bodies can be an effect of toxicity, whereas WBC type and count provide information about the immune status of the animal.

Histological part of this aim was to evaluate the status of neoplastic pancreatic lesions at histological level. We graded the Pancreatic intraepithelial Neoplasia (PanIN) based on morphology and criteria set by reference [31].

Specific aim 2:

To investigate the mouse pancreatic and liver tissue, for response to the dietary Garcinol at molecular level.

2a, To explore the change in the micro RNA profile of Garcinol treated vs. control animals.

2b, Real time Reverse Transcriptase PCR analysis (RTPCR) of tumor related and miRNA target genes in mouse pancreatic tissue.

2c, Real time Reverse Transcriptase PCR analysis tumor related and miRNA target genes in common metastatic site liver.

An important part of this aim was to investigate the changes in miRNA array analysis upon intervention with Garcinol. Garcinol has shown promising results previously reported invitro data by modulating the tumor promoter and tumor suppressor markers genes. These pathways were further investigated by measuring relative gene expressions by RT PCR in Pancreatic tissue. Since the liver is the primary or first site for metastasis, gene modulation in the liver tissue was also investigated by RTPCR.

Specific aim 3:

Metabolomic Analysis of Urine samples from treated and untreated groups.

3a, To investigate the differences in Urinary Metabolomic profiles of cancer control and Garcinol treated mice using Simca P+ software for multivariate data analysis

3b, To conduct target analysis to identify and quantify the differences in metabolite concentrations:

Urinary metabolomic profiling is a non-invasive approach to study the effects of any intervention. In this study we used this approach to investigate the changes in metabolomic profiles of the Garcinol treated Pancreatic cancer mice. Urinary NMR Spectra were processed and then subjected to multivariate statistical analysis to study similarities and differences based on variation in metabolite concentrations. Target analysis of the peaks/metabolites corresponding to the change, metabolites were identified and quantified using CHENOMX NMR suite.

Animals:

Mice for this study were obtained from Van Andel Institute Grand Rapids under mutual transfer agreement. The protocol for this project is approved by Department of Laboratory animal resources (DLAR) and all the mice were housed at Scott Hall DLAR facility

Protocol number: IACUC Protocol A 06-13-1.

1.4 KPC mice, clinically relevant mouse model for Pancreatic Cancer:

Kras and P53 conditional mutant mice (KPC) are clinically relevant model for pancreatic ductal adenocarcinoma as it develops full range of Pancreatic intraepithelial neoplasia (PanIN) and aggressive ductal adenocarcinoma with 100% penetrance. Orthotropic and Xenograft models of pancreatic cancer cannot fully explain the complexity of development of pancreatic ductal adenocarcinoma (PDA) and are therefore not true representative of the disease. Specifically the implanted tumor is not treated as primary tumor by the body and there may not face physiological challenges which are normally present with development of primary tumor. Typically in PDA, Kras is mutated (constantly turned on) in 90% of the cases, P53 is mutated (turned off) in 75% of the cases and SMAD 4 or DPC4 (turned off) is mutated in 55% of the cases [32]. According to Hruban et al (2000) more advanced PanIN accumulate more mutations and higher instability [32]. Higher Nuclear cytoplasmic ratio, genomic instability and abnormal mitosis are all hallmarks of carcinogenesis. KPC mice (Figure 2) are Kras, and p53 conditional mutant mice and with Pdx cre recombinase (krasLSL.G12D/+; p53R172H/+; PdxCretg/+). Pancreatic and duodenal homeobox (Pdx) is a protein expressed during embryonic development of the pancreas. Association with Pdx makes these mutations to appear only in the pancreatic tissue sparing rest of the body. Higher genomic instability, abnormal mitosis, anaphase bridges and more centrosomes were observed in this model. These mice develop ductal metaplasia, different stages of PanINs, ductal adenocarcinoma and macro-metastasis [32]. Median survival rate is 4.5 month [33]. Therefore Pancreatic ductal

adenocarcinoma in KPC mice resembles human tumors both patho-physiologically and at the molecular level [33].

CHAPTER 2: Dietary Garcinol Arrests the Progression of Pancreatic Cancer invivo in KRAS and p53 pancreas- specific mutant mouse model

2.1 Study Design:

Forty two male KPC mice (KrasLSL.G12D/+; p53R172H/+; PdxCretg/+) 6 to 8 weeks of age, were obtained from Van Andel Institute (Grand Rapids, MI ,USA). Mice were housed individually under standardized protocol approved by Division of Laboratory Animal Resources (DLAR), Wayne State University. Day and night cycle was maintained with controlled temperature (25° C) and humidity. Food and water were given adlibitum and 12hr dark and light cycle was maintained. Garcinol was purchased from Enzo Life Sciences (Plymouth Meeting, PA), Garcinol containing diet (0.05%) and the purified isocaloric diet were formulated and produced by Dyets Inc. (Bethlehem, PA). Mice were weighed and acclimatized for one week. After acclimatization mice were randomly assigned to four groups (Figure 2).

KC (n=8), KPC mutant mice on control diet group were fed isocaloric diet (Table-1) (AIN 93G purified rodents diet, Dyets, Inc., Bethlehem, PA, USA) and received intra-peritoneal saline injections (200 ul) from week 1 to week 5.

KGr (n=8) KPC mice on Garcinol diet mice were fed 0.05% Garcinol added diet(Table-1) (modified AIN 93G purified rodents diet, Dyets, Inc., Bethlehem, PA, USA) and received intra-peritoneal saline injections (200 ul) from week 1 to week 5.

KGm (n=8), KPC mice on control diet were fed isocaloric diet and received intra-peritoneal Gemcitabine (100mg/kg in final volume 200 ul, LC laboratories, Woburn, MA,USA) injections from week 1 to week 5.

KGG (n=8), KPC mice on Garcinol diet were fed 0.05% Garcinol diet and received intra-peritoneal Gemcitabine (100mg/kg in final volume 200 ul) injections from week 1 to week 5.

Littermates without mutations served as controls without cancer; these mice were divided into two groups.

CC (n=5), Control mice on control diet, were fed isocaloric diet and received intraperitoneal saline injections (200 ul) from week 1 to week 5.

CGr (n=5), Control mice on Garcinol diet were fed 0.05% Garcinol diet and received intraperitoneal saline (200 ul) injections from week 1 to week 5.

Garcinol and isocaloric diet both had similar composition besides addition of 0.05% Garcinol in Garcinol diet (Table-1). The dose of Garcinol was based on previously reported dietary study without any toxicity and side effects [21]. As Garcinol is a light sensitive compound all the precautions were taken during preparation and are kept in dark bags after preparation. Small amount of diet sufficient for three to four days was provided to the mice at one time.

Weight of the mice, their diet and water intake were monitored on a bi-weekly basis. As KPC mice have tendency to develop very aggressive form of pancreatic cancer (PaCa), 20 % weight loss or abdominal distention with respiratory distress were set as criteria for early euthanization. Groups receiving gemcitabine were monitored for

48 hours for toxicity symptoms of the dose including alertness, sudden weight loss and loose stools.

0.05% Garcinol added Diet				Isocaloric Diet			
Ingredient	**kcal/g**	**grams/kg**	**kcal/kg**	**Ingredient**	**kcal/g**	**grams/kg**	**kcal/kg**
Casein	3.58	200	716	**Casein**	3.58	200	716
L-Cystein	4	3	12	**L-Cystein**	4	3	12
Sucrose	4	100	400	**Sucrose**	4	100	400
Cornstarch	3.6	396.986	1429.1496	**Cornstarch**	3.6	397.486	1430.9496
Dextrose	3.8	132	501.6	**Dextrose**	3.8	132	501.6
Soybean Oil	9	70	630	**Soybean Oil**	9	70	630
t-Butyl hydroquinone	0	0.014	0	**t-Butyl hydroquinone**	0	0.014	0
Cellulose	0	50	0	**Cellulose**	0	50	0
Mineral Mix #210025	0.88	35	30.8	**Mineral Mix #210025**	0.88	35	30.8
Vitamin Mix #310025	3.87	10	38.7	**Vitamin Mix #310025**	3.87	10	38.7
Choline Bitartrate	0	2.5	0	**Choline Bitartrate**	0	2.5	0
Garcinol	0	0.5	0				
		1000.00	**3758.2496**			**1000.00**	**3760.0496**

Table 1- Composition of 0.05% Garcinol diet and isocaloric diet.

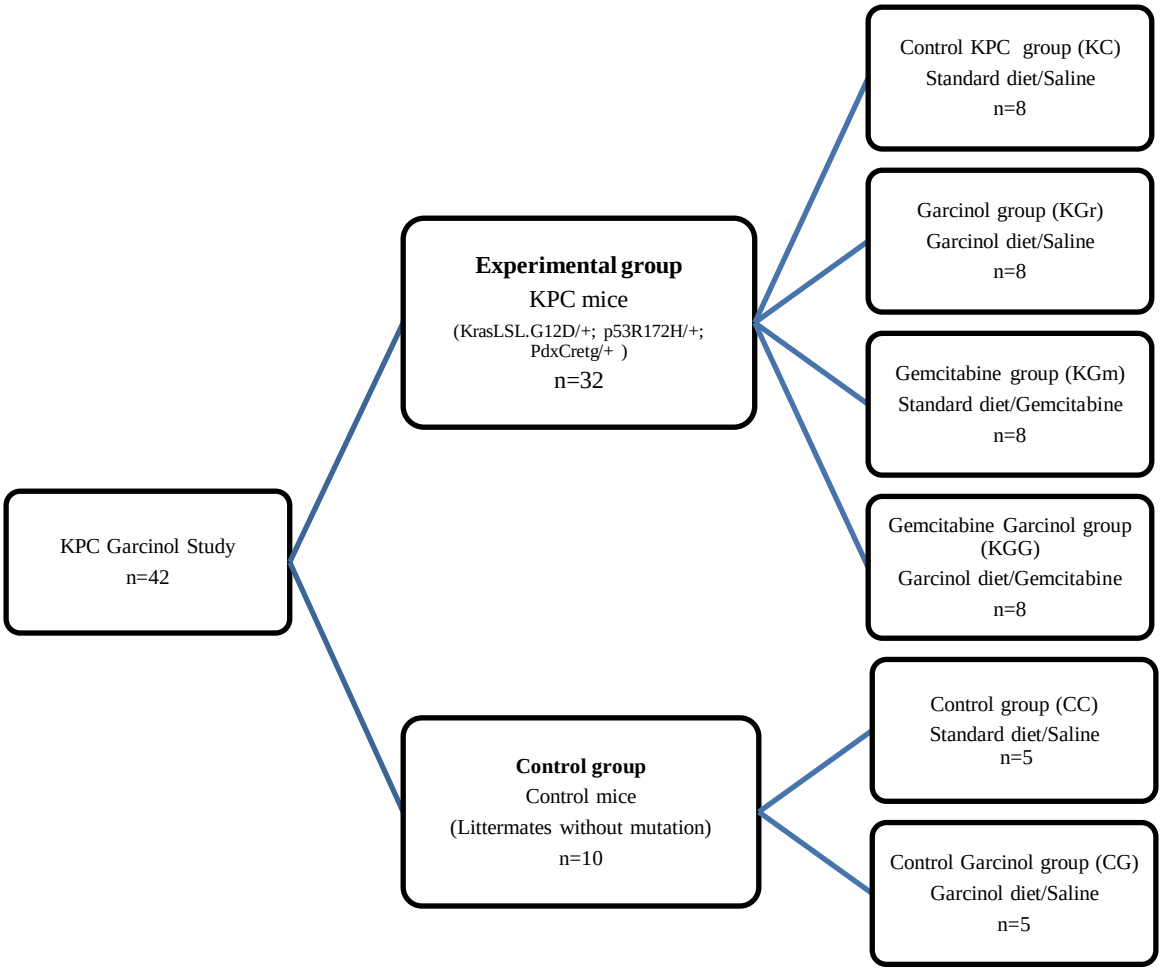

Figure 2- Study design

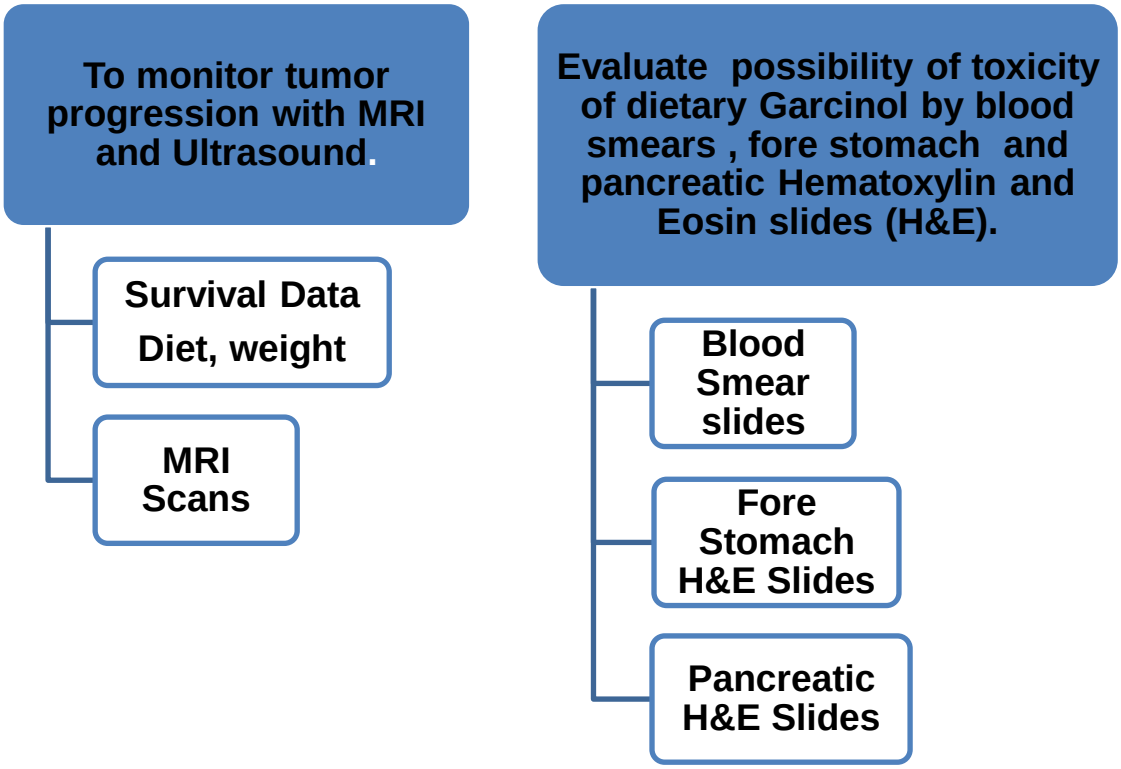

Figure 3: Specific aim 1-To investigate the invivo response of dietary Garcinol on PaCa in mouse model.

2.2 Methods:

Methods used for specific aim 1 are summarized in Figure 3 .

2.2.1 Magnetic Resonance Imaging (MRI):

MRI scans were conducted to monitor tumor growth in weeks 1 and 5 during the study. Mice were weighed and were anesthetized with 80mg/kg body weight Ketamine and 20mg/kg body weight Xylazine given intra-peritoneally and placed on heated platform for scanning. Ophthalmic ointment was used to keep the eyes moist. Scans were conducted on 7T scanner (ClinScan, Bruker, Karlsruhe, Germany). Overall inflammation status and tumor volumes were measured during the scans. After the scans, the mice were allowed to recover from anesthesia on the heated pads. A pallet of food was provided inside the cage for easy access during recovery.

2.2.2 Plasma and tissue sample collection:

Mice were anesthetized with 100mg/kg Ketamine and 20mg/kg Xylazine. Mice were euthanized at week 6 by exsanguination and removal of major organs. Abdominal cavity was opened and blood was collected directly from the heart with EDTA coated syringes and stored on ice in EDTA coated vials. Plasma was separated by centrifuging at 3500 rpm for 15 minutes, measured and stored at -80°C for further analysis. All the major organs were collected including Pancreas, liver, fore stomach, spleen, kidneys, heart and testis. Tissue samples for histology were fixed in 10% neutral buffered formalin.

2.2.3 Blood smear slides preparation:

Blood (3 ul) was collected directly from the heart to avoid contact with EDTA. This drop of blood was placed on the slide and smear was prepared by using a spreader slide. Slides were dried at room temperature and then fixed in 95% ethanol for one minute. Blood smears were stained by Wright Giemsa stain (Volu-Sol, Inc, Salt Lake City, UT) according to the provided protocol. Briefly each slide was first immersed into a jar of Wright-Giemsa staining solution for 30 seconds, then into a pH balanced buffer for 60 seconds and finally in the rinse solution for 10 seconds. The blood smears were observed for changes in the red and white blood cell morphology under the light microscope NIKON ECLISPE (NIKON Instruments Inc, Melville, NY, after drying.

2.2.4 Histological evaluation of the formalin fixed pancreatic tissue.

Pancreatic tissues collected at euthanization were fixed directly in 10% neutral buffered formalin. After fixing, the samples were transferred to 70% ethanol to avoid excessive drying of the tissue. The slides were stained with Hematoxylin and Eosin (H&E) stain at the Histopathology lab, at Michigan State University. Briefly, samples were vacuum infiltrated with paraffin on the Thermo Fisher Excelsior tissue processor; followed by embedding with the Thermo Fisher Histo Centre III. After cooling, excess paraffin was trimmed from the edges and the blocks were placed on a Reichert Jung 2030 rotary microtome. Blocks were faced to expose tissue sample, cooled and finely sectioned at 4-5 microns. Sliced Sections were dried at 56°C slide incubator to ensure adherence to the slides for 2 – 24 hours. Slides were removed from the incubator and stained with Hematoxylin and Eosin stain. The procedure involved two changes of

Xylene (5 minutes each), two changes of absolute ethanol (2 minutes each), two changes of 95% ethanol (2 minutes each), running tap water rinse (2 minutes), Gill 2 Hematoxylin (ThermoFisher, Pittsburgh, PA) for 1 ½ minutes followed directly by a 10 – 15 second differentiation in 1% aqueous glacial acetic acid and running tap water for 2 minutes to enhance nuclear detail. Upon completion of running tap water slides were placed in one change of 95% ethanol – 2 minutes, 1% Alcoholic Eosin-Phloxine B – 2 minutes to stain cytoplasm, one change of 95% ethanol for 2 minutes, four changes of 100% ethanol – 2 minutes each, four changes of Xylene – 2 minutes each followed by cover-slipping with synthetic mounting . Slides were then observed under the light microscope (Nikon Eclipse 80i).

2.2.5 Immuno-histostaining for S100P and DPC4:

To confirm the findings from the H&E slides immunohistochemistry was conducted using S100P (Abcam #ab166649) and SMAD4/DPC4 (Abcam [EP618Y] #ab40759) antibodies at the Histopathology lab (MSU, Lansing MI). The specimens fixed and embedded in paraffin blocks earlier in H&E staining were sectioned on rotary microtome at 4-5μ's. These sections were then placed on slides coated with 2% 3 - Aminopropyltriethoxysilane and dried at 56°C overnight. The slides were deparaffinized in Xylene and hydrated through ethyl alcohol to distilled water. Slides were then placed in Tris Buffered Saline pH 7.4 (Scytek Labs – Logan, UT) for 5 minutes for pH adjustment. Heat Induced Epitope Retrieval was performed utilizing Citrate Plus pH 6.0 buffer in a rice steamer for 30 minutes; followed by a 10 minute incubation at 25°C (Scytek). Endogenous Peroxidase was blocked utilizing 3% Hydrogen Peroxide / Methanol bath for 30 minutes followed by running tap and distilled water rinses.

Following pretreatment standard avidin-biotin complex staining steps were performed at room temperature on the DAKO Autostainer. All staining steps were followed by rinses in Tris Buffered Saline + Tween 20 (Scytek). After blocking for nonspecific protein with Normal Goat Serum (Vector Labs – Burlingame, CA) for 30 minutes; sections were incubated with Avidin / Biotin blocking system for 15 minutes each (Avidin D – Vector Labs / d-Biotin – St. Louis, MO).

S100P:

Primary antibody slides were incubated for 60 minutes with the Rabbit Polyclonal anti – S100P diluted at 1:200 (Abcam – Cambridge, MA) in Normal Antibody Diluent (NAD) (Scytek). Biotinylated Goat anti-Rabbit IgG (H + L) prepared at 11.0μg/ml in NAD incubated for 30 minutes (Vector); followed by R.T.U. Vectastain Elite ABC Reagent incubation for 30 minutes (Vector). Reaction development utilized Vector Nova Red peroxidase chromogen incubation of 15 minutes followed by counterstain in Gill 2 Hematoxylin (Thermo Fisher – Kalamazoo, MI) for 30 seconds then differentiation, dehydration, clearing and mounting.

DPC4/SMAD4:

Primary antibody slides were incubated for 60 minutes with the Rabbit Monoclonal anti – SMAD4/DPC4 diluted at 1:100 (Abcam – Cambridge, MA) in Normal Antibody Diluent (NAD) (Scytek). Biotinylated Goat anti-Rabbit IgG (H + L) prepared at 11.0 μg/ml in NAD incubated for 30 minutes (Vector); followed by R.T.U. Vectastain Elite ABC Reagent incubation for 30 minutes (Vector). Reaction development utilized Vector Nova Red peroxidase chromogen incubation of 15 minutes followed by

counterstain in Gill 2 Hematoxylin (Thermo Fisher – Kalamazoo, MI) for 30 seconds followed by differentiation, dehydration, clearing and mounting.

2.3 Statistical Analysis:

Analysis of variance (ANOVA) was conducted to evaluate the statistical significance of the data using SPSS software (IBM SPSS Statistics, IBM Corporation, Armonk NY). Significance level was set at p-value < 0.05, to be considered as significant in reporting the results.

2.4 Results and Discussion

2.4.1 Survival data, Body weights and diet intake:

All KPC mice in Garcinol fed group (KGr) survived the 6 week study period (100 percent survival). One mouse died due to complications of cancer in Cancer control (KC) group, two mice each from Gemcitabine(KGm) and Gemcitabine Garcinol group(KGG) were not able to complete the study(75% survival) either due to intestinal obstruction or more than 20 % weight loss. All the non-mutant mice from control without cancer groups (CC and CG) survived the study (Table 2). There was no significant difference in average diet intake (p value > 0.05) or increase in body weights (p value > 0.05) from week one to week 6 in all the groups (Figure 4 & 5).

Group	Total	Survived	Not Survived	% Survival rate	Animal not survived	Remarks
CC	5	5	0	100%		
CGr	5	5	0	100%		
KC	8	7	1	87%	KC2	KC2 died in Week 5 very weak
KGr	8	8	0	100%		
KGm	8	6	2	75%	KGm3 , KGm5	KGm3: Week 3 –Died (due to intestinal & urinary obstruction)
						KGm5: Week 5-Sacrificed (very weak & lost weight)
KGG	8	6	2	75%	KGG6 , KGG8	KGG6: Week 5 -Sacrificed (very weak & lost weight)
						KGG8: Week 6 -Died (due to intestinal & urinary obstruction)

Table 2: Survival data KPC Garcinol Study.

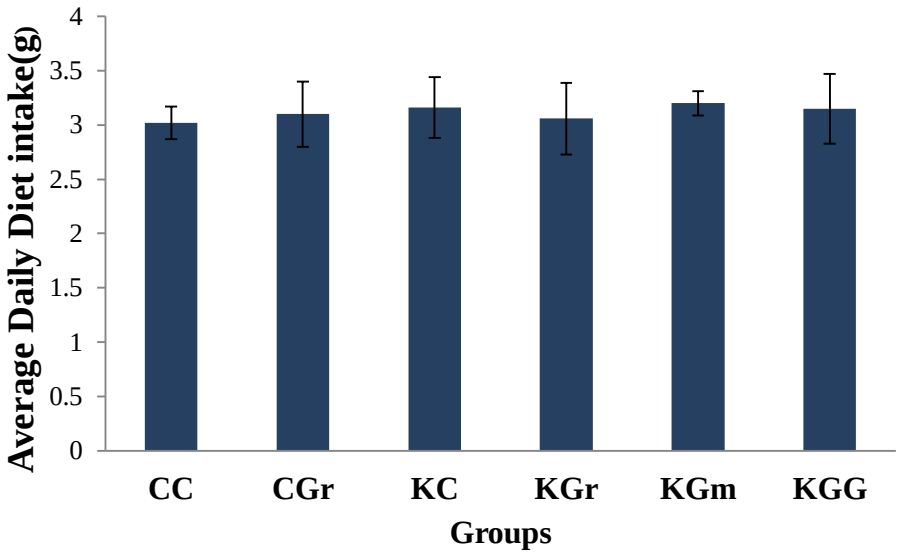

Figure 4: Average daily diet intake during 6 weeks study in all groups. Error bars represents ± mean standard deviation. No significant difference between the groups (p value > 0.05).

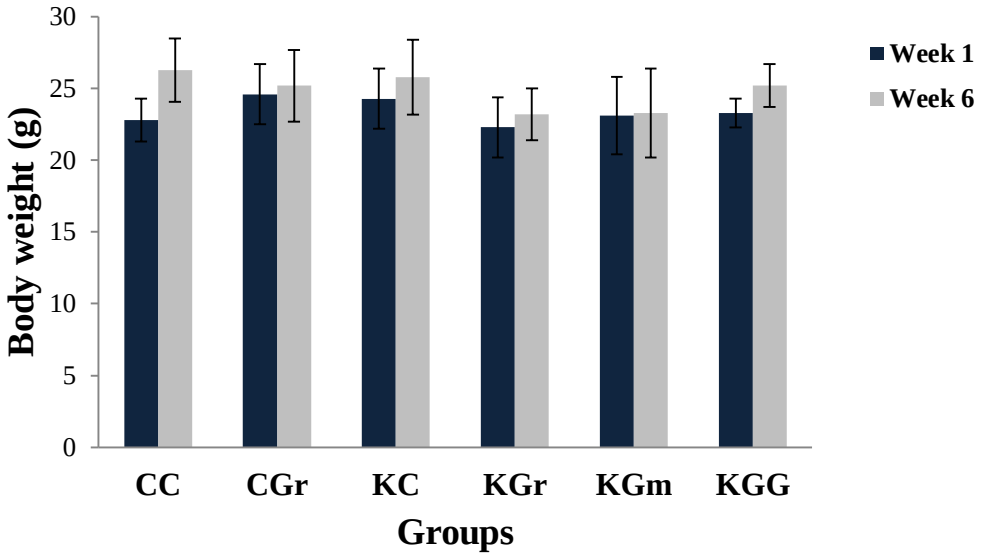

Figure 5- Average body weights compared week 1 to week 6 in all groups. Error bars represents ± mean standard deviation. No significant difference was found from week 1 to week 6 in all the groups (p value >0.05).

2.4.2 Tumor Progression in KPC mice:

Tumors volumes in live animals were monitored using MRI (T2 weighted image scans) and Ultrasound (20MHz transducer). Tumor progression was observed in KPC mice on control diet without Garcinol or Gemcitabine treatment in KC group (Figure-6). Ten tumors were monitored and seven of them grew in size from week 1 to week six in KC group (Table-3).

Dietary Garcinol retarded the progression of Pancreatic Cancer in KPC mice. Of the nine tumors monitored over 6 weeks' time, only one grew in size, four of which showed arrest in growth and four showed reduction in size (40% tumor reduction). In addition, there was a considerable reduction in inflammation of the peri-pancreatic area, stomach and intestinal tract in the Garcinol fed mice group (KGr). Intestinal obstruction due to inflammation and secondary tumors are common complications in KPC mice. Reduction in swelling and abdominal distention was apparent from the MRI scans of Garcinol fed mice from week one to week five (Figure-7).

Gemcitabine is a pyrimidine analog and works at two levels. It stops DNA synthesis by incorporation in the elongating stand and it also targets Ribonucleotide Reductase enzyme as it binds to the enzyme and inactivates it irreversibly. It is one of the drugs of choice in pancreatic cancer treatment. The Gemcitabine group (KGm) showed a mixed response to the drug, Figure 8 shows the MRI image from one mouse that showed significant reduction in tumor volume and can be referred to as Gemcitabine responder (10% response). Of the 10 tumors monitored and four of them grew in size indicating that some mice did not respond to the Gemcitabine treatment

(Table-3). Five tumors showed no difference in the tumor volume from week one to week to week 6 (growth arrest).

The mice in the Gemcitabine plus Garcinol group (KGG) showed a better response as compared to gemcitabine alone (Figure 9), 9 tumors were monitored and two of them showed reduction in size with treatment and 6 showed arrest in growth. One of the mice did not response to the treatment as indicated by the increase in tumor size from week one to week 5 (Table-3). Some tumors were associated with cysts. It was observed that Garcinol, Gemcitabine and Gemcitabine plus Garcinol groups showed cyst volume reduction upon treatment in some mice (Table-3).

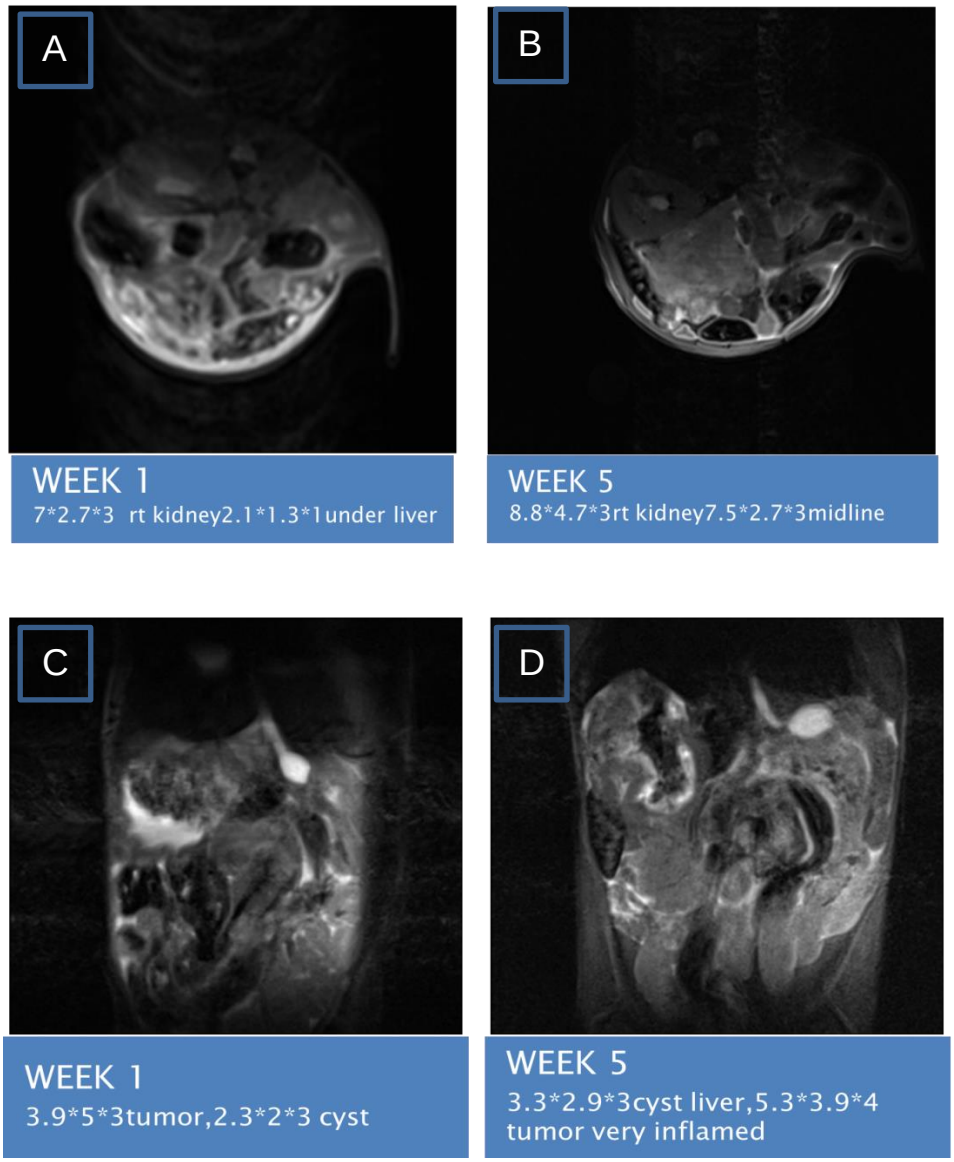

Figure 6: Progression of Pancreatic cancer in KC group.
A, KC transverse view week 1. B, KC transverse view week 5. C, KC coronal view week1. KC coronal view week 5.

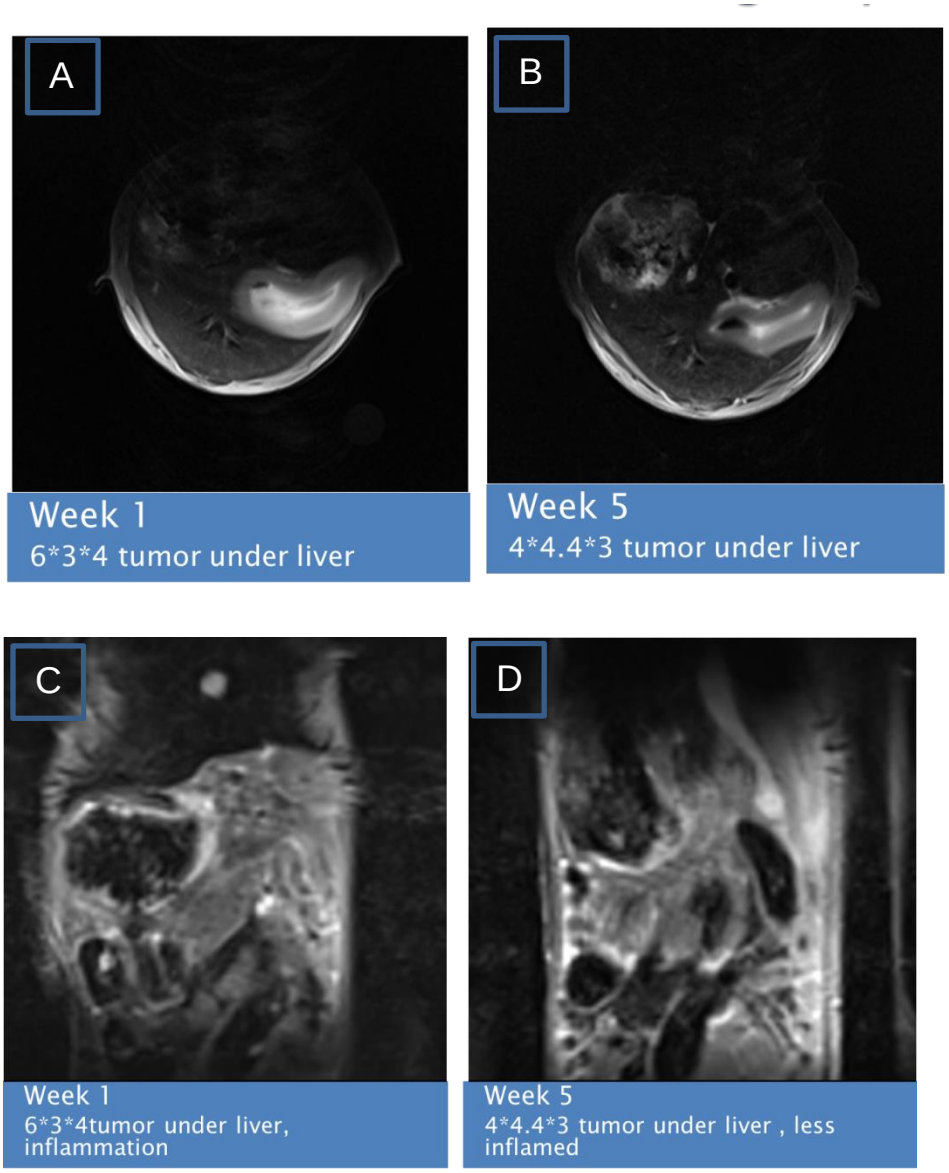

Figure 7: Reduction of tumor volume and inflammation in KGr group.
A, KGr transverse view week1. B, KGr transverse view week 5. C, KGr coronal view week 1. D, coronal view week 5

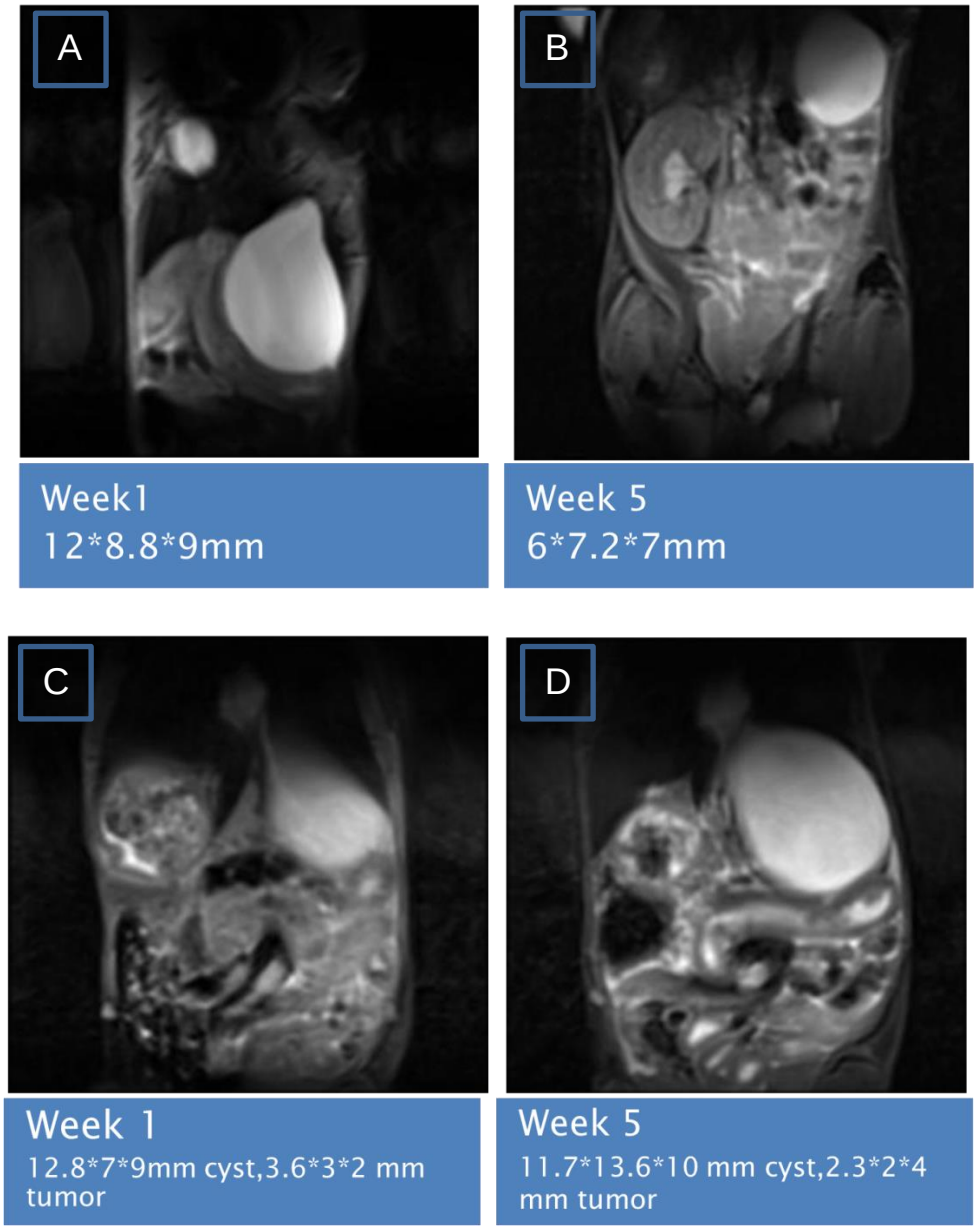

Figure 8: Gemcitabine responder and Non Responder.
Gemcitabine Responder- A, coronal view week 1 & B, week 5 and Gemcitabine non-responder C, week 1 & D, week 5.

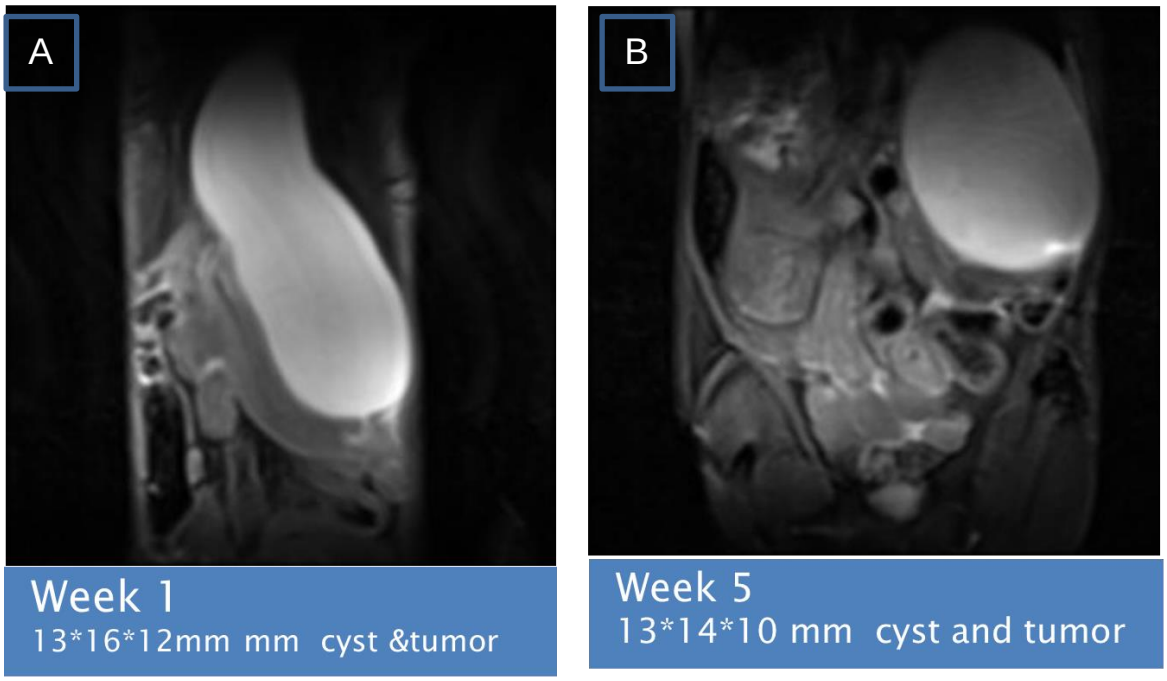

Figure 9: Garcinol and Gemcitabine combination (GG) showed reduction in tumor and Cyst.
A, KGG coronal view week 1. B, KGG coronal view week 5.

Group	Total Number of Tumors monitored	Number of tumors increased in size	Number of tumors decreased in size	Total Number of Cysts monitored	Number of cysts increased in size	Number of cysts decreased in size
KC	10	7	-	4	4	-
KGR	9	1	4	3	2	1
KGM	10	4	1	5	3	2
KGG	9	1	2	6	3	3

Table 3: Tumors and Cysts monitored by MRI in KPC mice.

2.4.3 Investigation of Fore- stomach H& E slides for possible toxicity of Dietary Garcinol:

As Garcinol was administered through diet, we investigated the fore- stomach H&E slides for possible toxicity of dietary Garcinol. Fore stomach the proximal third part of the stomach is non- glandular and has keratinized stratified squamous epithelium. The latter two third glandular part of the stomach has cap cells chief cells and parietal cells for gastric secretions [34]. Epithelial lining gets irritated and hypertrophied with ingestion of toxic substances. Fore stomach epithelium, mainly mucosal epithelium gets hypertrophied with repeated doses of toxic compounds. Sometimes this is associated with keratosis and inflammation and can leads to severe complications if not addressed

at earlier stages [35]. Along with chemical irritant , insecticides and drugs, some synthetic and naturally occurring anti-oxidants have shown fore stomach hyperplasia and toxic effects after oral administrations as early as four weeks[36].

As shown in Figure 10, we observed no toxicity of Garcinol to the fore stomach after oral administration for six weeks in control mice on Garcinol diet group (CG). The fore stomach lining was comparable to control mice on control diet group (CC) after dietary Garcinol ingestion for 6 weeks. This indicates that Garcinol ingestion does not cause any hyperplasia of fore-stomach lining mucosa.

Upon investigation of the fore- stomach from KPC mice (KC), a lot of inflammation, papilloma formation and hyperplasia of most of the fore stomach lining, consistent with the phenotype of these mice with stomach and intestinal obstruction, inflammation and swelling was observed. These papillomas were more evident near the junction of fore-stomach and glandular stomach (Figure- 10), referred to as squamo-columnar or fore-stomach/zymogenic junction in previous studies [34]. The histology and pathology was quite similar to the mataplastic, columnar and glandular gastric tumors reported earlier in a study with SMAD 3 zinc deficient mice [37]. Similar tumors were also reported in p53 null and zinc deficient mice with N-nitrosomethylbenzylamine (NMBA) administration [38]. Fore stomach in rodents is considered as a dilation of the esophagus and is comparable to human esophageal /stomach junction. This portion of stomach is more sensitive than the esophagus in mice, although both are lined by squamous epithelium [38].

Interestingly Garcinol fed KPC mice showed marked reduction in these papillomas. Even more fascinating was the fact that the stomach lining of some Garcinol

fed mice were comparable to the non-cancer groups (CC and CG) (Figure-3). This finding correlated with our MRI results where we observed reduction in inflammation and swelling of the intestinal tract specially stomach and duodenum with Garcinol administration. Intestinal obstruction is a major cause of weight loss and death in KPC mice. All the Garcinol fed mice (KGr) mice survived the study and didn't show any signs of these complications. This may be attributed to its protective effect on the stomach lining.

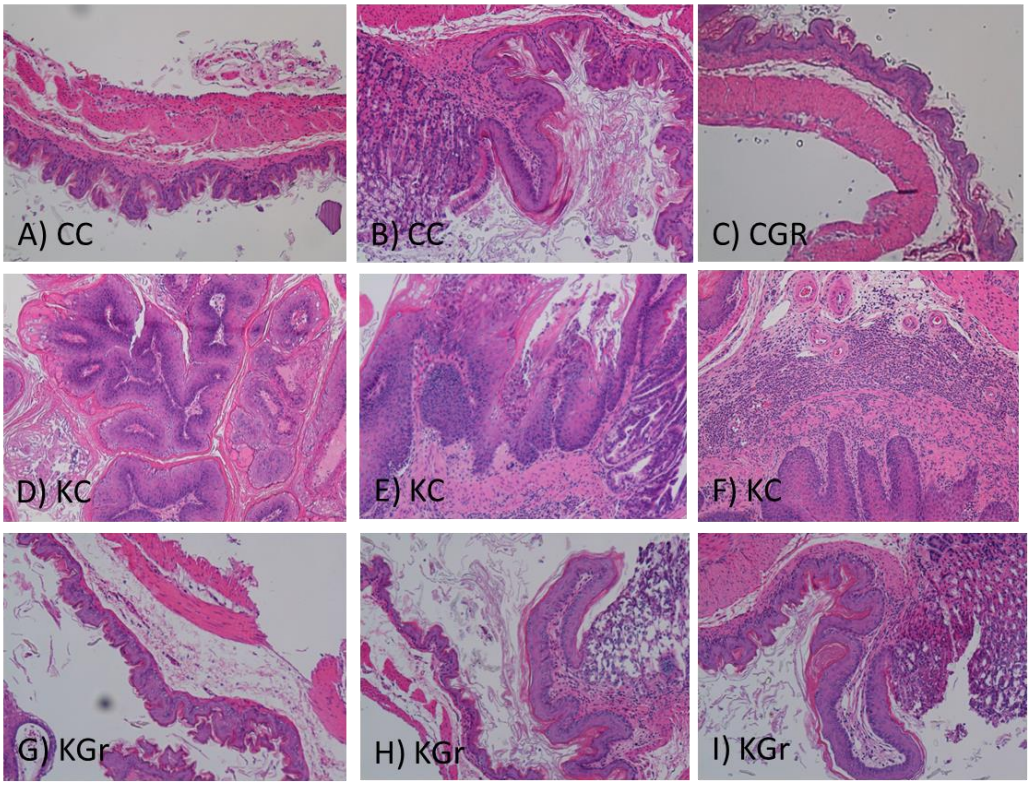

Figure 10 : Fore-Stomach H&E slides showed no toxicity to Dietary Garcinol

- Mice without cancer on control diet (CC)
  - (A): normal fore-stomach lining epithelium in (B): Normal Squamo/columnar junction in CC
- Mice without cancer on Garcinol diet (CGr)
  - (C): no sign of hypertrophy or toxicity
- KPC mice on control diet (KC)
  - D, Papilloma formations ; E, Squamo-columnar junction with papilloma like changes; F, Inflammation
- KPC mice on Garcinol diet (KGr)
  - G, H & I, normal fore-stomach lining and less papilloma like changes. Squamo-columnar junction in KGr group similar to CC group.

2.4.4 Investigation of Blood smears for possible toxicity and immune response in KPC mice:

Blood smears prepared at the end of the study, were stained with Wright and Giemsa stain and observed under light microscope (Nikon Eclipse), to explore the effects of dietary Garcinol on blood morphology and rule out possible toxicity. Changes in red blood cell following exposure to toxics/drugs are common. These include basophilic stippling with metal poisoning, bite cells and Heinz bodies in oxidative stress and blister cells in aromatic drugs exposure. No changes to red blood cells post Garcinol administration were observed in any of the Garcinol fed animals indicating that 0.05% dietary Garcinol did not cause any toxic effects on red blood cell of KPC or control (non-mutant) mice.

Total white blood cell count showed no significant differences in the experimental groups as compared to control group. However, while counting total lymphocytes it was noticed that there were more number of Large granular lymphocytes LGLs.(Figure 11, mainly Natural killer cells (NK cells) and Natural killer T cells (NKT cells), in the Garcinol fed group blood smears as compared to other KPC groups. NK cells are the first line of defense against tumor cells and represent the innate immune response [39]. NK and Natural kill T cells (NKT) have similar phenotype and function in response to tumor cells [40]. In order to investigate the innate immune response to pancreatic cancer in all the groups, we measured the number of the NK & NKT cells and compared it with the number of non NK lymphocytes in all the groups of mice (Figure- 12).

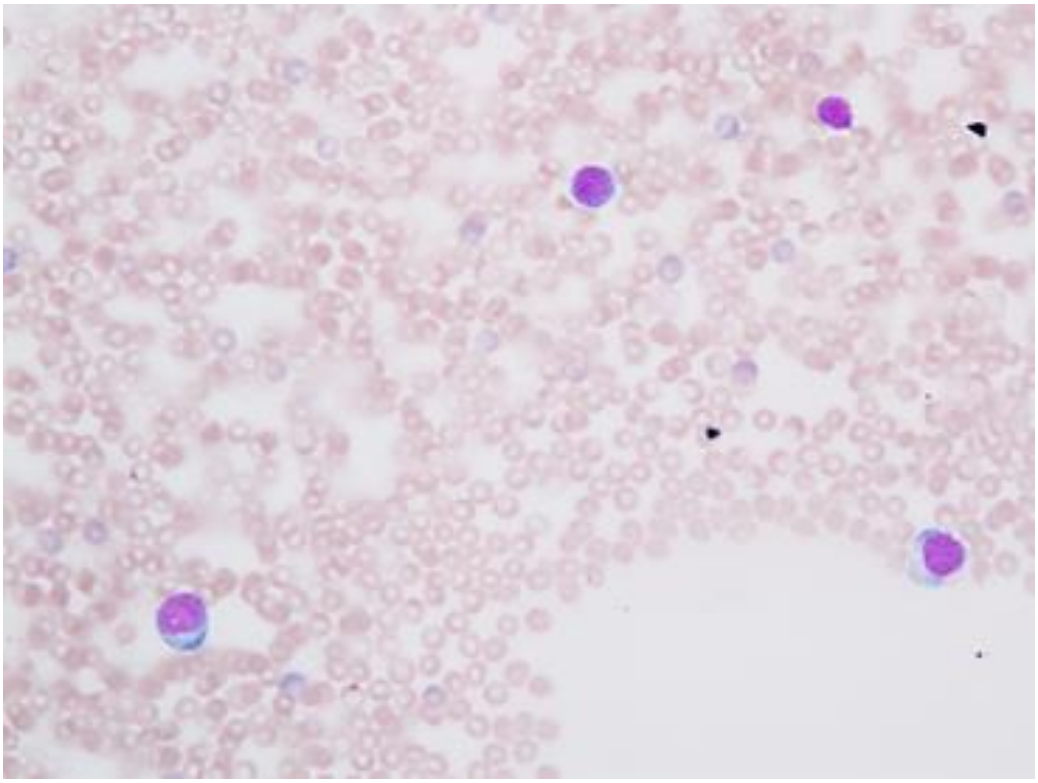

Figure 11: Large granular lymphocytes (NK & NKT)- In Garcinol fed group(Wright Giemsa stain), NK &NKT cells are larger in size and have granular, irregular nucleus. Non NK lymphocytes have round heterochromatic nucleus with thin rim of Cytoplasmic.

Large granular lymphocytes (LGL) have granules and an irregular-shaped nucleus. These are larger in size than other lymphocytes. Non NK Lymphocytes generally have a round, heterochromatic nucleus with thin rim of cytoplasm around it; they are much smaller in size compared to LGLs.

Interestingly the NK & NKT cells number compared to non NK lymphocytes was significantly high in Garcinol treated group (KGr) as compared to other groups with p value<0.001 (Figure - 12). Increase in NK & NKT cells can be a very valuable finding and warrants further investigation. A follow up study, measuring population of these cells by flow cytometry at different time points with Garcinol administration may be useful in understanding the mechanism of this effect.

The role of NK & NKT cells against tumor cells has been investigated in many studies including carcinogen induced and transgenic mouse models. NK &NKT cell can be helpful in cancer therapy in many ways. NK cells can target tumor cells through multiple pathways including release of perforins and granzymes, death receptor activation and gamma interferon and nitric oxide pathway [41]. NKT cells can also target tumor cells, by directly killing tumor cells or indirectly by activation of NK cells at early stages of cancer development by mechanisms that may or may not require antibody response. In addition invariant NKT (iNKT) cells can regulate production of angiogenic factors by tumor associated macrophages containing CD1d and can therefore have repressive effect on angiogenesis[40]. Recent studies have suggested use of NKT cultured cells supplementation along with CD1d antibodies as cancer therapy [40]. NK and NKT cells secrete cytokines like interferon-γ (IFNγ) that participate in adaptive immune response [40]. Adjuvant therapy with agents inhibiting formation of reactive

oxygen species like Histamine can assist in NK cell immunotherapy to overcome challenges produced by infiltrating monocytes and macrophages[42].

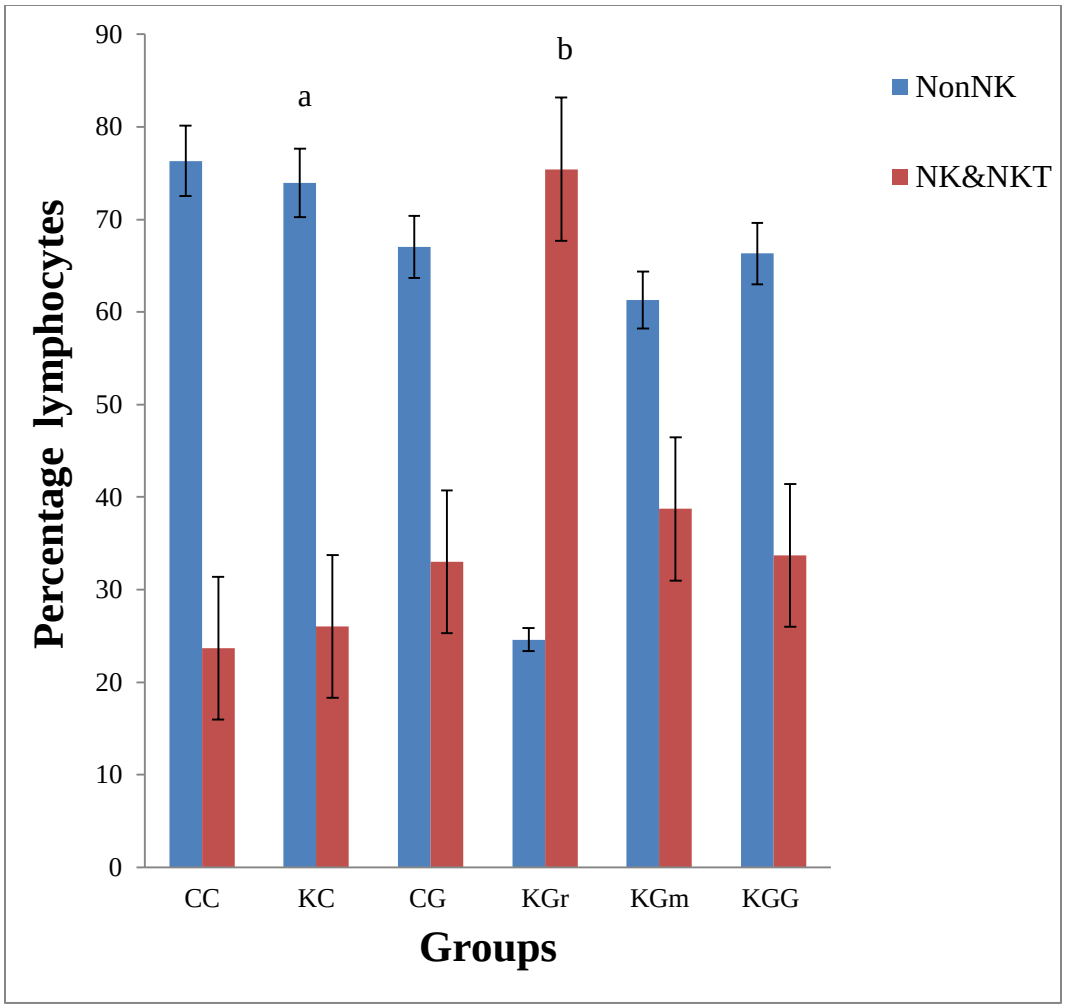

Figure 12: Change in lymphocyte population with dietary Garcinol. Percentages of NK and NKT compared to Non NK lymphocytes, KGr group (Garcinol fed) showed significantly high percentage of NK & NKT cells (‘a‘ is significantly different from ‘b’ pvalue<0.001), almost reversal of the ratio as observed in other groups. Error bars represents standard error of mean.

2.4.5 Histological investigation of pancreatic tissue:

KPC mice develop a wide range of changes in the pancreas comparable to changes that occurs during progression of ductal adenocarcinoma in humans. These changes include genetic instability, increased nuclear cytoplasmic ratio, loss of acinar tissue organization, nuclear pleomorphism and loss of cell differentiation [32].These mice shows premalignant Pancreatic intraepithelial neoplasia similar to those in human disease. These lesions usually contain mucin and are cytokeratin 19 positive [32]. They have 100% penetrance with a variable latency period along with an average median survival of four and half months.

In order to investigate the pancreatic lesions in our mice we used the criteria established by the International workshop held in University of Pennsylvania, co-sponsored by National Cancer Institute in 2004 [31]. One of the goals of this work shop was to evaluate different models of Pancreatic exocrine neoplasia and set uniform criteria to describe pathology of these genetically engineered mice so it will enable the comparison with human disease [31].

There are architectural and cytologic changes which need to be observed for in-depth evaluation of pancreatic lesions. Architectural changes includes the formation of abnormal structures like masses and cysts, changes in the location of structures and transformation of tissue, invasion and of new cells to the tissue which does not belong to the area. Cytological changes include cellular hypertrophy, atrophy, metaplasia, hyperplasia, apoptosis and cell necrosis. In addition changes of the interstitial tissues including fibrosis, desmoplasia and inflammation should also be noted in complete investigation of the tissue.

Pancreatic lesions; those meeting specific criteria, including ductal proliferation should be within native pancreatic duct, involved duct should measure less than 1mm and should be differentiated from acinar ductal metaplasia were classified as mouse Pancreatic intraepithelial neoplasia (mPanIN). The word mouse was added as these lesions were similar to human pancreatic intraepithelial neoplasia but they all progress to invasive ductal adenocarcinoma in mice [31].

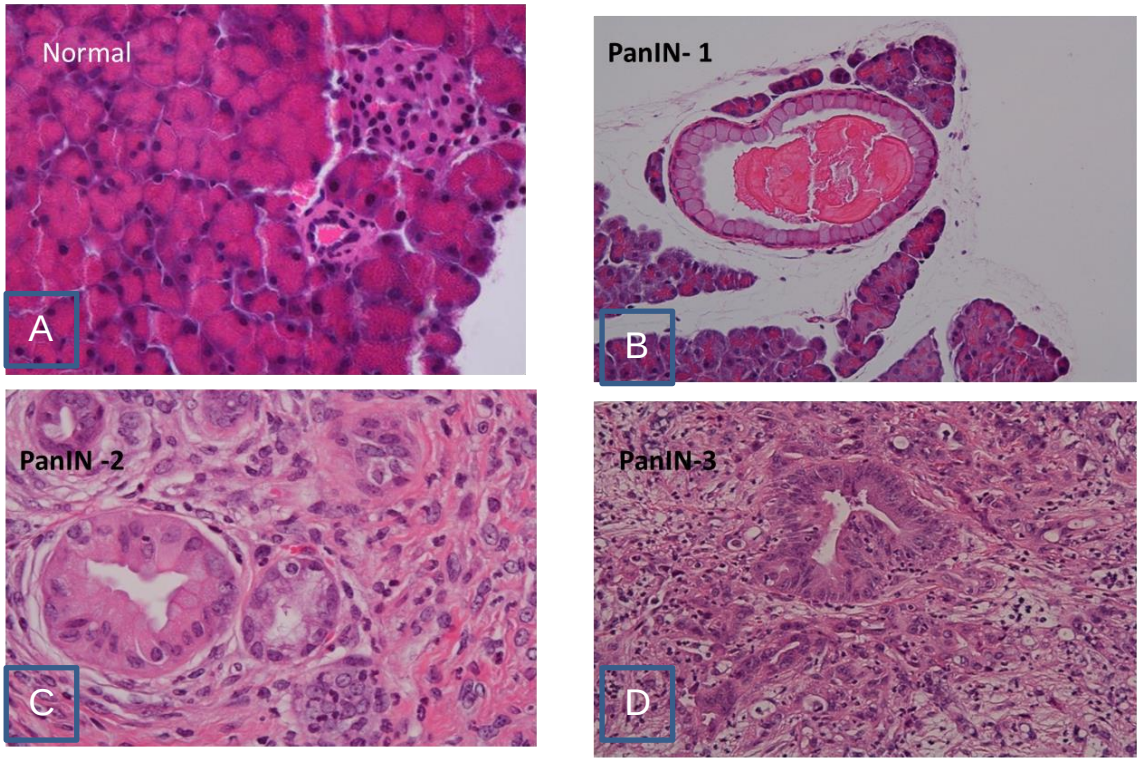

Figure 13: mPancreatic Intraepithelial Neoplasia (mPanIN).
A, Normal pancreatic tissue. B, PanIN-1. C, PanIN-2. D, PanIN-3.

Grading of mPanIN was based on architectural and cytological changes, starting with normal pancreatic ductal epithelium which is cuboidal to low columnar with amphophilic cytoplasm with no atypia. mPanIN-1a has tall columnar cells with basally located round to oval nuclei and large amount of mucin (Figure-13). They also may have papillary or micropapillary with a single layer of nuclei (mPanIN 1b). mPanIN-2 contains mostly papillary structures but may be flat. These some cytological changes like loss of polarity, nuclear crowding, enlarged nuclei and hyperchromatism (Figure-13 C). mPanIN 3 are papillary and micropapillary lesions. Budding of clusters of epithelial cells into the lumen with luminal necrosis (Figure-13 D). Cells show loss of polarity, abnormal mitosis and goblet cells. These lesions have all the characteristics of invasive carcinoma but the basal membrane is not breached.

Invasive pancreatic ductal adenocarcinoma (PDA) can be well or poorly differentiated. It is defined as malignant epithelial neoplasm with ductal differentiation that has penetrated through the ductal basement membrane [31]. In KPC mouse model PDA is mostly undifferentiated carcinoma which is invasive neoplasm with no glandular, acinar, endocrine or squamous differentiation. Loss of lobular normal pancreatic architecture is also evident in these lesions [31].

KPC mice showed all stages of mPanIN along with invasive Pancreatic ductal adenocarcinoma (PDA). Full array of architectural, cytological and interstitial changes was observed validating the clinical relevance of this mouse model. PDA lesions were associated with cyst formation in number of cases. Acinar ductal metaplasia was prevalent in the almost all of the mice included in the study. Most of the mice showed untouched endocrine with slight compensatory hyperplasia in cases where fibrosis has

damaged lobular structure of the pancreas. Acute and chronic inflammations leading to formation of granuloma like aggregates were observed. Fibrosis and desmoplsia were widespread in the mice with PDA. In addition to peri-pancreatic lymph nodes, intra-pancreatic lymphoid tissue aggregates with sinus histocytosis were also observed with advanced PDA lesions.

Overall the total number of mPanINs were decreased in KGr, KGm and KGG groups with lowest number observed in the KGG group ($p = 0.005$). Highest numbers of mPanIN3s were observed in KC group and lowest number in KGG group ($p = 0.002$). This indicates slower progression of mPanIN lesions from mPanIN1 to mPanIN 3 in the Garcinol fed groups as compared to KC group (Figure-14).

According to histology we saw improvement in three gemcitabine treated mice, slow responders although in MRI we saw only one clear Gemcitabine responder based on tumor volumes. KGG group showed well preserved lobular structure, ductal, acinar and endocrine pancreas among all groups (Figure- 14).

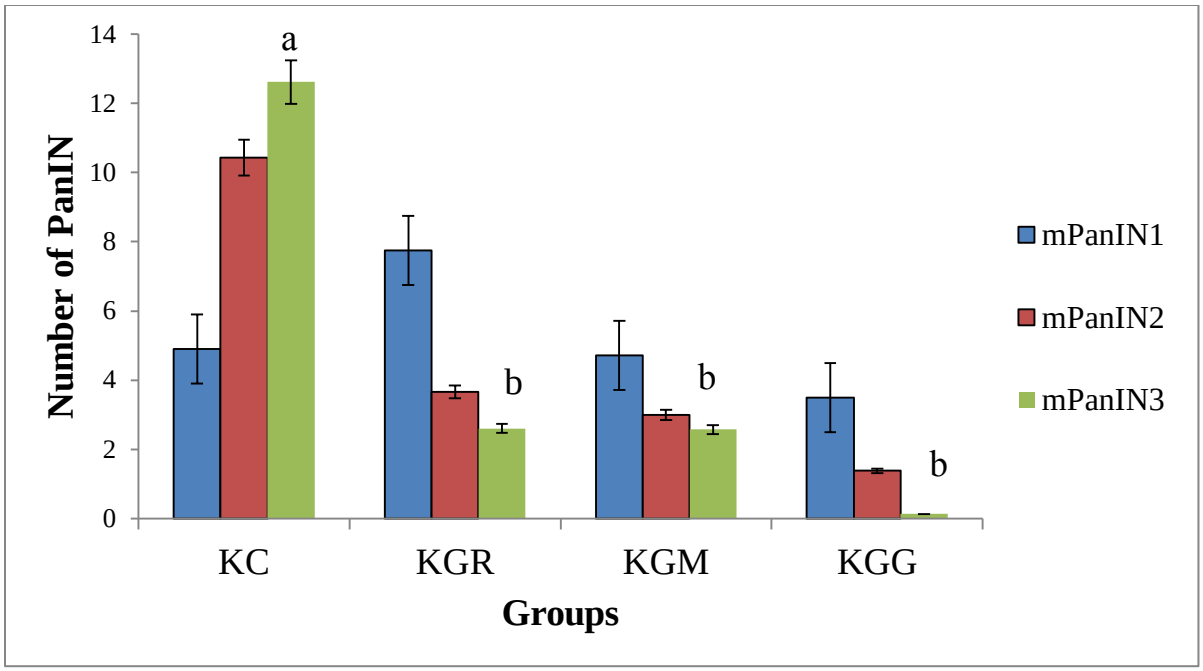

Figure 14: Comparison of mPanIN numbers and stages in different groups.
('a' is significantly different from 'b')
KC group had highest number total number of mPanIN (p value < 0.05) and KGG had lowest number of mPanIN (p value< 0.05). Reduction of mPanIN 2 and 3 was observed with Garcinol and Gemcitabine treatment (p value < 0.05). KGG had lowest number of mPanIN 3 (p value < 0.05).

2.4.6 Immunohistochemistry with S100p and DPC4 antibodies:

S100p is a member of s100 family of proteins and is not usually expressed in pancreas. However it is reported to be expressed in pancreatic cancer [43]. This is primarily due to hypo-methylation of the gene as reported in earlier studies. Overexpression of s100p normally correlates with resistance to chemotherapy and increased metastatic potential [43]. S100p provided support to cancer cell proliferation leading to pancreatic cancer cell survival [43]. This protein interacts with the RAGE receptor which in turn activates different cell signaling pathways including MAP kinase and Fib, causing increased survival, growth and metastasis of tumor cells. S100p also takes part in degradation of β catenin through interaction with Cacy/SIP, a component of the ubiquitination pathway. It has been reported that s100p is a good marker for Pan IN progression and there is a considerable increase in expression from PanIN 1 (13% expression) to PanIN2 (31% expression) and PanIN3 (41% expression) [44]. Lesions positive for S100P have been reported to be significantly related to progression into invasive ductal adenocarcinoma [44]. Expression of S100P was shown to be very effective in diagnosis of Pancreatic ductal adenocarcinoma (PDA). In a study conducted on fine needle biopsy samples from patients with different pancreatic tumors, S100P immunostaining was found to be positive for all PDA samples. The immunoreactivity was reported negative for all endocrine tumors and only one benign sample was found positive [45]. In another study S100P was shown to be one of the best immunomarker of ductal adenocarcinoma of pancreas along with pVHL, maspin, and IMP-3 [46]

Immunohistochemistry with S100P antibody showed that these mPanIN lesions in KPC mice are positive to S100P. Upon detailed examination of the slides, expression of S100P increases with progression of mPanIN and was highest in PDA. KC group showed very strong staining (Figure 15) in mPanINs confirming our findings from H& E slides that the KC group had the highest number of advanced mPanINs and PDA. Lymphoid tissue from KC mice showed S100P labeling in lymph node with stained cells in the center of lymph node. S100P stained cells were also observed on ducts and blood vessels (Figure 16). KGr group showed much cleaner S100P stained slides, with few mPanIN lesions stained for S100P (Figure 17). Lymphoid tissue also have very few s100P positive cells, if present they were in the periphery of the lymph nodes (Figure 18). KGm mice showed less S100P staining in the responders and more expression in the non-responders consistent with H&E findings (Figure 19). KGG group confirmed to be the best response group to the treatments with least expression of S100P (Figure20). S100P staining is not reported in KPC mice before. Expression of S100P can be very useful predictor of progression of PDA in this clinically relevant mouse model of pancreatic cancer.

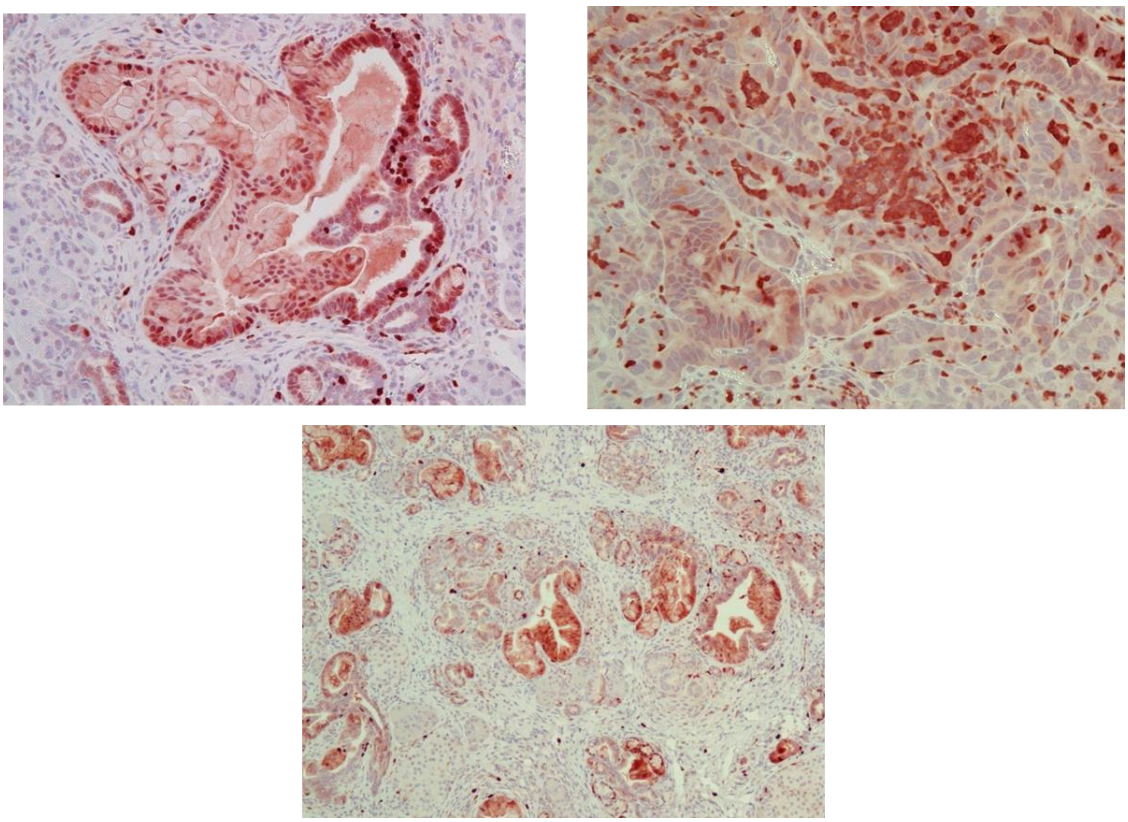

Figure 15: higher expression of S100P in PanIN and PDA in KC group (KPC on control diet).
Three different sections from KC group showing advanced pancreatic lesions with high S100P staining.

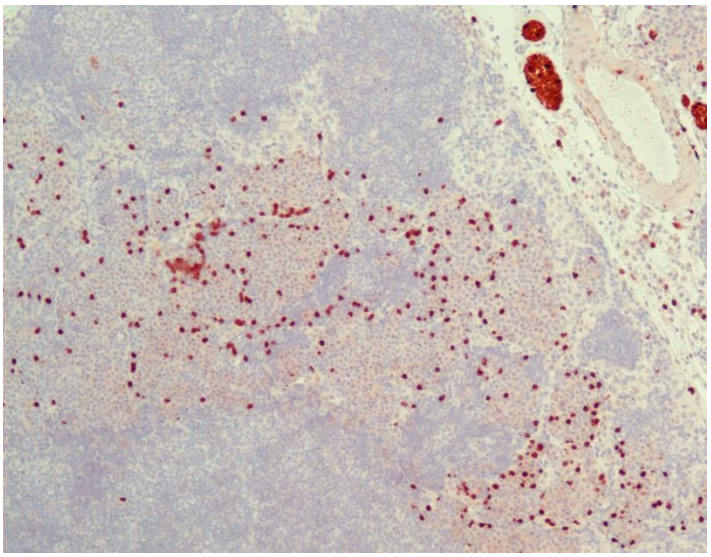

Figure 16: Peri-pancreatic lymph node in KC mice, showed many S100P positive cells in the center of lymph node.

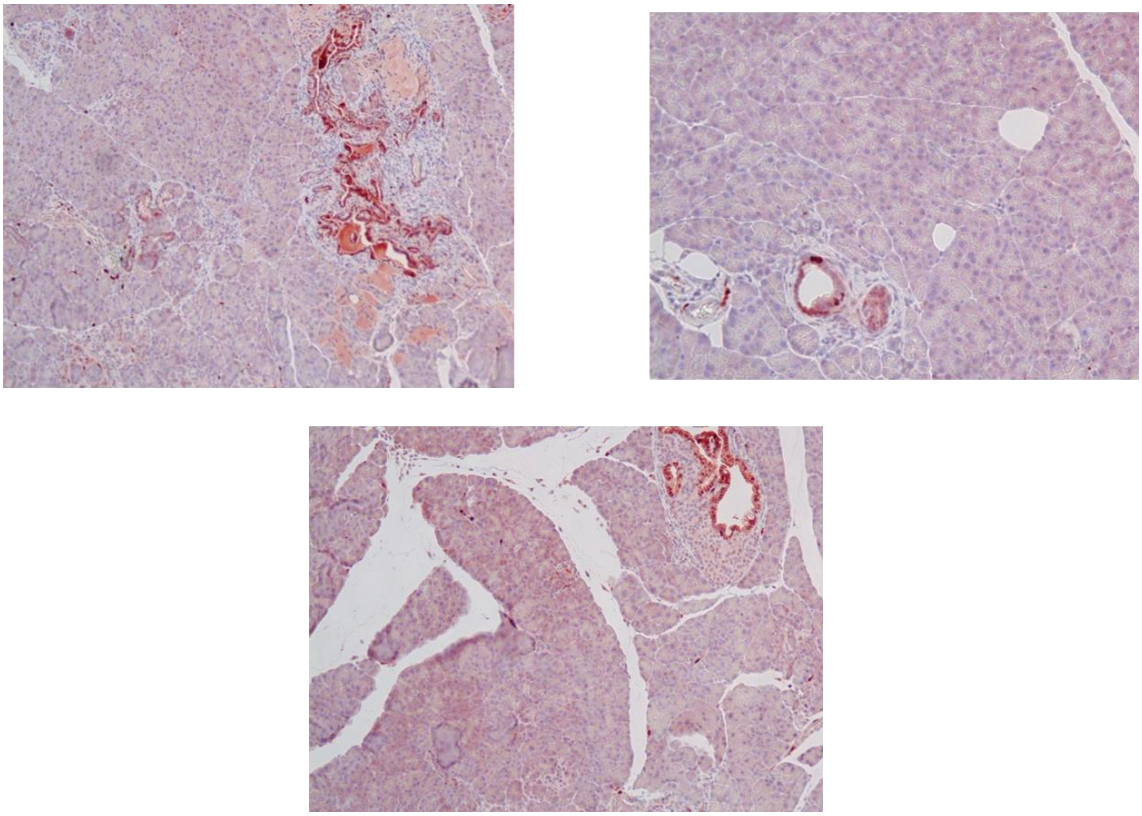

Figure 17: KGr group (KPC Garcinol fed) showed lower expression of S100P compared to KC group.
Three different sections from KGr group showing less S100P staining compared to KC group.

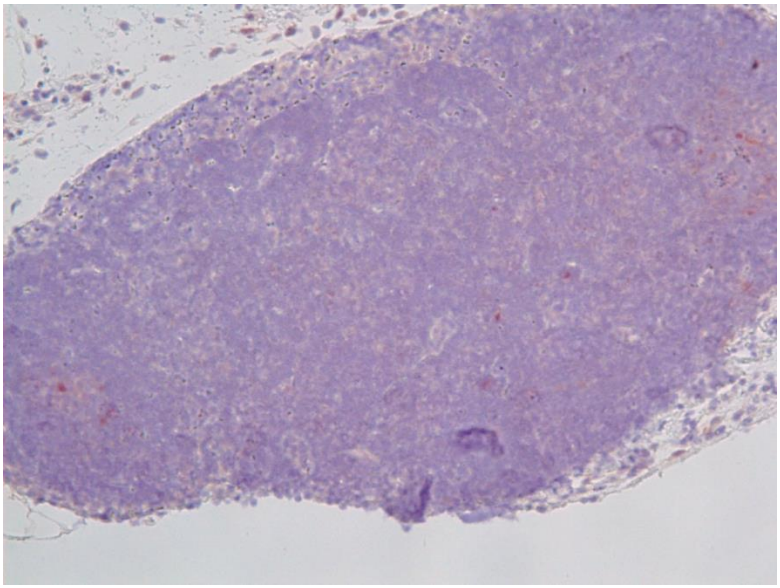

Figure 18: Lymph node in KGr group with very less S100P staining.

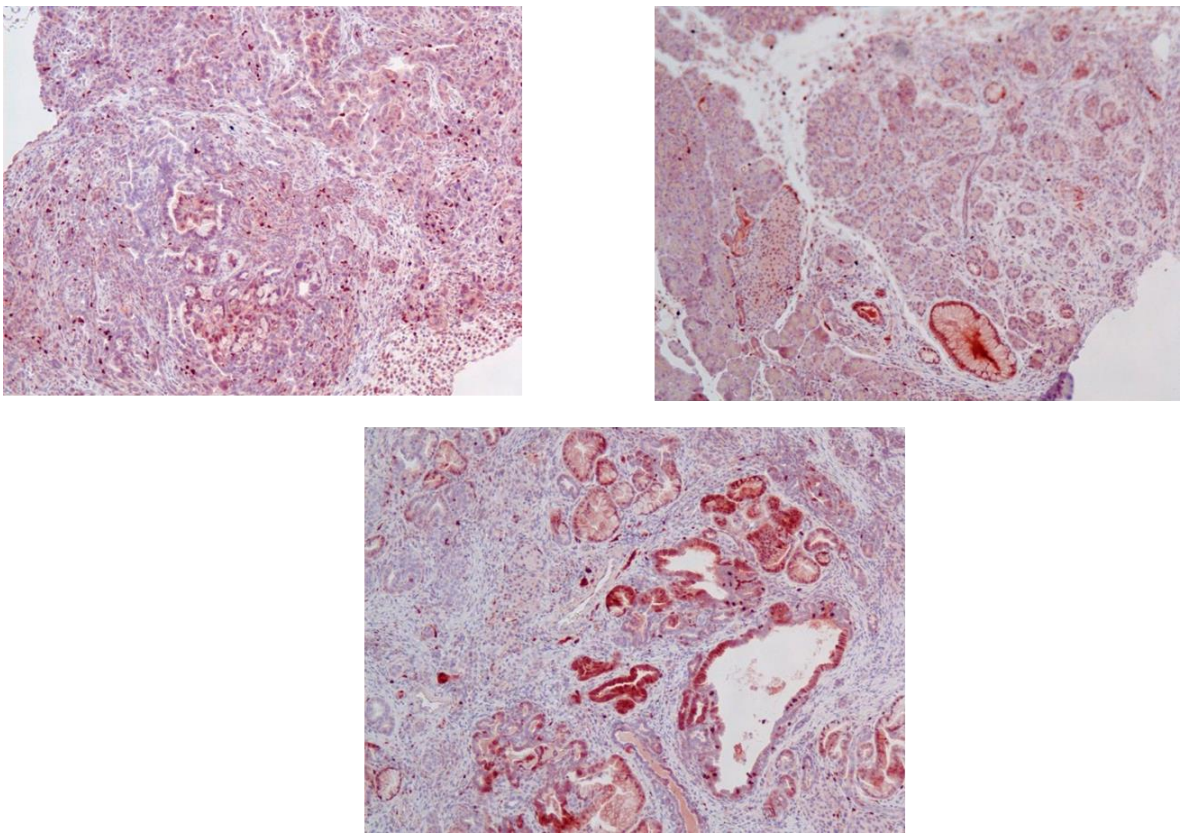

Figure 19: S100P staining in KGm group. KGm group (KPC Gemcitabine treated) showing less staining and fibrotic tissue in responder and more S100P staining in non-responders

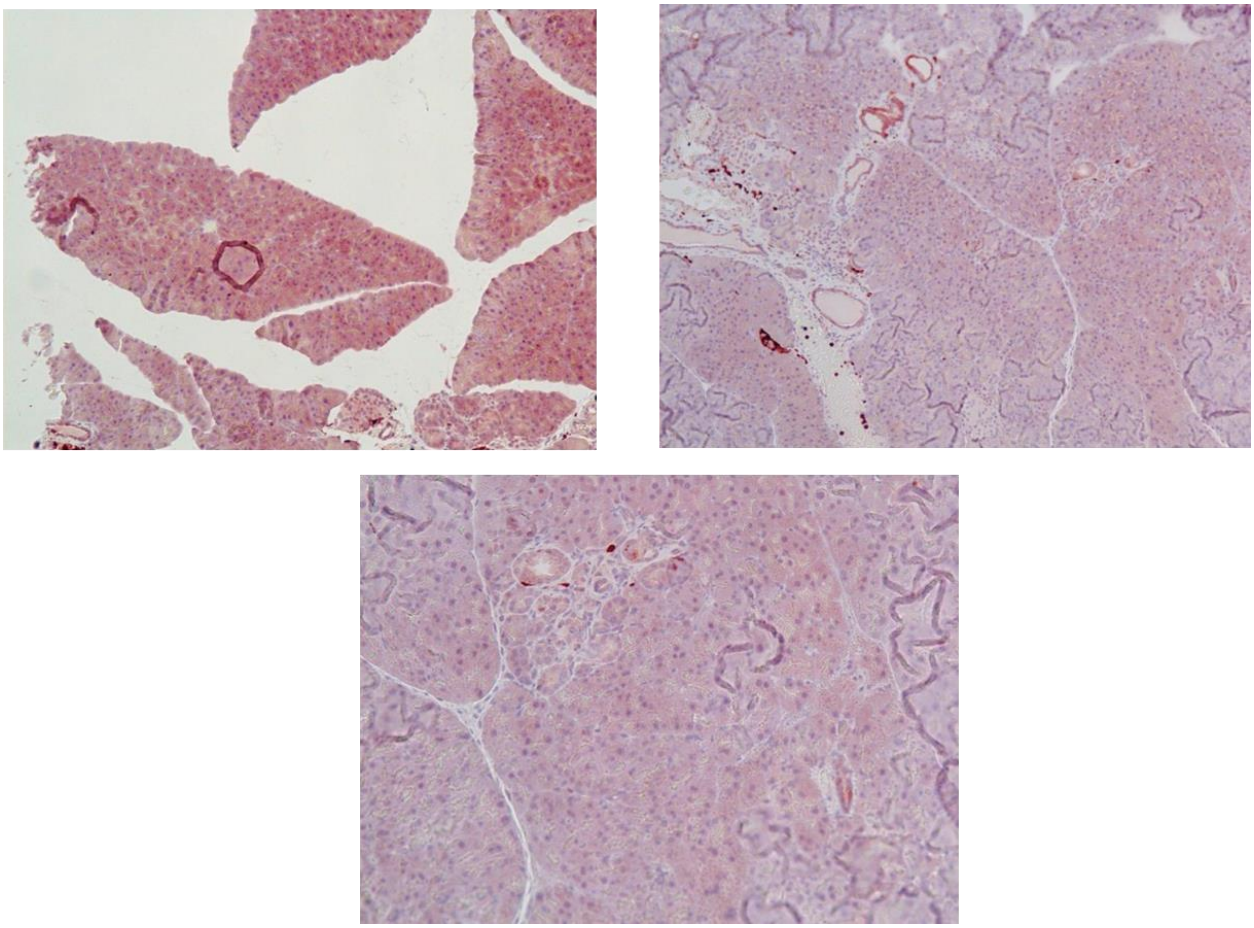

Figure 20: S100P staining in KGG group-showing more consistent lower expression of S100P in KGG group (KPC Gemcitabine plus Garcinol)among all the groups.

Deleted in pancreatic cancer (DPC4)/ Mothers against decapentaplegic homolog 4 (SMAD4) is a tumor suppressor gene normally inactivated in pancreatic cancer. It usually occurs by heterozygous deletion and mutation in other allele or by homozygous deletion of the gene during progression of the disease [47]. Inactivation of is DPC4 is specific to pancreatic cancer and it occurs mostly late in PanIN3 stage. Loss of DPC4 can be predictive of invasive properties of the PanIN lesions [48]. Although there was not much difference in the pathology and characteristics of pancreatic tumors, DPC4 positive Pancreatic cancer patients have shown longer survival trend in clinical setting[47]. We have p53 and K-ras conditional mutations in KPC mouse model, in order to investigate whether DPC4 is also affected during the development and progression of pancreatic lesions in this model, we explored paraffin fixed pancreatic tissue with DPC4/SMAD4 antibody. KPC mice without any treatment (KC) showed loss of DPC4 labeling with antibody in advanced mPanINs and PDA. Additionally there were areas with generalized fading in normal structures of pancreas in some KC mice indicating that loss of DPC4 can come as an earlier event in some cases before the area gets aggressive PDA lesion (Figure 21). KGr group overall showed higher expression of DPC4 correlating with H&E findings with less mPanIN lesions and preserved lobular structure, ducts and endocrine regions (Figure 22). There were some areas of advanced mPanINs and PDA that showed loss of DPC4 indicating that loss of DPC4 due to advancement of the disease, leading to genetic instability. KGm showed mixed response as some of them showed diffuse labeling with DPC4 antibody but some of them were generally faded most of the pancreatic tissue (Figure 23). Interestingly one of the responders to Gemcitabine showed over all fading with very little area of normal

DPC4 staining where as one of the non-responder has more ducts with DPC4 labeling. Garcinol plus Gemcitabine treatment in KGG groups showed the most staining and well preserved DPC4 expression representing preservation of normal morphology of most of the pancreas in this group, consistent with our previous H&E and S100P observations (Figure 24).

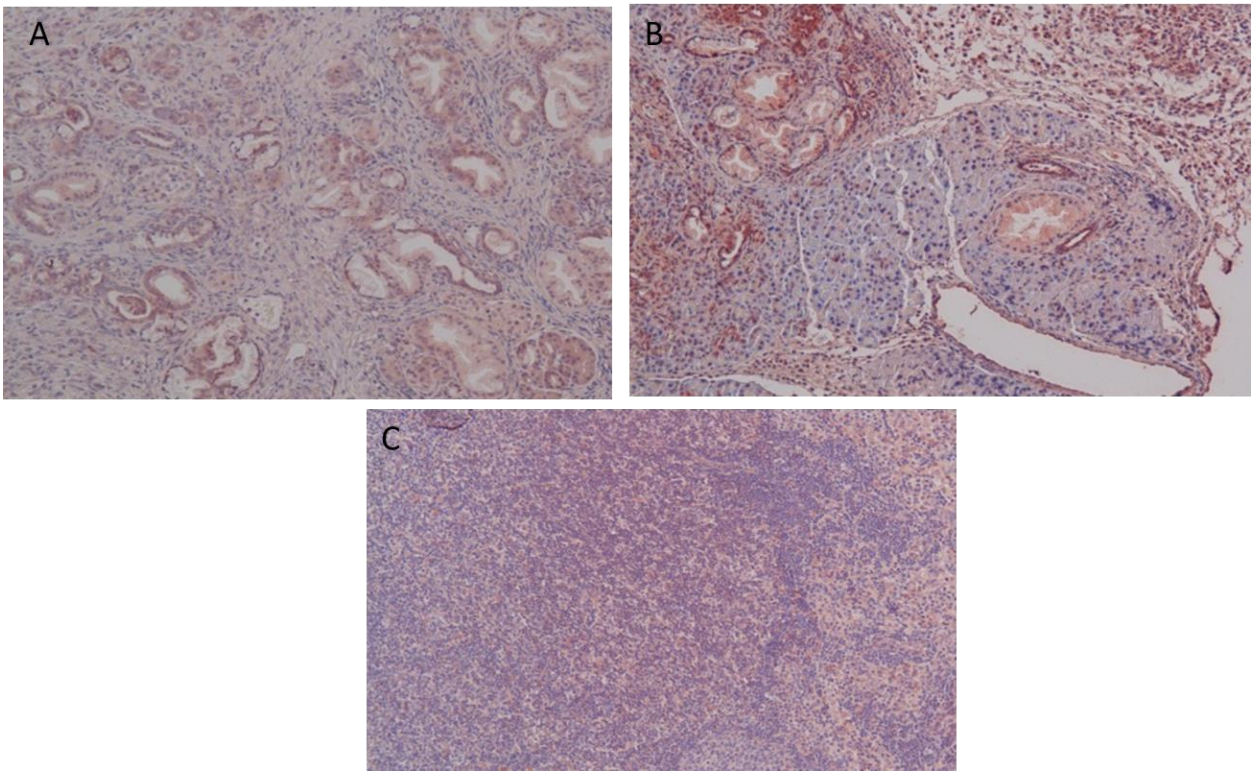

Figure 21: DPC4 Staining in KC Group. A&B, Very less DPC4 staining in KC group(KPC on control diet) with progression of PanIN and PDA.C, lymphoid tissue in KC group showed almost no DPC4 positive cells

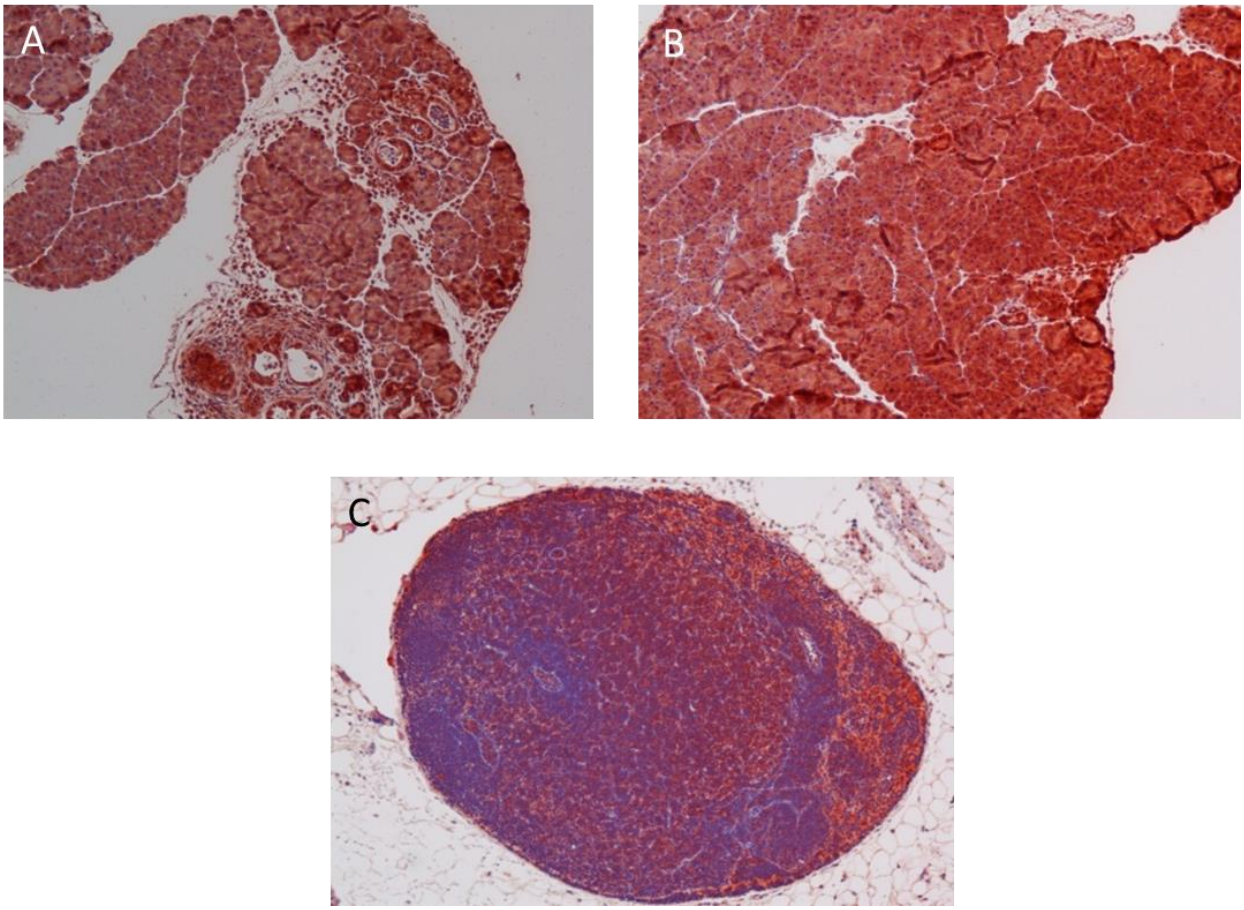

Figure 22: DPC4 staining in KGr group- A&B KGr group (KPC Garcinol fed) Showed preserved DPC4 in pancreatic tissue. C, Lymphoid tissue in KGr group with DPC4 staining.

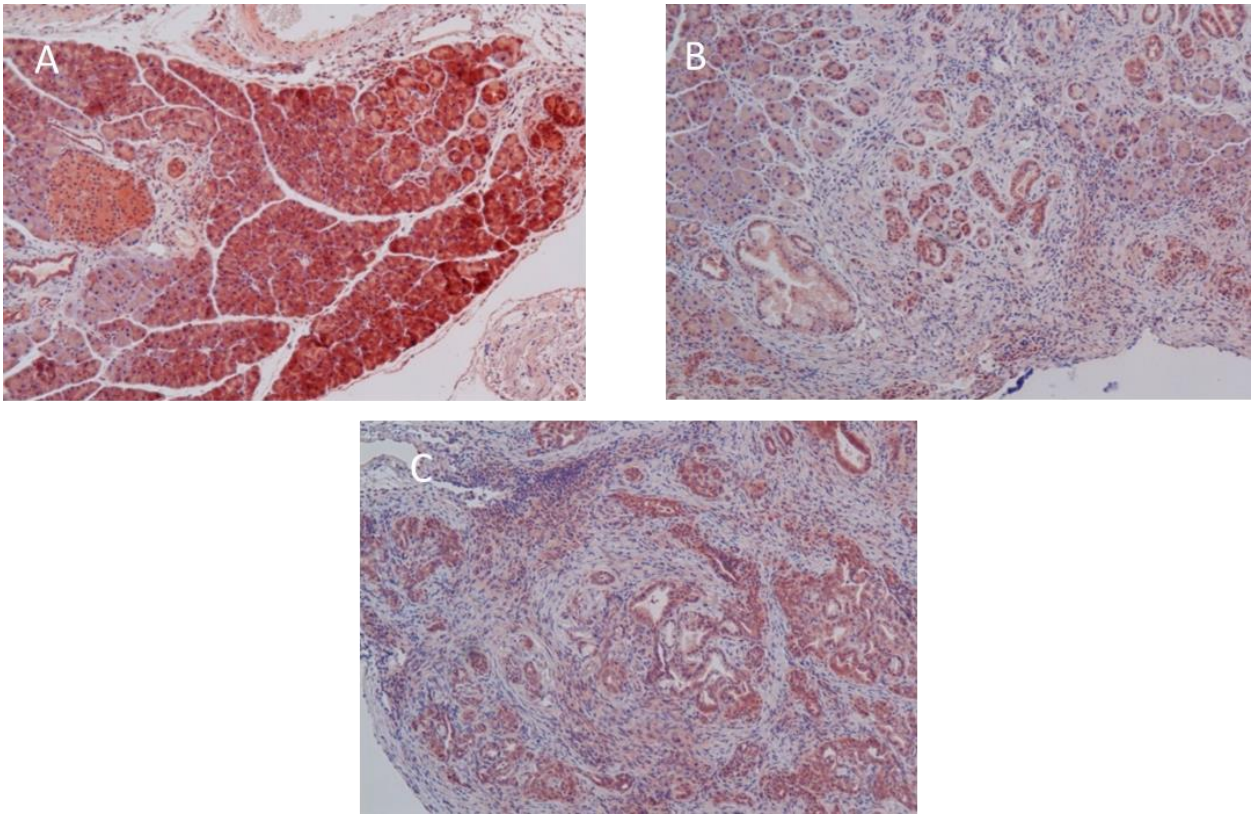

Figure 23: DPC4 Staining in KGm group- A, DPC4 positive Gemcitabine responder. B& C, Less staining in Gemcitabine non-responders.

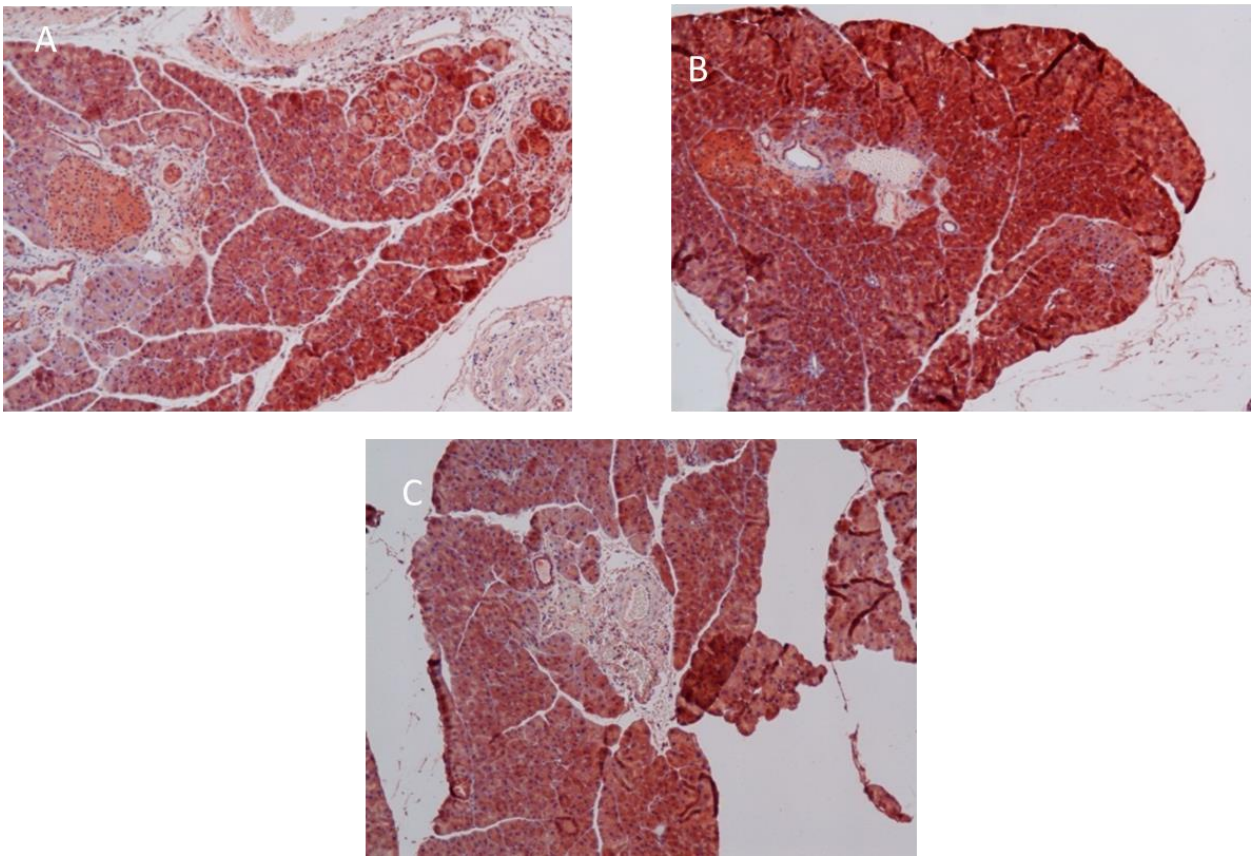

Figure 24: DPC4 Staining in KGG Group- A, B & C Higher expression of DPC4 in KGG group(KPC Gemcitabine plus Garcinol).

CHAPTER 3: Epigenetic Modulation of Tumor Promoter Genes Through microRNAs in Garcinol fed Transgenic Pancreatic Cancer Mouse Model

MicroRNA are small ~20 nucleotide long, noncoding RNAs which have the potential of silencing mRNAs for specific genes. Although the exact mechanism of gene silencing is under investigation, 3' UTR of mRNA and first 8 nucleotides of miRNA play important roles. One mRNA can be repressed by multiple miRNAs [49, 50]. Although there is little complementation between 3'UTR and seed region (2-8 nt in 5'region) of miRNA, it is sufficient to cause repression of mRNA and sometimes leads to degradation of mRNA itself. If there are multiple target sites of lesser complementarity, these can lead to Ribonuclear protein (RNP formation) which leads to translational inhibition but can spare degradation of mRNA. Some of the genes have single predicted target site but mostly target genes have multiple sites which leads to cooperative binding [51]. The level of suppression also depends on the availability of the mRNA and miRNAs and they compete for binding. Although miRNA genes comprise only one percent of our human genome, they can affect up to ten percent of the total protein production [51]. These small RNAs can be responsible for major alterations in key metabolic pathways through their target genes[52].

Pancreatic cancer has a very complex stroma and miRNAs can cause alterations to this microenvironment. Additionally Pancreatic tumors are glucose dependent and some miRNA target genes are involved in major glucose metabolic pathways. Metabolic pathways can regulate production of some miRNAs and alternatively some miRNAs are

responsible for changes in metabolism in pancreatic cancer. Based on some research studies specific miRNA can differentiate among normal Pancreas and Pancreatic Cancer [52]. Reactive oxygen species (ROS), hypoxia, glucose status and major tumor related genes alter different sets of miRNA including up regulation of miR23a/b, miR155, miR125, miR21, miR181b, miR210, miR212, miR409 and miR 132 in Pancreatic cancer [52]. Pancreatic Cancer and other pancreatic diseases like chronic pancreatitis have miRNA signatures which can differentiate them from normal pancreas. These miRNA signatures have potential to identify long term and short term survivors [53].

Recently several studies s have shown potential of natural bioactive food components in modulation of miRNA profiles leading to suppression of tumor promotor miRNAs and up regulation of tumor suppressor miRNAs. Agents investigated includes curcumin , isoflavones, resveratrol, Indoles, catechins and Ellagitannin [54].

Garcinol has modulated miRNA profiles in positive manner, invitro studies in our lab. Oncogenic miRNA 21, 196a and 495 were down regulated and miRNA 638 and 453 tumor suppressor miRNA were up regulated (in a pancreatic cancer cell line when treated with Garcinol). In this study we investigated miRNA profile and some of the target genes to study the effects of Garcinol *invivo*.

3.1 Methods:

3.1.1 RNA Extraction:

Total RNA extraction was performed with a RNeasy Mini Kit (Qiagen Valencia, CA, USA) according to the manufacturer's instructions. Briefly, first, an approximate

weight of 30mg of frozen liver and pancreatic tissues were excised and placed into 700 uL QIAzol Lysis Reagent for disruption and homogenization using tissue homogenizer until sample was uniformly homogenous. Tube containing homogenate was then placed at room temperature (15-25˚C) for 5 minutes. 140 uL of chloroform was then added and tube was capped securely followed by vigorous shaking for 15 seconds. The tube was then placed at room temperature for 3 minutes prior to centrifugation for 15 minutes at 12,000 rcf at 4˚C. Following centrifugation, the upper aqueous phase was transferred to a new collection tube. 525 uL of 100% ethanol was added and mixed thoroughly by pipetting. Next, 700 uL of sample including any precipitate was pipetted into RNeasy Mini spin column in 2 ml collection tube and centrifuged at 10,000 rpm for 15 seconds. The flow-through was discarded and this step was repeated with remainder of sample. 700 uL of Buffer RWT was then added to RNeasy Mini spin column, centrifuged at 10,000 rpm for 15 seconds and flow-through was discarded. 500 uL of Buffer RPE was then pipetted onto RNeasy Mini spin column and again and centrifuged at 10,000 rpm for 15 seconds. The flow-through was discarded and another 500 uL of Buffer RPE was added to RNeasy Mini column, centrifuged at 10,000 rpm for 2 minutes. RNeasy Mini spin column was then places into a new 2 ml collection tube and centrifuged at full speed for 1 minute. The collection tube was discarded with the flow through. Finally, the RNeasy Mini spin column was transferred to a new 1.5 ml collection tube, 40uL of RNase-free water was pipetted directly on the RNeasy Mini spin column membrane and centrifuged for 1 minute at 10,000 rpm to elute the RNA. Quantity measurement and spectrophotometric quality assessment ($A_{260/280}$ and $A_{260/230}$ ratios) of RNA were then carried out using the Nanodrop spectrophotometer.

3.1.2 CDNA Preparation:

Reverse transcription for pancreatic RNA was performed using miScript II RT Kit (Qiagen GmbH, Hilden, Germany). The reverse transcription master mix consisted of 4 uL 5x miScript HiFlex Buffer, 2 uL miScript Nucleic Mix, 2 uL miScript Reverse Transcriptase Mix and 4 uL RNase-free water prepared in 0.2 mL PCR tube, gently mixed and stored on ice. Next, 8 uL template RNA (equal concentrations of 1000 ng/ul for all samples) was added to each tube containing reverse transcription master mix, gently mixed and briefly centrifuged. These tubes were then loaded into Eppendorf mastercycler realplex 4 (Eppendorf, Hauppauge, NY) for reverse transcription process, incubated at the following temperatures; 37˚C for 60 minutes, 95˚C for 5 minutes and kept at 4˚C until retrieve for immediate use for qRT-PCR analysis or transferred to a -20˚C freezer.

Reverse transcription for liver RNA was performed using High Capacity RNA to cDNA Master Mix kit (Applied Biosystems, Carlsbad, CA). Briefly, 20 uL of RT buffer mix, 2 uL of RT enzyme mix, 8 uL of RNA sample (equal concentrations of 1000 ng/ul for all samples) and 10 uL of nuclease-free water were mixed into 0.2 mL PCR tube and centrifuged for few seconds. Prepared samples were then loaded into Eppendorf mastercycler realplex 4 (Eppendorf, Hauppauge, NY) for reverse transcription process with the following temperature setting; 25˚C for 5 minutes, 42˚C for 30 minutes, 85˚C for 5 minutes and kept at 4˚C until retrieve for immediate use for qRT-PCR analysis or transferred to a -20˚C freezer.

3.1.3 MicroRNA microarray:

Microarray analyses were performed at LC Sciences (Houston, TX). Briefly, total RNA was extracted as described above, RNA integrity was determined and all the samples were subjected to Quality control Analysis(QC). After QC RNA samples were enriched for micro RNAs, enriched samples were then labeled with fluorescent dye (C5). Hybridization was performed overnight on a µParaflo microfluidic chip probed with a chemically modified nucleotide coding segment complementary to miRNA transcripts listed in Sanger miRBase.

Multiple quality control steps were incorporated to various stages of assay including multiple sets of control probes were distributed throughout the array. Data normalization was achieved by using cyclic LOWESS (locally weighted regression) method to remove system related variations in the data. ANOVA was performed on signal intensities to evaluate significance of data.

Normalized data was also subjected to Principle component (PCA) multi-variate analysis using SIMCA P+ (Umetrics, San Jose, CA).

3.1.4 Quantitative Real-Time Polymerase Chain Reaction (qPCR) for miRNA expression:

cDNA prepared from pancreatic tissue samples using miScript HiFlex Buffer served as the template for real-time PCR using an miRNA-specific miScript Primer Assay and the miScript SYBR Green PCR Kit (Qiagen, Venlo, Netherlands & Hilden, Germany). Based on microRNA microarray analysis two miRNA mmu-miR- 451a and mmu-miR-23a for PCR validation. Briefly, final reaction volume of 25 uL consisted of 12.5 uL 2x QuantiTect SYBR Green PCR Master Mix, 2.5 uL of 10x miScript Universal

Primer, 2.5 uL 10x miScript Primer Assay, 5.5 uL of RNase-free water and 2 uL of cDNA (equal concentrations of 10ng/ul for all samples). qRT-PCR was carried out on the Eppendorf mastercycler realplex 4 instrument (Eppendorf, Hauppauge, NY) in Mx3000P 96-Well Plates (Agilent Technologies) with the following program; initial denaturing: 95˚C for 15 minutes, 40 repeats of denaturing: 94˚C (15 seconds), annealing: 55 ˚C (30 seconds) and extension : 70˚C (30 seconds). Each miRNA sample was analyzed in triplicate with single NTC. miRNA expression levels in the samples were calculated relative to KPC control (KC) using the comparative C_T method: $\Delta\Delta C_T = \Delta C_T$ *sample - ΔCT control, fold change =* $2\text{-}\Delta\Delta C_T$. Small nuclear RNA, snRNA RNU6B (RNU6-2) was used as PCR control and to normalize the expression values *(*ΔC_T*).*

3.1.5 Quantitative Real-Time Polymerase Chain Reaction (qPCR) for mRNA expression:

Some of the target genes expressions were investigated using RTPCR . In pancreatic tissue we selected Cyclin D1 from cell cycle, MMP9 from metastasis and invasion pathway, BCL2 and Notch 1 from apoptosis and tumor progression. Three genes were tested in common metastasis site in liver, CyclinD1, MMP9 and BCL2. The primer sequence of these genes are listed in Table 4. The final reaction volume of 25 uL consisted of 12.5 uL SYBR Green PCR Master Mix (Applied Biosystems, Warrington, UK), 1 uL of 20 uM reverse and forward primer mixture, 9.5 uL nuclease-free water and 2 uL of cDNA (equal concentrations of 10ng/ul for all samples). qRT-PCR was carried out on the Eppendorf mastercycler realplex 4 instrument (Eppendorf, Hauppauge, NY) in Mx3000P 96-Well Plates (Agilent Technologies) with the following

program; initial denaturing: 95˚C for 10 minutes, 45 repeats of denaturing: 95˚C (15 seconds) and elongation: 60˚C (1 minute), dissociation curve: 95˚C for 1 minute, 60˚C for 30 seconds followed by gradual temperature increase from 60˚C to 95˚C in 20 minutes and finally at 95˚C for 30 seconds. Each group was represented by n=4 samples in pancreas and n=5 samples in liver. Each gene was analyzed in triplicate with single NTC for each sample. mRNA expression levels in the samples were calculated relative to control, isocaloric diet-no chemotherapy group (KC) using the comparative C_T method: $\Delta\Delta C_T = \Delta C_T$ sample - ΔCT control, fold *change* = $2^{-\Delta\Delta C_T}$ β-actin was used to normalized the expression values (ΔC_T).

Primer's Name	Forward Sequence	Reverse Sequence
COX 2	5'-GTCCCTCACCCTCCCAAAAG-3'	5'-GCTGCCTCAACACCTCAACCC-3'
BCl_2	5'-CCTGTGGATGACTGAGTACC-3'	5'-GAGACAGCCAGGAGAAATCA-3'
CyclinD1	5'-CCTCCAGAGGGCTGTCGGCGCAGTAGCAGA-3	5'-TCTTACCTCCAGCATCCAGGTGGCCACGAT-3'
MMP9	5'- GCTCCTGGTCTCCTGGCTT-3'	5'-GTCCCACTTGAGGCCTTTGA-3'
β-Actin	5′-ACCAACTGGGACGACATGGAGAAG-3′	5′-TACGACCAGAGGCATACAGGGACT-3′
NOTCH1	5'-ATTGAAAGCACATATGGAGAT-3'	5'-GTATAAGCATGAAGTGGTCCA-3'

Table 4: Primer sequences used for RTPCR .

3.2 Results and Discussion:

3.2.1 MircoRNA microarray:

Number of MicroRNA in the Garcinol treated group were found to be significantly differently expressed in the microarray data (p value ≤ 0.05) as compared to non-treated KC group (Figure 25) . Most of the miRNA were up or down regulated in the favorable manner based on previous research studies in the field. Many of miRNAs modulated were related to cancer and some of them were found to be directly related to Pancreatic Cancer after search through different databases like miR Base (Manchester, UK) miR2Disease Base(Harbin institute of technology, School Of Medicine, Indiana University) , miRCancer (microRNA Cancer association database) and IPA (Ingenuity Systems Inc, Redwood City, CA).

Table 5 lists miRNAs differently expressed in treated KPC mice groups(KGr, KGm and KGG) compared to untreated group KC (p value ≤ 0.05). The table also includes seed regions of the miRNA, up or down regulation with Garcinol treatment and their relation to cancer, and pancreatic cancer.

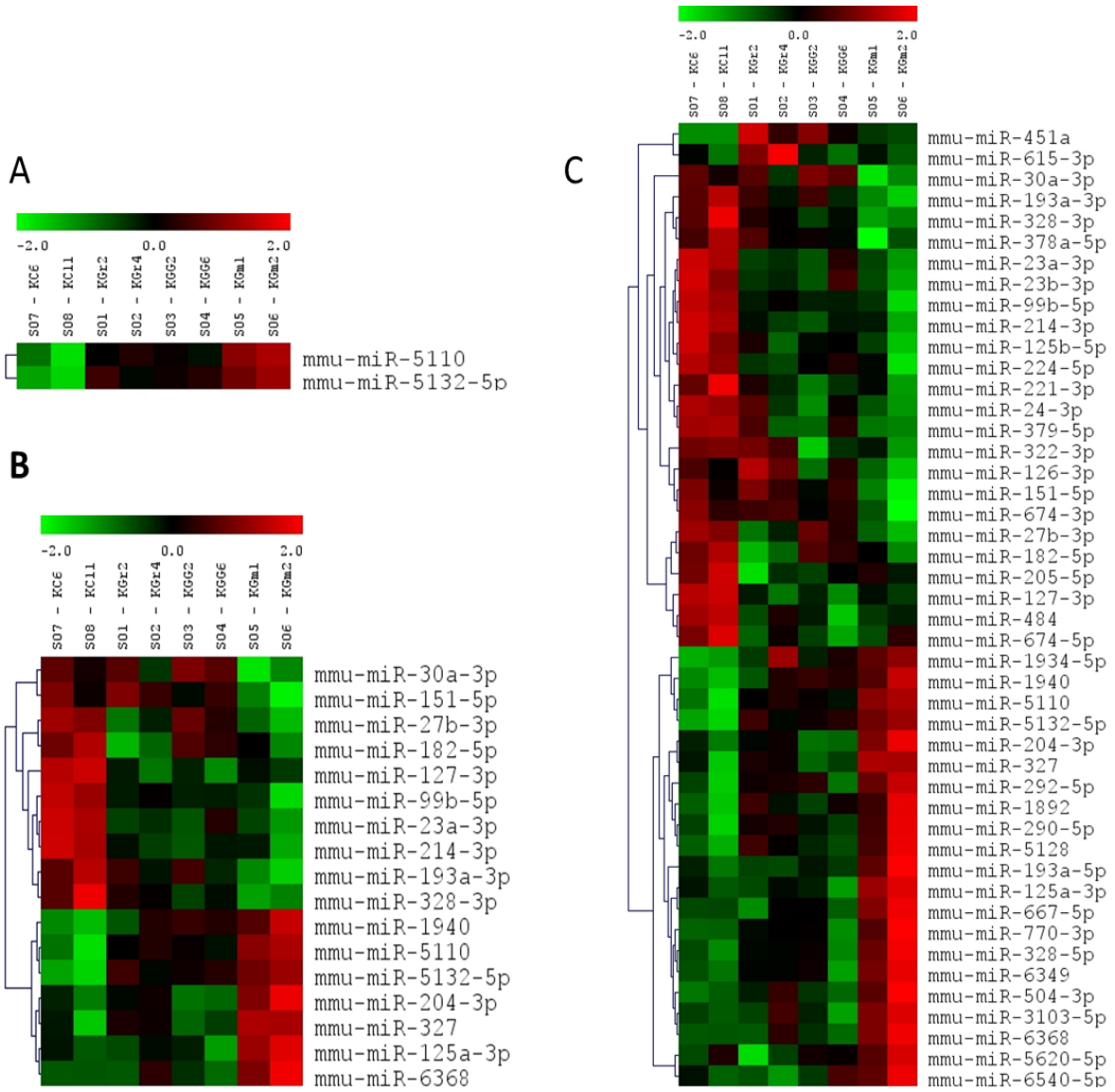

Figure 25: Heat maps and Hierarchical Clustering of miRNA microarray statistical significance < 0.01.

A, represents miRNA differently expressed with statistical significance <0.001. B, represents miRNA differently expressed with statistical significance < 0.05 and C, represents miRNA differently expressed statistical significance <0.1.

MicroRNA	Seed region	Garcinol treated	PaCa link	Cancer link
mmu-miR-23a-3p	AUCACAUUGCCAGGGAUUUCC	↓	Yes ↑	Yes↑
mmu-miR-27b-3p	UUCACAGUGGCUAAGUUCUGC	↓	UNK	Yes↑
mmu-miR-214-3p	ACAGCAGGCACAGACAGGCAGU	↓	Yes ↑	Yes↑↓
mmu-miR-99b-5p	CACCCGUAGAACCGACCUUGCG	↓	Yes ↑↓	Yes↓
mmu-miR-23b-3p	AUCACAUUGCCAGGGAUUACC	↓	Yes ↑	Yes↑↓
mmu-miR-451a	AAACCGUUACCAUUACUGAGUU	↑	Yes ↑↓	Yes ↓
mmu-miR-125b-5p	UCCCUGAGACCCUAACUUGUGA	↓	Yes ↑	Yes↑↓
mmu-miR-125a-5p	UCCCUGAGACCCUUUAACCUGUGA	↓	Yes ↑	Yes ↓
Low signals but Statistically significant p≤0.05				
mmu-miR-5132-5p	GCGUGGGGUGGUGGACUCAGG	↑	UNK	UNK
mmu-miR-6368	CUGGGAAGCAGUGGAGGGGAG	↑	UNK	UNK
mmu-miR-127-3p	UCGGAUCCGUCUGAGCUUGGCU	↓	Yes	Yes ↓
mmu-miR-504-3p	AGGGAGAGCAGGGCAGGGUUUC	↑	UNK	UNK
mmu-miR-328-3p	CUGGCCCUCUCUGCCCUUCCGU	↓	UNK	Yes↑↓
mmu-miR-193a-3p	AACUGGCCUACAAAGUCCCAGU	↑	UNK	Yes↑↓
mmu-miR-667-5p	CGGUGCUGGUGGAGCAGUGAGCACG	↓	UNK	UNK
mmu-miR-224-5p	UAAGUCACUAGUGGUUCCGUU	↓	Yes	Yes ↑
mmu-miR-466m-3p	UACAUACACACAUACACACGCA	↑	UNK	Yes ↑
mmu-miR-327	ACUUGAGGGGCAUGAGGAU	↑	UNK	Yes
mmu-miR-5620-5p	ACGAGGCAGGGGCUUUGACUGUG	↑↓	UNK	UNK
mmu-miR-183-5p	UAUGGCACUGGUAGAAUUCACU	↓	Yes ↑	Yes↑↓
mmu-miR-3100-5p	UUGGGAACGGGGUGUCUUUGGGA	↑	UNK	UNK
mmu-miR-193a-5p	UGGGUCUUUGCGGGCAAGAUGA	↑↓	UNK	Yes↓
mmu-miR-5110	GGAGGAGGUAGAGGGUGGUGGAAUU	↑	UNK	UNK
mmu-miR-378a-5p	CUCCUGACUCCAGGUCCUGUGU	↑↓	UNK	Yes↑↓
mmu-miR-204-3p	GCUGGGAAGGCAAAGGGACGU	↑	UNK	Yes↑↓
mmu-miR-770-3p	CGUGGGCCUGACGUGGAGCUGG	↑	UNK	Yes ↓
mmu-miR-30a-3p	CUUUCAGUCGGAUGUUUGCAGC	↓	Yes	Yes↑↓
mmu-miR-1940	AUGGAGGACUGAGAAGGUGGAGCAGUU	↑	UNK	Yes↑
mmu-miR-674-5p	GCACUGAGAUGGGAGUGGUGUA	↑	UNK	Yes↑
mmu-miR-5128	CAAUUGGGGCUGGCGAGAUGGCU	↑	UNK	UNK
mmu-miR-182-5p	UUUGGCAAUGGUAGAACUCACACCG	↓	Yes	Yes↑
mmu-miR-151-5p	UCGAGGAGCUCACAGUCUAGU	↓	UNK	Yes↑↓
mmu-miR-125a-3p	ACAGGUGAGGUUCUUGGGAGCC	↑	UNK	Yes ↓

Table 5 : MicroRNA differently(p≤ 0.05) expressed in Treated (KGr, KGm and KGG) compared to Untreated KPC mice[55, 56]. ↑= up regulated, ↓= down regulated, UNK= unknown.

3.2.2 Principle Component Analysis of microRNA Microarray data:

In order to investigate the complete miRNA profiles and observe the differences between treatment and non-treated groups we uploaded our whole miRNA data to SIMCA P+ 13 software for multivariate analysis. Principle component Analysis is unsupervised multivariate analysis which compresses large data sets into 2-3 principle components. Based on the differences in these variables, each group was assigned a point on the score plot. The separation between the groups represents differences in microRNAs (variables). Score plot of the model with Untreated group (KC) compared to Garcinol group (KGr) showed clear separation between the two groups. The corresponding loading plot points toward the microRNAs responsible for this separation Figure 26 and 27.

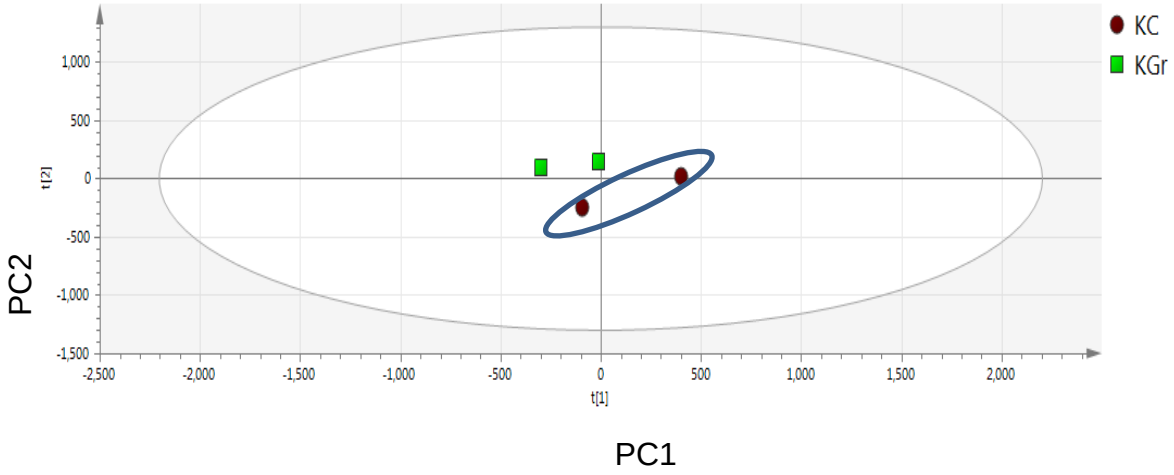

Figure 26: PCA Score plot comparing microRNA profiles of KC and KGr group (pvalue < 0.05).

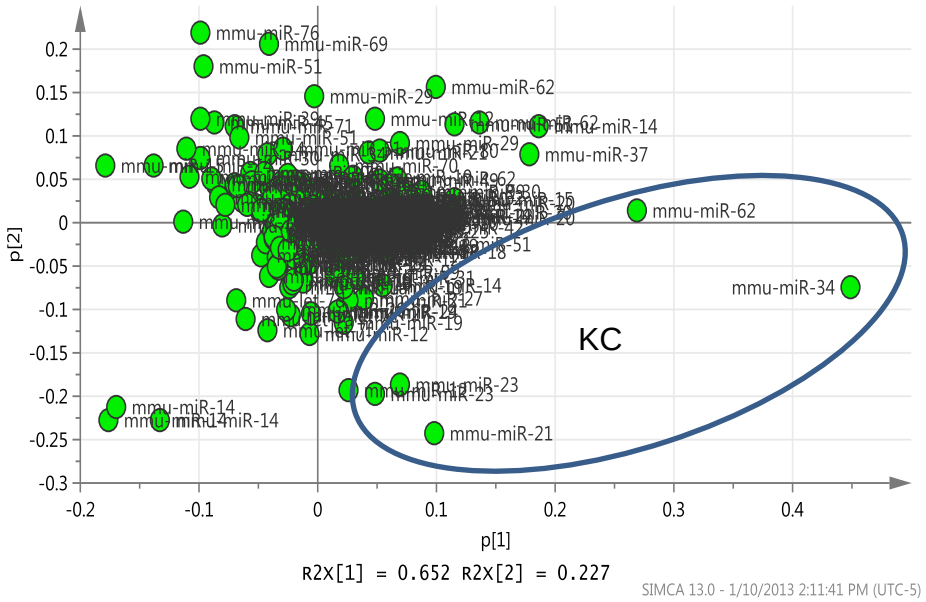

Figure 27: Loading plot of model comparing KC with KGr group showed miRNA responsible for separation of the two group.

Loading plot of the model comparing KC group with KGr group (Figure 27) clearly indicate that miRNA 21, miRNA 23 and miR 34 are responsible for KC score's and location and separation from KGr. These miRNA are reported to be tumor promoter miRNA by several studies and microRNA data bases [55, 56].

In order to compare and to further investigate, we added a positive control group (gemcitabine responders) KGm to this model. The score plot after addition of gemcitabine responders, indicate that the separation of KGr is in the direction of Gemcitabine treated mice. The score plot can also be predictive of response to Gemcitabine and Garcinol. We can see that one Gemcitabine responder responded more to the treatment compared to the other, as implicated by the distance of separation from KC group Figure 28.

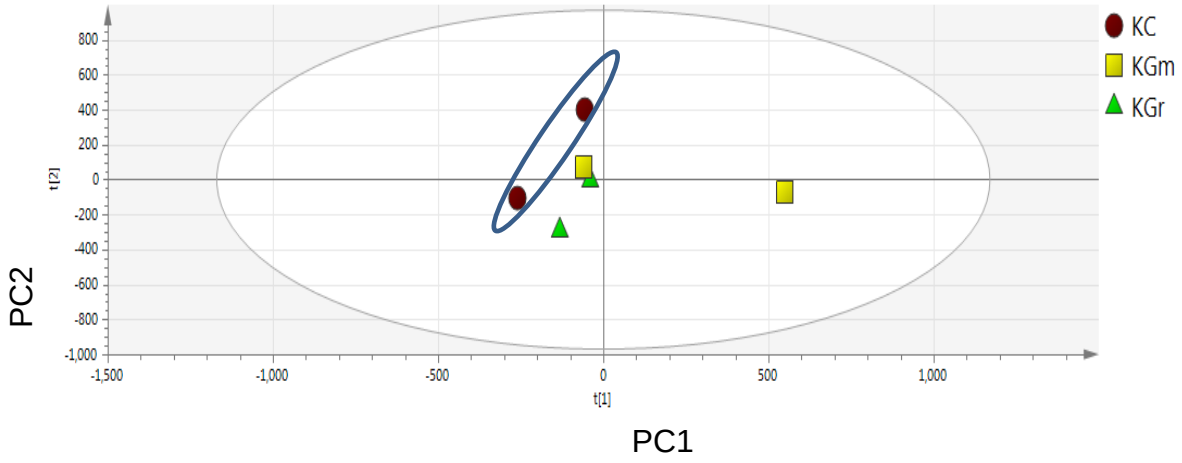

Figure 28: PCA Score plot comparing microRNA profiles of KC, KGr and KGm (responder) groups.

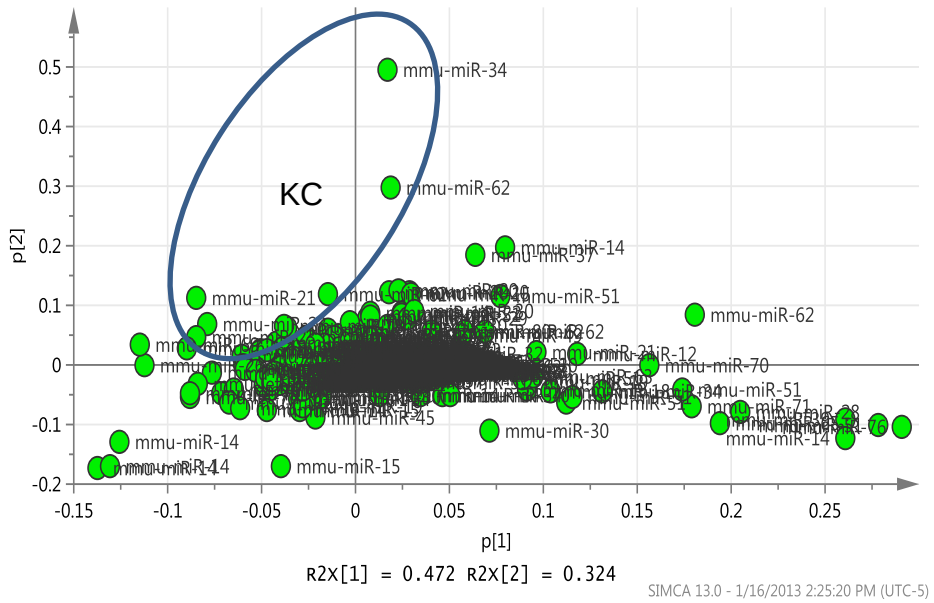

Figure 29: Loading plot of the model comparing KC with KGr and KGM (responder) groups clearly showed miRNA responsible for separation of the KC group.

Loading plot of the model with three groups (KC, KGr and KGm) Figure 29 again pointed towards miRNA 21, miRNA 23 and miR34 responsible for separation of un-treated KPC mice KC group from treated (KGm and KGr) groups. In order to specifically look at the effect Garcinol on the whole miRNA profile, we plotted contribution plots of Garcinol points in the score plot (Figure 28).

The contribution plot gives us the information about the variable contributions (microRNA) and their values for assigning certain location or locations in the score plot. We can have contribution plot for one point and compare it to rest to see contributions of that point , or we can have contribution plot of the whole group by selecting all the score points from that group. We looked at the contributions of the whole KGr group. The Contribution plot (Figure 30) indicated that positions of Garcinol scores on the score plot were due to high values of many tumor suppressor miRNA and low values of many tumor promotor miRNA labeled on the plot (Figure 30). Some of the tumor suppressor miRNA found to have high values include miR 451a,miR 126-3p, mir5126, miR149-3p, miR338,miR142 and miR29-3p. Tumor promotor miRNA with low values includes miR23, miR243, miR27a, miR let 7, miR 21a-5p and miR341-5p and miR19b-3p. Many of these miRNA were found statistically significant by ANOVA on Microarray data validating this approach. Additionally it pointed out some miRNA responsible for separation of complete miRNA profiles on score plot which were not statistically significant but contributing in favorable manner as a group. This technique can be quite useful with intervention studies where we have responders, non- responders to the drug and also have variation in the data due to individual's response to the drug.

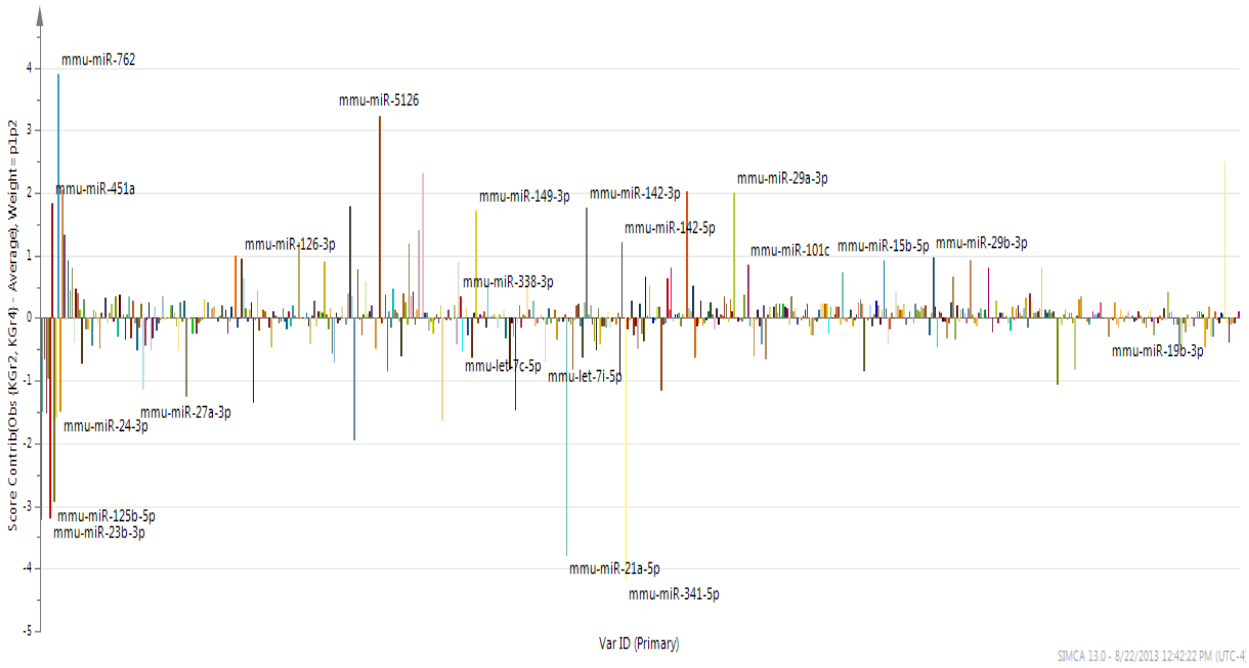

Figure 30: Contribution plot of KGr group explaining variables.

3.2.3 mmu-miR 23a-3p:

MicroRNA 23a was found to be down regulated in Garcinol treated groups compared to KC group (p value ≤ 0.05). This miRNA belongs to miR-130, miR-23 and miR-23c family, it is located in the cytoplasm and is functional as mature miRNA. It is considered to be an oncogenic miRNA, as it plays an important role in cell proliferation and growth. MicroRNA mmu-miR-23a was found to be down regulated with Garcinol treatment (KGr and KGG) compared to untreated KC group (p value ≤ 0.02).

This miRNA was shown to be up regulated in several Gastrointestinal tract Cancers including pancreatic cancer [53]. MicroRNA 23a is also reported to be up regulated in lung cancer, endometrial cancer, uterine cancer, hepatocellular carcinoma, melanoma and nasopharyngeal cancer. This microRNA is also deregulated in other diseases including non -insulin dependent diabetes mellitus, cardiac fibrosis and endometrial carcinoma (IPA, Ingenuity Systems Inc, Redwood City, CA).

Important targets for this microRNA includes IL6, FBX032 and TRIM63. In addition it also binds to HES1, MDH2, ATAT1, LMNB1, SEPT3, SMAD5, SMAD3 & SMAD4.

It can be regulated by multiple drugs like isoproterenol, decitabine, trichostatin A, medroxyprogesterone acetate, beta-estradiol, androgen, 5-fluorouracil and proteins like PASMC cells, AGO2, EPHB6, DIC ER1, SPI1, TNFSF12, E2F3, E2F2 (miRBase [57], DIANA[58] & IPA, Ingenuity Systems Inc, Redwood City, CA).

3.2.4 miR-23a~27a~24-2 cluster:

As many miRNA also exists in clusters and miR 23a is one of them. It is some time observed to coexist as miR-23a~27a~24-2 cluster located at chromosome 8 . These clusters are evolutionary conserved. Based on data from multiple research studies it can take part in cell proliferation, differentiation and hematopoiesis together [59]. This cluster can target Wnt signaling pathway, MAPK pathway, TGF-beta signaling pathway, T cell receptor pathway, and Insulin signaling pathway, cytoskeletal rho/GTPase pathway. This cluster can alter Wnt signaling pathway through different target genes including APC,PP2A, CCND1[59].

In another study miR 23a regulated MTSS1 metastasis suppressor gene and miR27a Targeted Ubiquitin ligase FBXW7 in colorectal carcinoma cell line , consistent with the proposed role of miR23a as promotor of migration and invasion and miR 27 in proliferation[60]. MicroRNA 23a is up regulated in intestinal adenocarcinoma at the stage where they change from preinvasive to locally invasive stage where as miR27 is normally up regulated in invasive and metastatic colorectal cancer[60].

In our study microRNA microarray data showed down regulation of miR23(p value ≤0.02) , miR 27 (p value≤ 0.02) and miR24 (p value≤ 0.08). Further exploration of this cluster's target genes is warranted to understand the mechanisms and molecular pathways involved in this pancreatic cancer mouse model. In a recent study from our lab we have noticed down regulation of miR23a in Garcinol treated pancreatic cancer cell lines. Data from this invivo study supported our invitro findings and points towards possible relationship between Garcinol treatment and miRNA 23a.

3.2.5 mmu-miR451a:

MicroRNA 451a was up regulated (p value ≤ 0.05) in Garcinol treated mice (KGr and KGG) this response was not observed in Gemcitabine responders (KGm) in microarray data.

miRNA- 451 is cytoplasmic miRNA and functionally active in its mature form. Its gene is located on chromosome 17, 100bp downstream of miR-144 gene[61]. According to the recent literature this microRNA behaves as tumor suppressor in several cancer types. It is found to be one of the most stable miRNA and can be secreted into blood in exosome affecting distant sites of its release location [62]. MicroRNA 451 is conserved among vertebrates. Processing of miR 451 is little different than canonical miRNA pathway as it bypass Drosha- mediated processing step [61].

It is reported to be involved in reducing tumor invasiveness, apoptosis and arresting at Go/G1 phase. Links to several cancers have been reported especially colorectal cancer, gastric cancer, lung cancer, renal cancer, acute lymphoblastic leukemia and breast cancer. Some other disease where this microRNA was shown to be involved are fatty liver, hyperglycemia with or without diabetes mellitus and myelodysplastic syndrome.

Most common targets for miR 451 are CKND1B, CCND1, ABC B1, MMP9, BCL2 2 AKT1 and MMP 2. The expression of miRNA 451 gene can be regulated by monocrotaline, acetoaminophen, proteins EPHB6 and AGO2. It can also bind to AKTIP, MIF and FBX033 genes (miRBase [57], DIANA[58] & IPA, Ingenuity Systems Inc, Redwood City, CA). Notch 1 was also reported to be regulating levels of miR451 in

T cell acute lymphoblastic leukemia, when intracellular notch 1 was induced it led to down regulation of miR451 along with miR 709[63].

In a study conducted on colorectal cancer stem cell to identify markers for self-renewal of cancer stem cells and drug resistance it was pointed out that miR 451 plays a major role in both of these pathways[64]. After transfection with miR 451 reduced number of colon spheres formation was observed, along with growth arrest and sensitization to drug Irinecan metabolite in vivo. They also investigated Cycloxygenase-2(COX2) and Wnt signaling pathway as possible mechanisms of these effects.

Additionally miRNA 451 can also act as biomarker for several cancers due to its stability and presence in blood and other fluids. In recent studies healthy Gastric tissue was shown to have higher concentration as compared to lower concentrations reported in gastric cancer, likewise lower levels of miR451 about 170.9 fold reduction was reported in non-small cell carcinoma[61]. In some of the recent studies specially in formalin fixed paraffin-embedded (FFPE) cell blocks they have reported higher levels of preserved mi451 levels as compared to other miRNAs in gastric cancer and Pancreatic cancer FFPE blocks [61, 65].

Furthermore miR451 can also be used in cancer therapy to overcome drug resistance and can be predictive of overall cancer survival as seen in Non-small cell lung cancer patients. Patients with down regulation of miR451 were related to less differentiation of tumors , late stage disease and lymph node metastasis [61].

3.2.6 RTPCR Validation of miRNA 23a and miR451:

In order to validate our microarray data we selected microRNA 23a and microRNA 451 for real time reverse transcriptase polymerase chain reaction (RTPCR)

gene expression analysis. As miR23a was found to be down regulated and miR 451 was up regulated looking at the expression profiles of these miRNA clearly supported microarray findings. MicroRNA 23a was found to down regulated in KGr and KGm responders groups (Figure 31). Expression of miRNA 451a was up regulated only in Garcinol treated groups (KGr and KGG) Figure 32 compared to KC and KGm group.

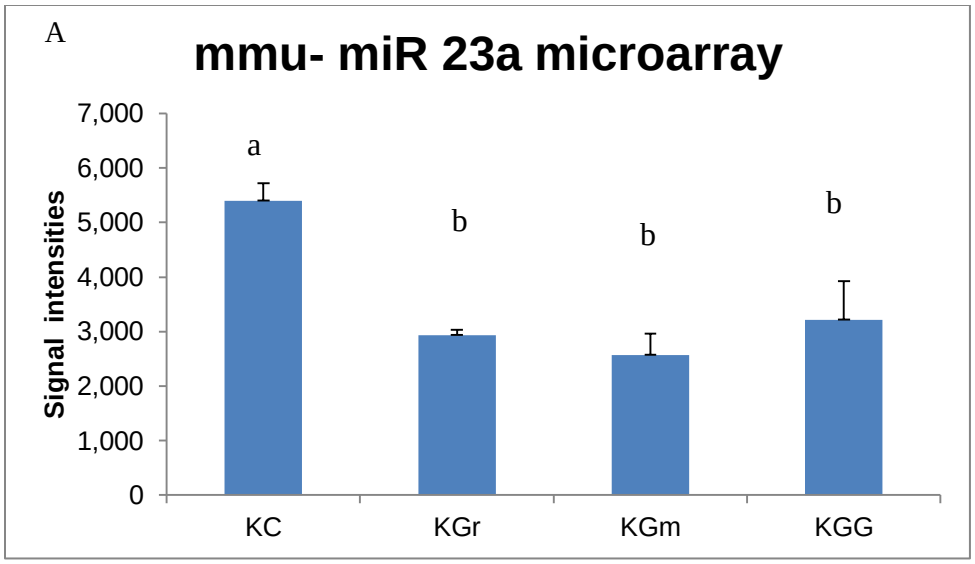

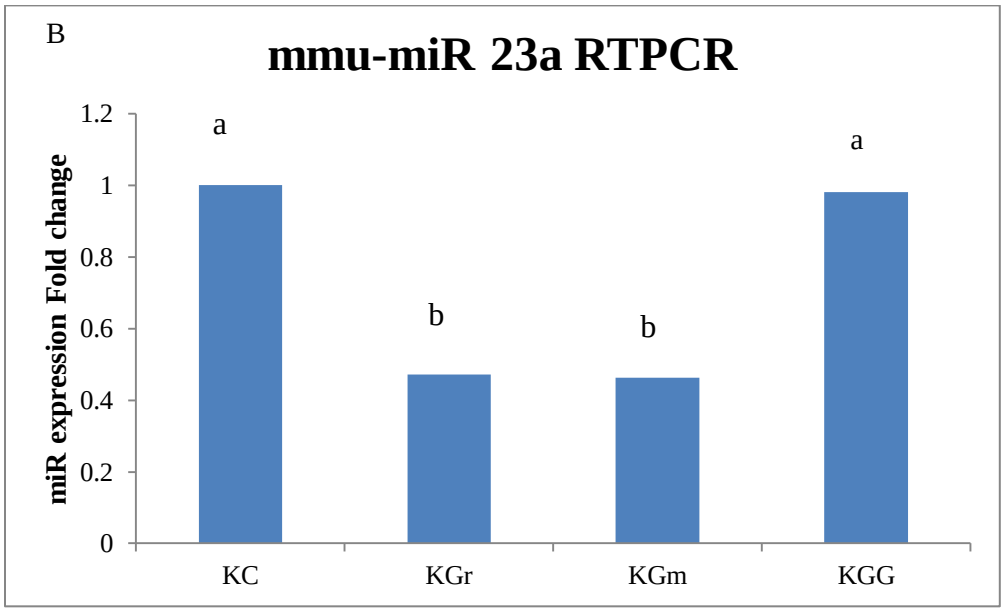

Figure 31: MicroRNA 23a levels by microarray and RTPCR. A, miRNA 23a microarray levels were found to be lower in KGr, KGm responder and KGG ('a' is significantly different to 'b' pvalue ≤ 0.05) Error bars represents ± mean standard deviation. B, miRNA 23a expressions RTPCR were down regulated in KGr and KGm responder (less than 0.5 fold compared to KC). KGr and KGm were significant based on t-test ('a' is significantly different from 'b' p value ≤ 0.05)

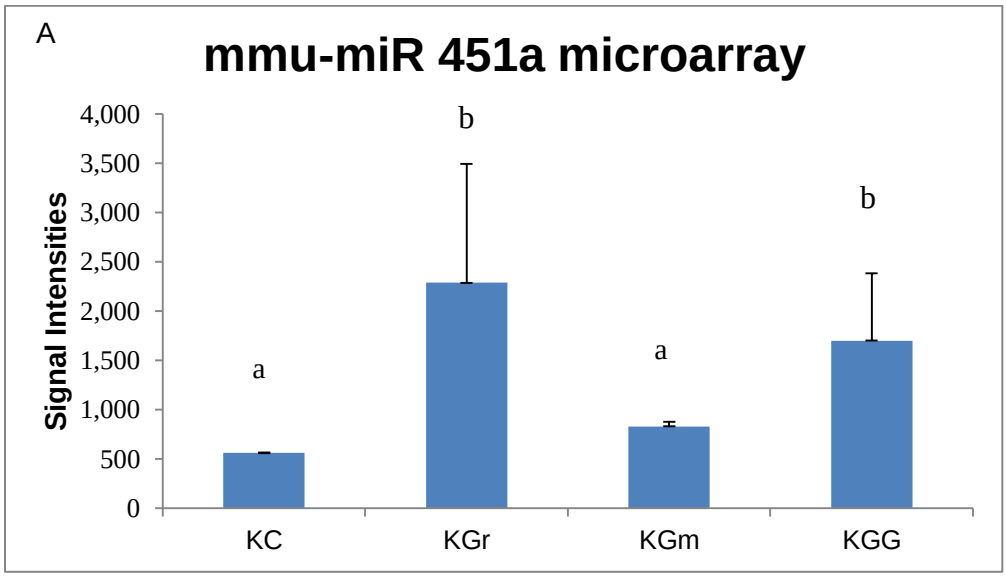

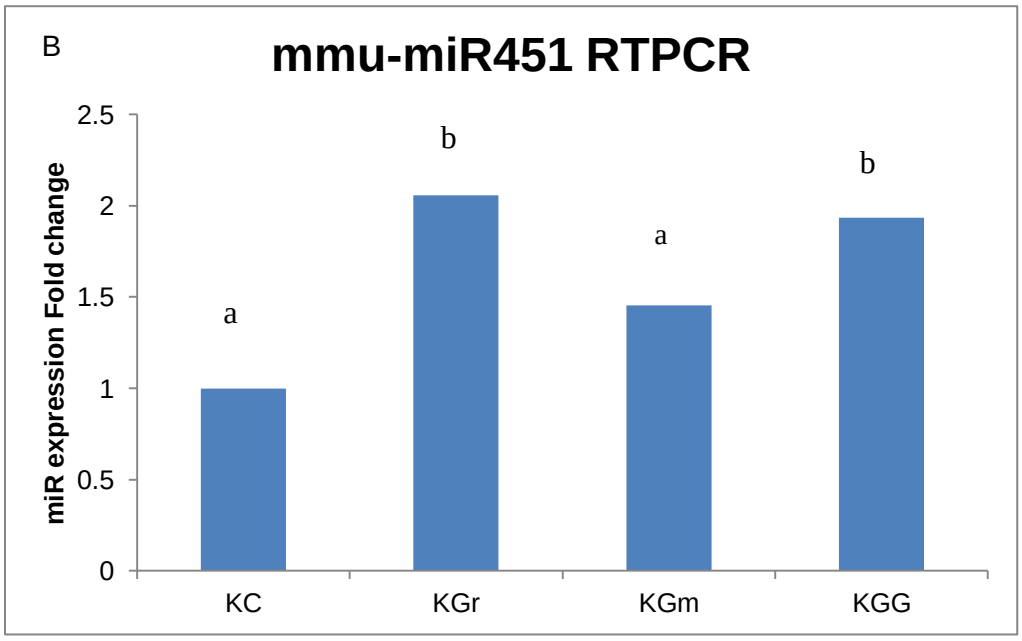

Figure 32: MicroRNA 451a levels by microarray and RTPCR. A, miRNA 451 levels were found to be higher in KGr and KGG ('a' is significantly different to 'b' pvalue ≤ 0.05). Error bars represent ± mean standard deviation. B, miRNA 451a expressions were up regulated in KGr and KGG (almost 2 fold compared to KC). KGr and KGG were significant based on t-test ('a' is significantly different from 'b' p value ≤ 0.05)

Pancreatic mRNA expression levels of some of target genes by RT PCR:

Four target genes from miRNA found to be differently expressed with Garcinol treatment were selected for investigation in pancreatic tissue. These four genes were Matrix metalloproteinase 9 (MMP9), Cyclin D1, B-cell lymphoma 2 (Bcl2) and Notch 1. These genes belongs to four different pathways of tumorogenesis and are considered as tumor promotor genes.

3.2.7 Matrix metalloproteinase-9 (MMP9):

Pancreatic mRNA expressions of MMP-9 gene were found to be significantly decreased in Garcinol (KGr) and Gemcitabine plus Garcinol (KGG) group compared to non-treated KC group(fold change). Interestingly Garcinol groups (KGr and KGG significant based on ttest pvalue <0.05) showed lower MMP 9 levels compared to KGm group due to KGm responders and non-responders the average for KGm was even higher than KC. The combination group KGG showed the lowest levels of MMP9 among all groups (Figure 33).

MMP9 belongs to matrix metalloproteinases (MMPs) family they are Zinc – dependent endopeptidases can also be called as matrixins. Involvement of metaloproteinases in tumor metastasis is been investigated in many studies. They have shown to increase angiogenesis, enhance invasion and aid secondary tumors growth at metastatic sites[66]. In this Family of proteins, MMP9 has been repeatedly reported to be involved in angiogenesis and invasion. High levels of serum MMP 9 was reported to be linked with proliferation, metastasis and poor survival in melanoma patients. In another study MMP9 serum and plasma levels were related to metastasis of rat

mammary tumors[66]. Additionally it can be a marker of invasiveness, as higher MMP 9 expressions were shown to be related to chemically induced skin tumors specially invasive carcinoma[66]. High expression of MMP 9 was also associated with lymph node metastasis of ovarian carcinoma cells[67]. Additionally higher MMP 9 expression was related to poor prognosis in breast cancer patients[67]. Lower expressions of MMP9 in Garcinol groups can be indicative of lower invasiveness of pancreatic cancer in these mice.

Lower expressions of MMP 9 levels in this study correlates with the invitro data from our lab in Pancreatic cancer cell line with Garcinol treatment. Gemcitabine only had 10-15% response based on our MRI data but the combination of Gemcitabine and Garcinol had lower MMP9 expressions as a group (more consistent).

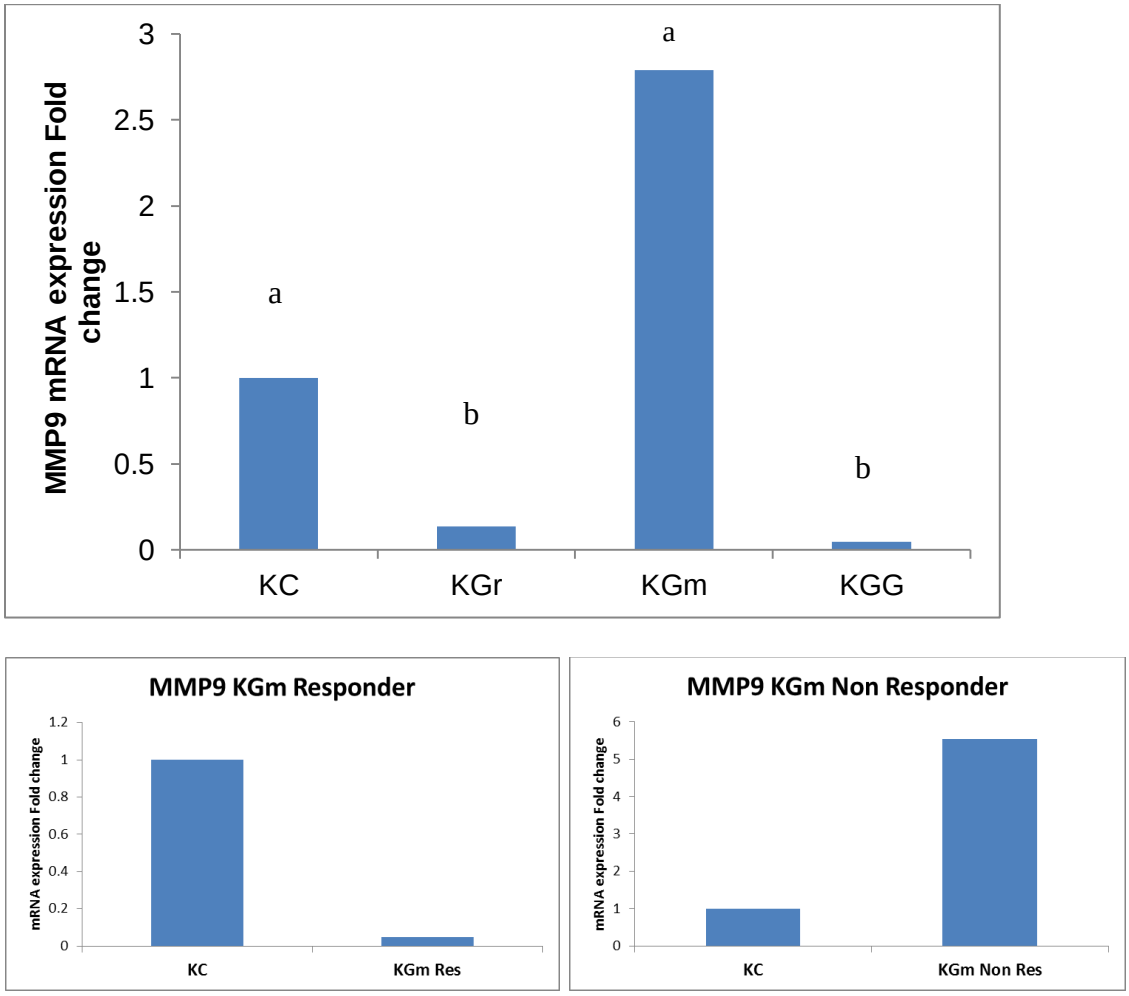

Figure 33: RTPCR mRNA expression of MMP 9 in KC, KGr, KGm and KGG groups. KGr and KGG had lower expression relative to KC (less than 0.5 fold). Fold change was calculated by 2-ΔΔCT method. β-actin was used as house-keeping gene to normalize CT values. KGr and KGG statistically significant (t-test- 'a' is significantly different from 'b' p value < 0.05). MMP9 expressions were very different in KGm responder and Non responder (not significant)..

3.2.8 Cyclin D1 (CCND1):

Relative mRNA expression of CCND1 gene in pancreatic tissue samples indicate lower expression levels for KGr, KGm and KGG groups compared to non- treated KC group. Additionally dietary Garcinol (KGr and KGG groups) was found to be more effective in reducing CCND1 levels in comparison to Gemcitabine treatment (KGm group) Figure 34.

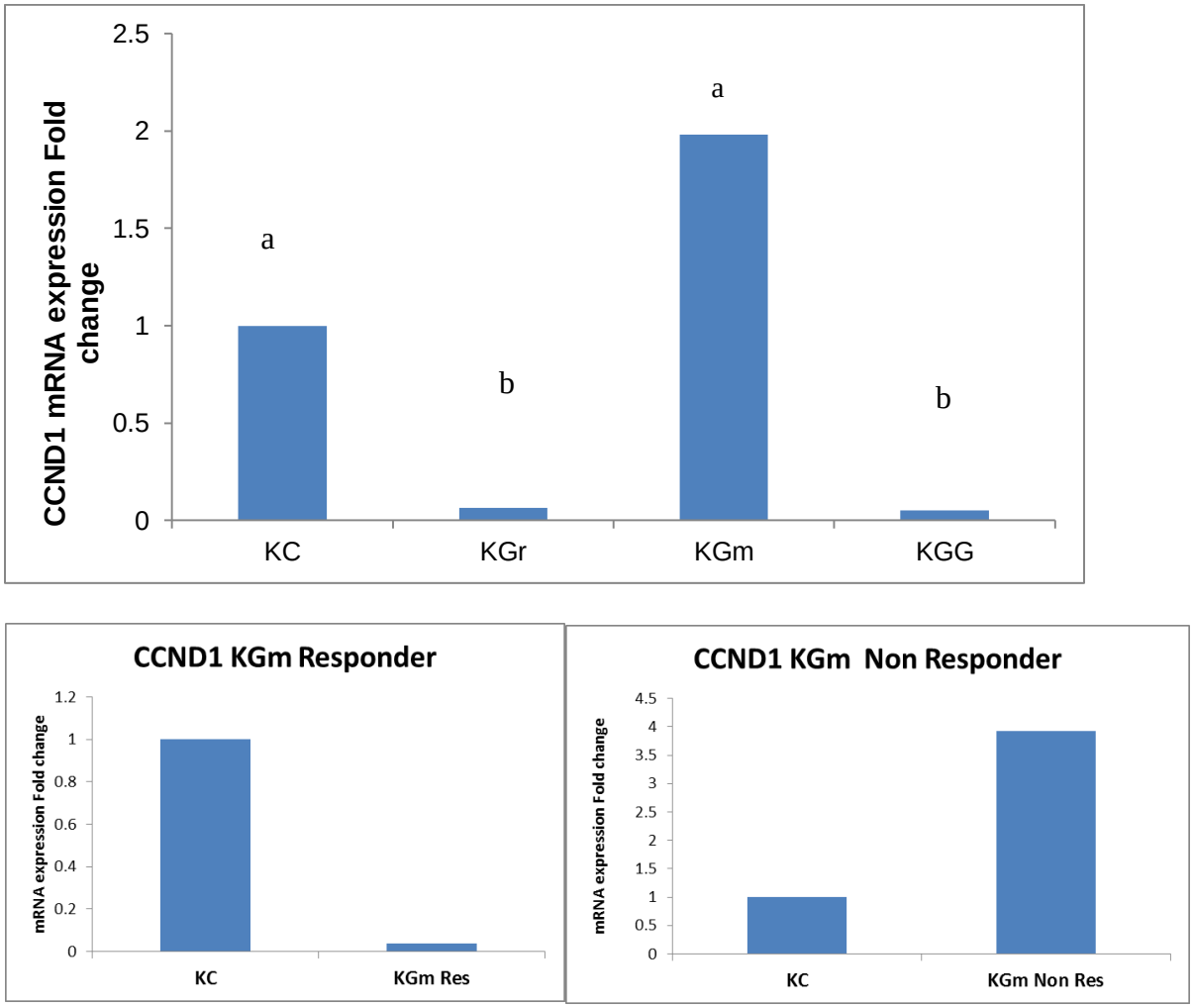

Figure 34: RTPCR mRNA expression of CCND1 in KC, KGr, KGm and KGG groups. KGr and KGG had lower expression relative to KC (less than 0.5 fold). Fold change was calculated by 2-ΔΔCT method. β-actin was used as house-keeping gene to normalize CT values, KGr and KGG significantly different from KC (t-test - 'a' is significantly different from 'b' p value < 0.05). KGm responder and non-responder had very different mRNA expressions (not significant).

Cyclin D1 is a cell cycle gene involve in progression through the G1-S phase, it phosphorylates retinoblastoma gene (Rb) promoting cell proliferation. Up regulation of CCND1 gene is observed in many cancers[68]. It belongs to cyclin Family members of which is phosphorylated by cyclin dependent kinases CDK. Beside its function in cell cycle, it also act as regulator of transcription factors and other coactivators and corepressors. These factors can lead to histone acetylation and chromatin remodeling[68]. It is also reported to be involved in cell differentiation, migration and metabolism[68]. Overexpression of CCND1 is shown to be related to gene amplification and deregulation at post translational level [69]. Our non- treated group showed higher levels of CCND1 and these levels are were significantly reduced after Garcinol treatment. CCND1 can be regulated by miRNA 451a and miRNA 23a. As reported by earlier studies, overexpression of CCND1 is not solely due to genetic reasons, epigenetic regulation also plays important role, further investigation with miRNA mimics and inhibitors can provide valuable information. We saw the similar response as MMP9 in CCND1 with Gemcitabine and Garcinol treatment, as the Garcinol treated groups were more consistent in lowering CCND1 levels.

3.2.9 B-cell lymphoma-2 (Bcl2):

RTPCR mRNA expression profile shows no significant fold change in treated groups (KGr, KGm and KGG) compared to non-treated group (KC) Figure 35. Bcl2 belongs to Bcl family of proteins these proteins can be pro apoptotic or antiapoptotic [70] . Bcl2 is particularly is an antiapoptotic protein involved in Bax dependent mitochondrial apoptotic pathway. Bcl 2 is documented to be overexpressed various

cancers[71].. Bcl2 blocks the release of cytochrome C from mitochondria resulting in disruption of caspase dependent apoptosis [72].

Bcl2 can be regulated by miR 451a (Gene View, IPA , Ingenuity Systems Inc, Redwood City, CA) but results from pancreatic tissue were expected as our model was p53 conditional mutant in pancreas. Protein p53 acts as check and regulator of Bcl2 through Puma and noxa [73]. Furthermore p53 induce Bax, an pro apoptotic protein which minimize the effects of Bcl2 on apoptosis[73]. This is the reason why Bcl2 vs. bax ratio actually gives the complete picture of effects Bcl2 on apoptosis. In addition to this, in case of crises like situations, in most tumor environment p53 can directly repress Bcl2 as Bcl2 promotor has p53 negative response element[73]. We can assume that high levels of Bcl2 could be due to lack of p53 in the pancreatic tissue.

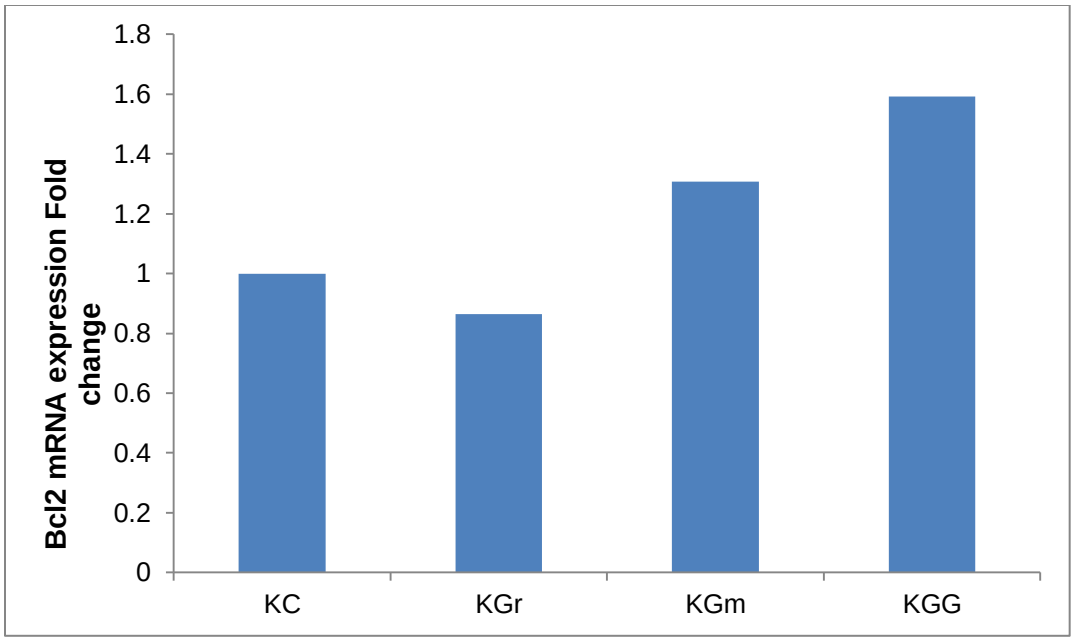

Figure 35: RTPCR mRNA expression of Bcl 2 in KC, KGr, KGm and KGG groups. There was no significant change observed among all the groups. Fold change was calculated by 2-ΔΔCT method. β-actin was used as house-keeping gene to normalize CT values (t-test - p value > 0.05).

3.2.10 Notch1:

Relative expression of mRNA RTPCR analysis with Notch1 genes showed significant down regulation of Notch1 in both Garcinol treated groups (KGr and KGG) in comparison to non-treated KC group. Garcinol treatment showed reduction of Notch1 mRNA profile when compared to KGm (Gemcitabine).also. Surprisingly Garcinol alone had lowest values among all the groups (Figure 36). KGr and KGG showed more consistent values compared to KGm which had clear responders and non- responders and the average of the group showed higher expression compared to KC, when we separated responders and non-responders, we were able to the response of Gemcitabine in KGm group on Notch1 mRNA levels.

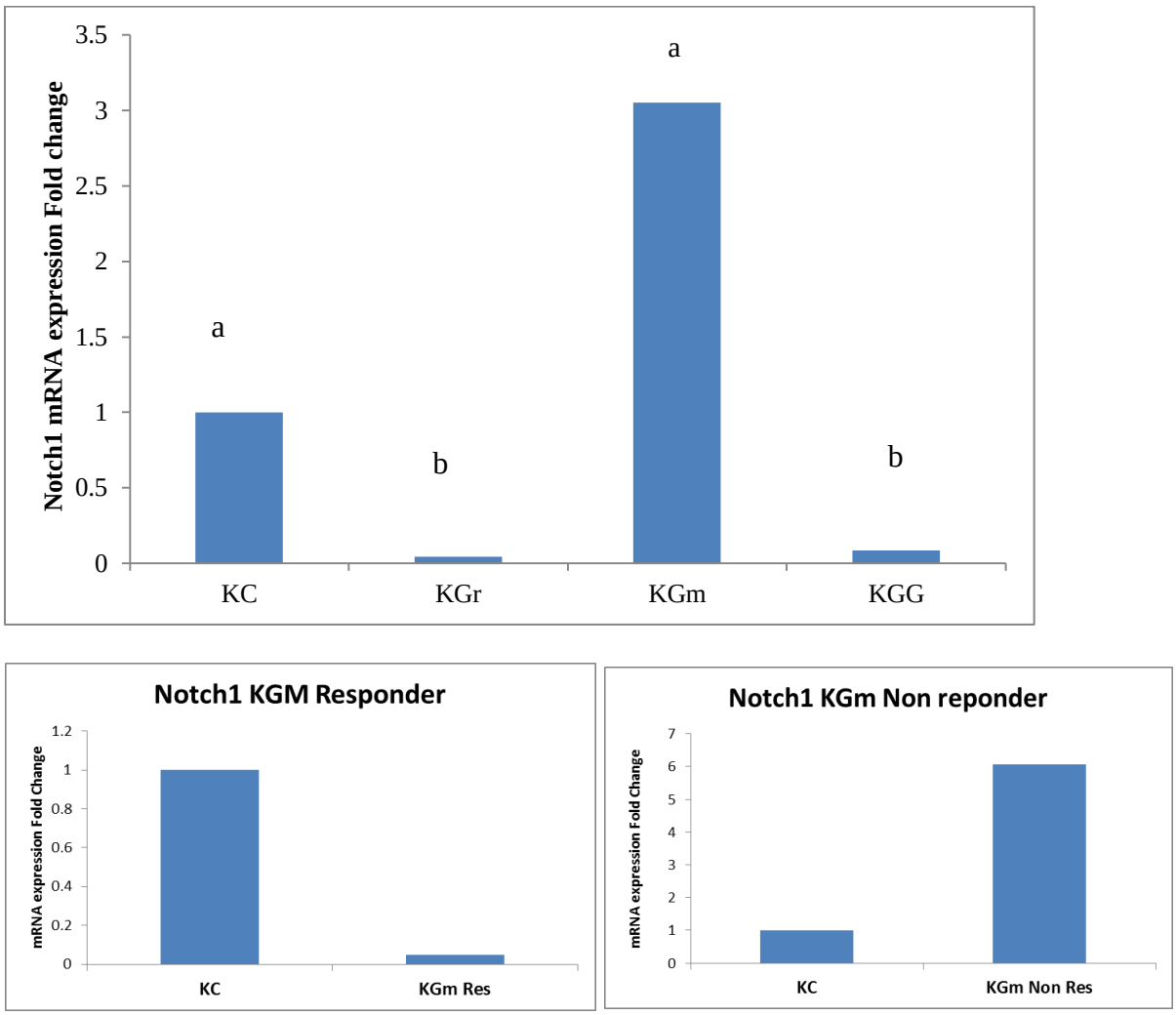

Figure 36: RTPCR mRNA expression of Notch 1 in KC, KGr, KGm and KGG groups. KGr and KGG had lower expression compared to KC (less than 0.5 fold). Fold change was calculated by 2-ΔΔCT method. β-actin was used as house-keeping gene to normalize CT values. KGr and KGG were significantly different from KC (t-test - 'a' is significantly different from 'b' p value < 0.05).

Activation of Notch1 is reported in multiple cancers. Although the mechanistic targets and molecular mechanisms are still under investigation, it plays a critical role in tumor proliferation [63] . Notch signaling is dependent upon its interaction with family of ligands leading to activation of these proteins[74]. Upon activation, the cleaved Notch enters the nucleus. This cleaved Notch along with transcription factors can regulate gene expression of target genes. Notch is also reported to be involved in cellular differentiation and its dysfunction can leads to tumor progression. Notch1 can also regulate and inhibit apoptosis through its interaction with NFkB and other related factors [75]. In a recent study a link between miRNA 451 suppression after induction of intracellular Notch1 had been investigated. They have reported that Notch 1 overexpression can degrade tumor suppressor E2a which is responsible for transcriptional activation of microRNA 451 and microRNA 709. Activation of miR451 and miR 709 are responsible for suppression of Myc, Akt and Ras-GRF1 (reported oncogenes)[63]. Our investigation of Notch1 leads to a possibility that Notch1 overexpression in KC mice might have a correlation with lower miRNA 451 levels. Treatment with Garcinol have shown to decrease Notch1 levels along with up regulation of miR451.

3.2.11 Liver mRNA expression levels of some of target genes by RT PCR:

In order to investigate the mRNA expression profiles of target genes at one of the common metastatic site we selected liver. Liver is one of the first organ where Pancreatic ductal adenocarcinoma metastasize.

3.2.12 Liver CCND1 mRNA expression:

Liver CCND1 mRNA expression showed significant reduction in All treated groups (KGr, KGm and KGG) compared to non-treated KC group. KGG group shows lowest expression among all three treated groups Figure 37. Lower levels of cyclin D1 can be representative of lower metastasis proliferation in treated groups. Liver CCND1 profile correlate with pancreatic CCND1 mRNA profiles from Garcinol treated mice supporting the anti-cancer effect of Garcinol.

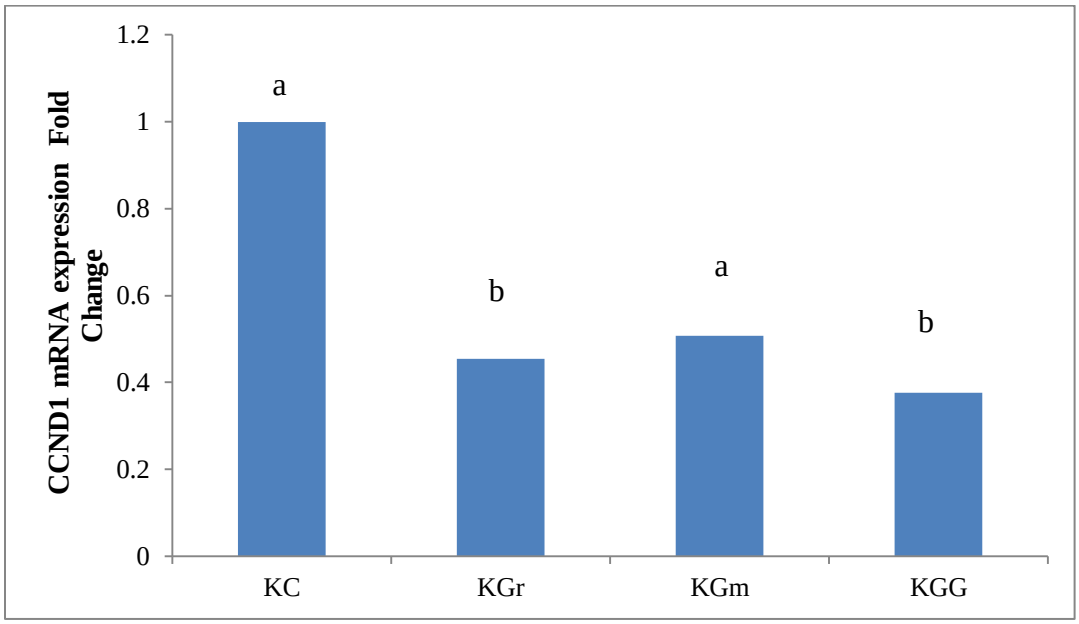

Figure 37: Liver RTPCR mRNA expression of CCND1 gene in KC, KGr, KGm and KGG groups. KGr, KGm and KGG had lower expression relative to KC (less than 0.5 fold). Fold change was calculated by 2-ΔΔCT method. β-actin was used as house-keeping gene to normalize CT values. KGr and KGG were significantly different from KC (t-test - 'a' is significantly different from 'b' p value < 0.05)

3.2.13 Liver MMP9 mRNA expression :

Liver MMP9 mRNA profiles from Garcinol treated groups (KGr and KGG) showed significant reduction relative to non- treated KC group. KGm group showed trend of reduction in mRNA expression but was not significant (more than 0.5 fold) Figure 38. Liver MMP9 mRNA expression profiles correlate with pancreatic mRNA levels and both showed significant reduction with dietary Garcinol treatment.

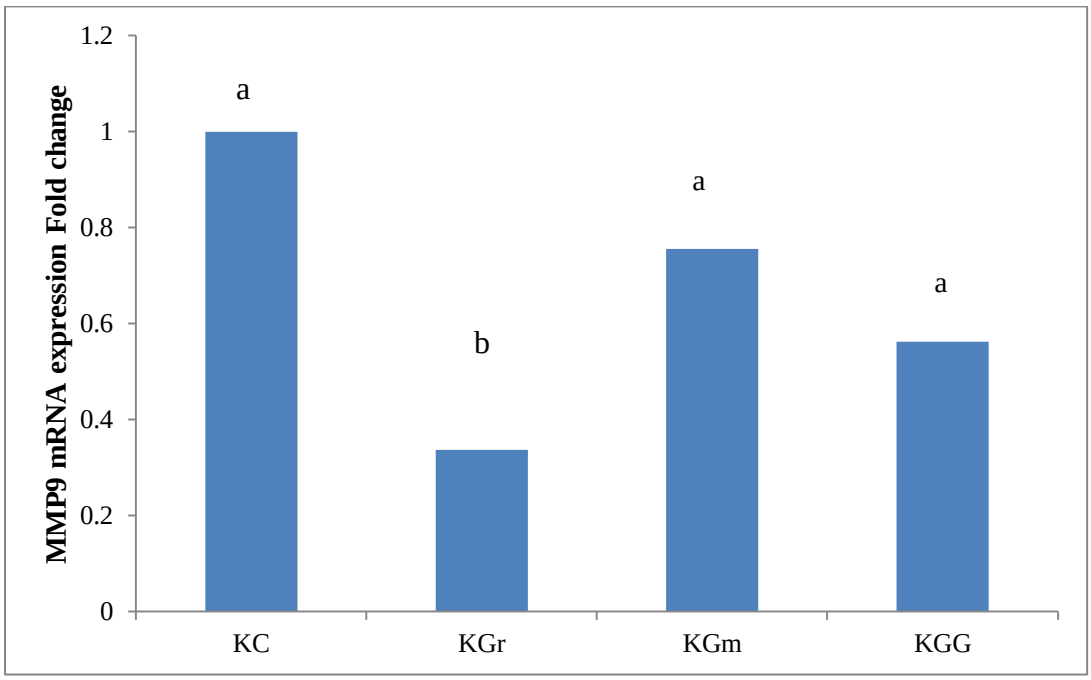

Figure 38: Liver RTPCR mRNA expression of MMP9 in KC, KGr, KGm and KGG groups. KGr and KGG had lower expression compared to KC (less than 0.5 fold).KGm showed lower expression trend but not significant. Fold change was calculated by 2-ΔΔCT method. β-actin was used as house-keeping gene to normalize CT values. KGr was significantly different from KC (t-test - 'a' is significantly different from 'b' p value < 0.05)

3.2.14 Liver Bcl2 mRNA expression :

Relative expressions of Bcl2 gene compared to KC group in liver tissue showed significant reduction in both Gemcitabine (KGm) and Combination group (KGG). A trend was observed in KGr group but was no significant reduction compared to KC group Figure 39. Gemcitabine treatment was able to reduce Bcl2 levels significantly in liver tissue compared to no effect in P53 mutant pancreatic tissue.

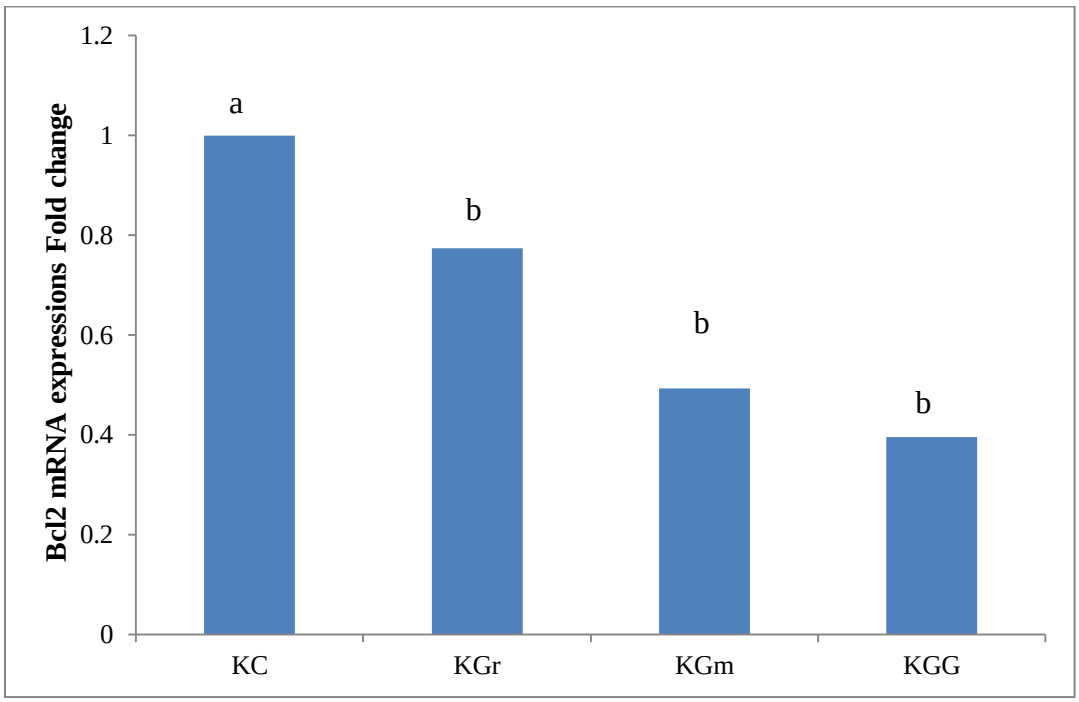

Figure 39: Liver RTPCR mRNA expression of Bcl2 in KC, KGr, KGm and KGG groups. KGm and KGG had lower expression compared to KC (less than 0.5 fold). KGr showed trend (more than 0.5). Fold change was calculated by 2-ΔΔCT method. β-actin was used as house-keeping gene to normalize CT value. KGr, KGm and KGG were significantly different from KC (t-test -'a' is significantly different from 'b' p value < 0.05)

CHAPTER 4: Urinary Metabolomics profiles of Garcinol treated Pancreatic Cancer transgenic mice

Metabolomics is a relatively new approach to identify differences in the larger complex data sets usually collected from biological samples. It is one of the omics approach dealing with the overall changes in the metabolism associated with either disease processes or treatment interventions. With growing advances in the omics fields, it can change current concepts of diagnosis and treatment, making it more tailored for custom need of the individuals. These advancements have rendered traditional approaches to be limited and less appropriate for today's clinical environment, where we have genome and metabolome wide information available. Complex metabolic diseases are usually associated with interconnections of variable factors leading to overall presentation of the disease state [76].

There is an added interest in the biomarker discovery for early diagnosis and treatment, making metabolomics one of the technique most pursued in this field. It is the study of low molecular weight, less than 1500 Daltons compounds. These compounds collectively make the metabolome, which can potentially provide exclusive information about the disease or tested treatment outcome[77]. Recently the introduction of latest data analysis tools including multivariate data analysis and pattern recognition software have aided analyzing complex data such as those produced from metabolomics, with much ease [76].

Investigation of urinary metabolomics profiles is a non -invasive and cost effective technique, which can provide unique signatures and information about the

alterations in metabolism with disease, treatment and environmental changes. In this study, we first studied the biomarkers of Pancreatic cancer in urinary metabolomics profiles of KPC mice by comparing them with those of the control littermates without mutations leading to cancer. Secondly, we investigated the changes associated with the progression of pancreatic cancer. Additionally the main goal of the study was to investigate the effects of Dietary Garcinol treatment on urinary metabolomics profiles of KPC mice.

4.1 Methods:

4.1.1 Urine Sample preparations:

Urine samples were collected in weeks 2, 4 and 6. Mice were kept in suspender for 24 hours. The Urine samples were collected. Samples were centrifuged at 1500 rpm for 2 minutes to remove solid debris and 0.02% wt/vol sodium azide (NaN3) was added to urine samples as an antibacterial agent. Urine samples were stored in -80° C till NMR analysis. For NMR spectroscopy samples were thawed at room temperature and diluted in a ratio of 1:4 with Deuterium oxide (D2O).

A reference buffer solution of 5mM DSS (disodium-2, 2-dimethyl 2-silapentane-5-sulphonate) and 10mM imidazole (pH indicator) in D_2O (Deuterium Oxide) (Sigma-Aldrich, Mississauga, ON) were added in a ratio of 9:1 (9 urine: 1 NMR solvent) to the diluted samples. Samples were mixed by vortexing and were transferred to 8 inch NMR tubes (Kontes glass, Vineland, NJ) [78].

Samples were prepared based on recommendations from CHENOMX software database which was used for interpretation of peaks in NMR spectra. Samples were prepared in the morning of NMR as they can detoriate over time.

4.1.2 ^{1}H-NMR Spectroscopy:

^{1}H-NMR spectroscopy was conducted on Varian 500 MHz with oxford magnet (Varian, Palo Alto, CA). It is equipped with 5mm AutoX , broadband (15N-31P/1H-19F) probe with variable temperature capabilities. VNMRJ software was used to collect spectral data in the form of free induction decay (FID) files in time domain. NMR spectroscopy was conducted according to the setting and pulse sequence required by CHENOMX software-1D version of noesyprtp; with pre-saturation during relaxation delay and mixing time. Briefly temperature of the probe was set at 25° C with pulse sequence tnnoesy. Total of 64 scans were collected using acquisition time of 4 seconds with sweep width of 6009.62 hzs and 32768 number of points at 500 MHz frequency.

4.1.3 Pre- processing of NMR spectra using ACD 1D NMR software:

NMR spectra were collected in Free Induction Decay (Fid) time domain format we converted them in frequency domain in order to analyze them by the multivariate analysis software. Fid files were Fourier transformed to frequency domain Figure 40. Fourier transformed spectra are represented by spectral width of 10 ppm, with spectral regions (peaks) representative of different metabolites in the sample. We used 1D

NMR preprocessing software, ACD/Spec Manager 7.00 software (Advanced Chemistry Development, Inc. Toronto, Ontario, Canada) for this processing. The spectra obtained were pre-processed in one file, baseline corrected and auto phasing was done using DSS peak as a reference at 0.0 ppm. The spectra after preprocessing had straighter base line and sharper peaks Figure 41. The spectra were divided into 1000 bins by intelligent binning, to avoid splitting of the peaks into two bins. These binned spectra were digitized into table of integrals and were exported to Simca P+ (13) software.

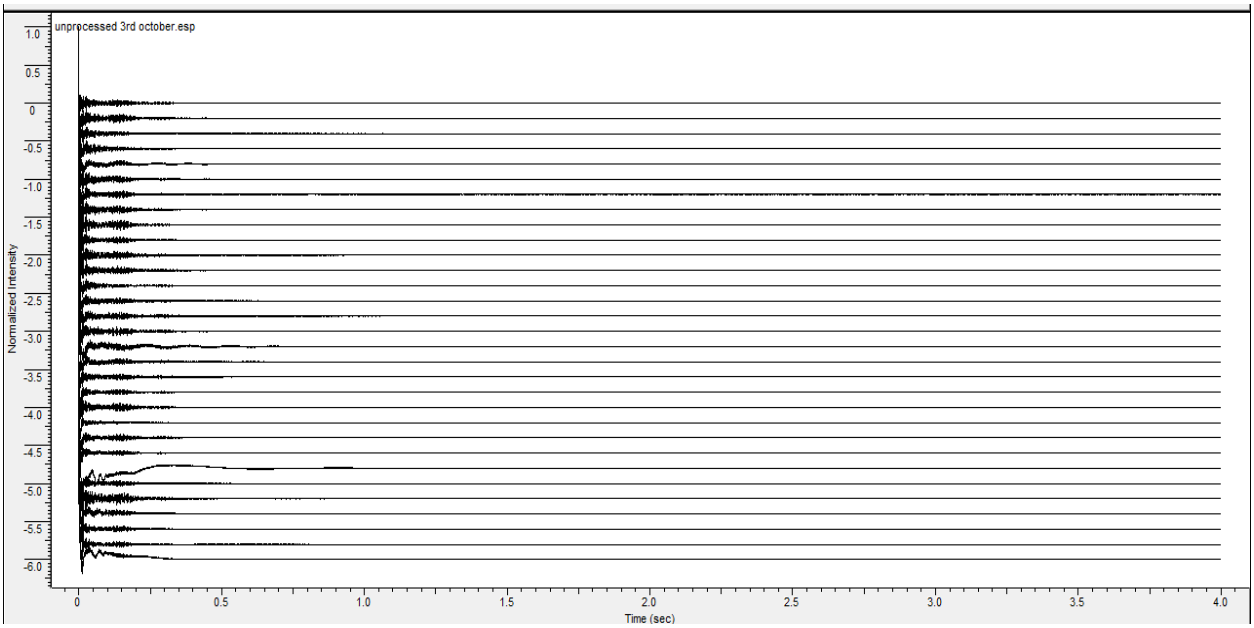

Figure 40: Fid files from NMR 500 stacked in one file in ACD/Spec Manager 7.00 software

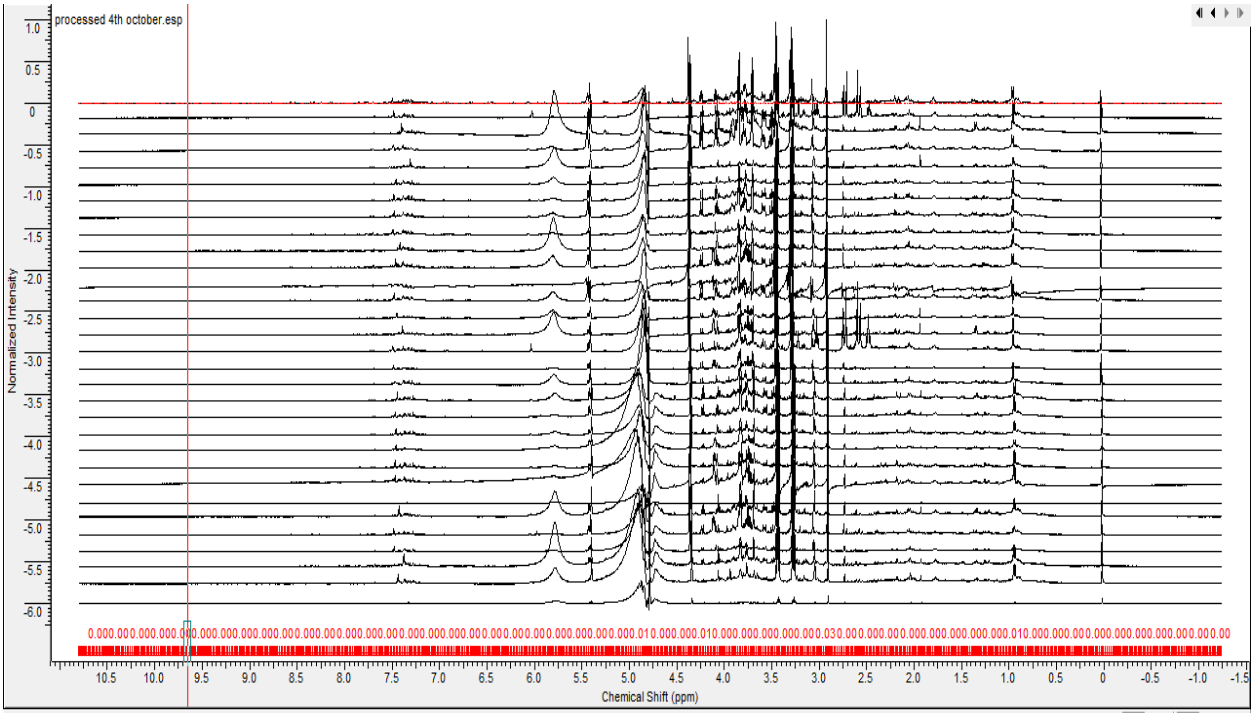

Figure 41: Fourier transformed spectra stacked using ACD/Spec Manager 7.00 software.

4.1.4 Multivariate data Analysis:

The table of integrals from ACD software were imported in the SIMCA P+ software (Umetrics Academy, Sweden) for Multivariate data analysis (MVDA). The imported data was converted to a model, using Principle component analysis (PCA). PCA is an unsupervised mathematical algorithm which can be used as a screening tool to study the differences between the urinary spectra from different groups. A Principle component (PC) is a weighted linear combination of all the NMR variables. The huge data set of original variables is compressed into few PCs [79]. Normally NMR data is compressed into 3-4 PCs, while most of the variation is explained in first principle component. The area of spectrum before 0.5 ppm and area from 4.5 to 5.5 was removed from the spectrum before analyzing the data with PCA. This region contains peaks from water, urea and other exchangeable protons. The NMR spectra also contains small peaks due the metabolites present in small concentrations. In order to give them equal importance as the larger peaks (metabolites present in higher concentrations), we used Pareto scaling. Pareto scaling is mean centering followed by dividing with square root of standard deviation of the original variables. Scatter plots and loading plots were analyzed and groupings were observed based on the differences in the urinary HNMR spectra.

Large complex data set like NMR spectra have large number of X variables. This kind of data set cannot be analyzed by traditionally used statistical analysis tools. The margin of error increases with rise in number of X. variables with techniques like ANOVA etc. PCA, a mathematical algorithm which compress the original data matrix

and can successfully project observations on scatter plot based on the loadings of that observation.

Loading plots pointed toward the ppm responsible for these separations. The ppm identified by loading plot responsible for separation of the different groups, were further investigated to identify the metabolites responsible.

4.1.5 Analysis to identify and quantify the differences in metabolites concentrations:

The areas on the spectrum responsible for separations in the PCA were explored and the metabolites in the area were identified and quantified using CHENOMX NMR suite (CHENOMX INC, Edmonton, Alberta). The fid files from the 1D 1H –NMR spectra were imported to the CHENOMX software. This software had its own processing interface where spectra were Fourier transformed and base line was corrected. Phasing was done using DSS reference peak at 0.0 ppm and water peak was deleted. The processed spectra were analyzed in the profiler module of the software. The 500 MHz library with corresponding pH was selected; this library contained more than 300 metabolites. Identification and concentrations of different metabolites was calculated by fitting the set of peaks for those compounds in the sample spectrum. If the area was crowded with many peaks then multiple metabolites were fitted at one time to match the reference spectrum closest to the sample spectrum [79]. The identified and quantified compounds were then exported to the Excel sheet and ANOVA and t test were done to calculate the statistical significance of the differences in spectra.

DSS is used as chemical shape indicator and reference standard to calculate the concentrations of different metabolites. It is very important to have sharp and clear DSS

peak in the spectra to identify and quantify the metabolites using CHENOMX software. Imidazole added to the samples was used to as pH indicator. As the peaks shifts with differences in pH, the metabolite library was selected based on pH. Pathways involved were explored using KEGG database. Summary of methods used for metabolomics analysis of urinary HNMR spectra are listed in Figure 42.

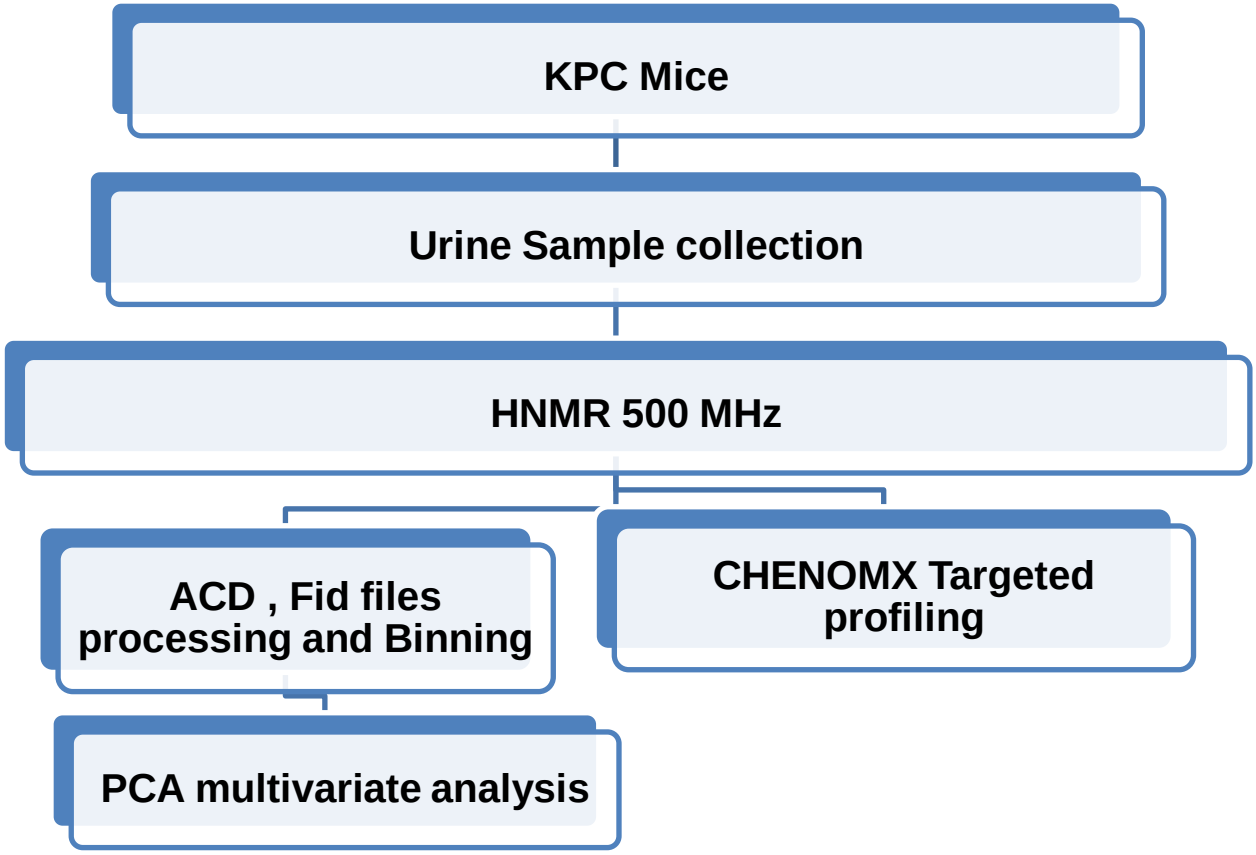

Figure 42: Flow chart of steps required to investigate the differences in Urinary Metabolomic profiles.

4.2 Results and Discussion:

NMR is a suitable technique for bio fluids as the samples preparation is comparatively simple and samples can be reused after the spectroscopy. We have very detailed database for metabolite available in CHENOMX. NMR technique provide quantative information and is reproducible, hence suitable for multivariate analysis[80]. NMR is not dependent on the hydrophobicity of the metabolite and is more suitable for metabolomics analysis of complex biological systems[80]. DSS was used as a reference for NMR spectra due to its less electronegative structure. It has shielded 9 methyl groups due low electronegativity of silicon. It gives signal upfeild and usually set as 0.0 ppm as this signal is further upfeild as compared to all organic compound .TMS is used as solvent for organics, as DSS is more water soluble it is used in most biological water based samples like urine saliva etc. As the CHENOMX software has the library for metabolites which are dependent on pH of the sample, Imidazole was added as pH indicator. The peaks of imidazole are pH dependent and its chemically inert nature makes it a perfect pH indicator in the biological samples[81].

4.2.1 Principle component Analysis (PCA):

4.2.2 To investigate the differences in metabolomic profiles of mice with and without pancreatic cancer.

In order to find the differences between urinary metabolomics profiles (MP) of control no cancer CC group and non-treated cancer group (KC). We made a model with ^{1}H-NMR spectra from CC and KC at week 6 of the study. As shown in Figure 43, the two groups were separated in the score plot along PC1 which contains the maximum

explained variation in the data, indicating that there were differences in metabolomics profiles of cancer group compared to non- cancer group. The corresponding Loading plot for this PCA model pointed towards the metabolites (ppm) responsible for this separation (Figure 44). These peaks responsible for separation of the two groups could be potential biomarkers of Pancreatic Cancer in this p53 and Kras conditional mutant pancreatic cancer mouse model.

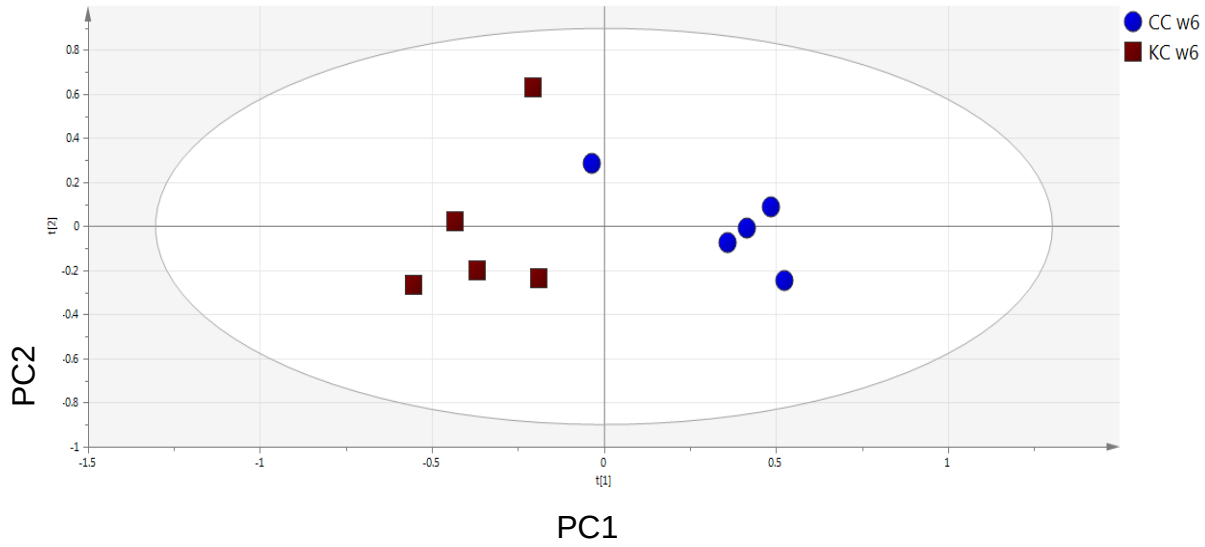

Figure 43: PCA Score plot showing differences metabolomics profiles of Cancer (KC) and no cancer (CC) groups.
(p value < 0.05)

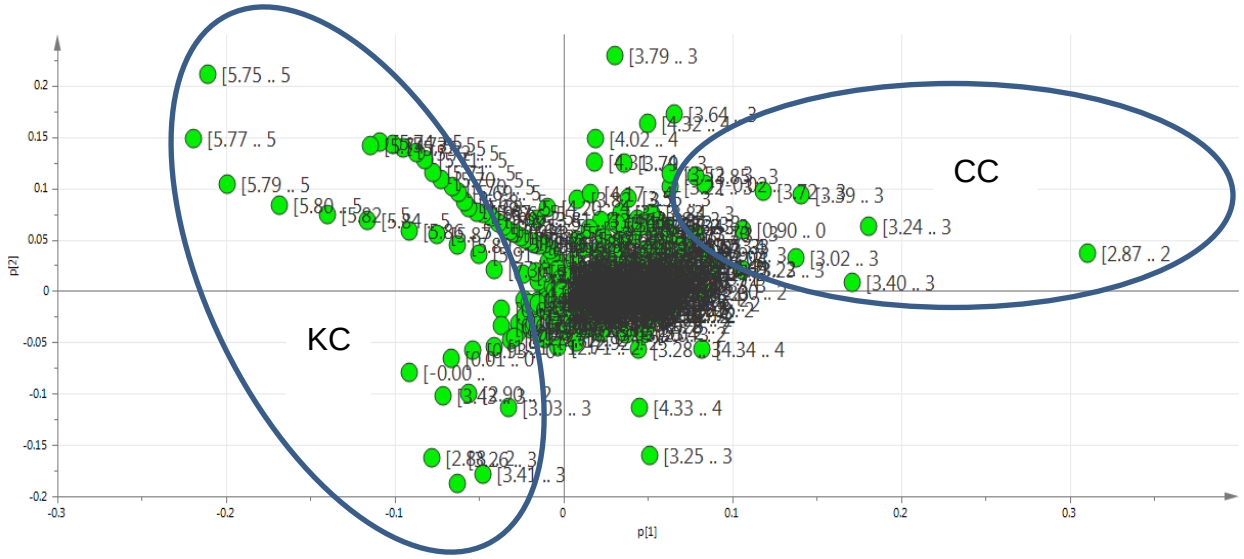

Figure 44: Potential biomarkers of cancer in KPC mice model.
PCA loading plot showing regions of NMR spectra responsible for the differences in MP of CC and KC groups shown in corresponding score plot (Figure 43).

4.2.3 To investigate changes in urinary metabolomics profiles upon progression of pancreatic cancer.

In order to investigate the changes in metabolism and metabolite excretion with progression of Pancreatic Cancer (PaCa) from week 2 to week 6 in non- treated KC group, we made a model with ^{1}H-NMR spectral files from KC group at weeks 2 and 6. The score plot showed separation of the two groups along PC 1 and PC2. Separation of the two groups on the score plot represents differences in urinary metabolomics profiles (MP) of KC group at week 2 and 6 (Figure 45). The corresponding loading plot of the model showed the regions of spectra (ppm) responsible for the separation in the score plot. These metabolites represented in the spectral regions could be possible biomarkers for PaCa progression in KC mice. Interestingly some of the spectral regions responsible for differences in the MP between week 2 and 6 of KC mice were similar to the areas responsible for differences in Control no cancer CC and non-treated KC mice at week 6. These results indicate that some of the metabolites (ppm) which were altered due to Pancreatic cancer incidence can also be changed, possibly in concentration with PaCa progression. These metabolites need to be studied further for their potential use as biomarkers for progression and diagnosis.

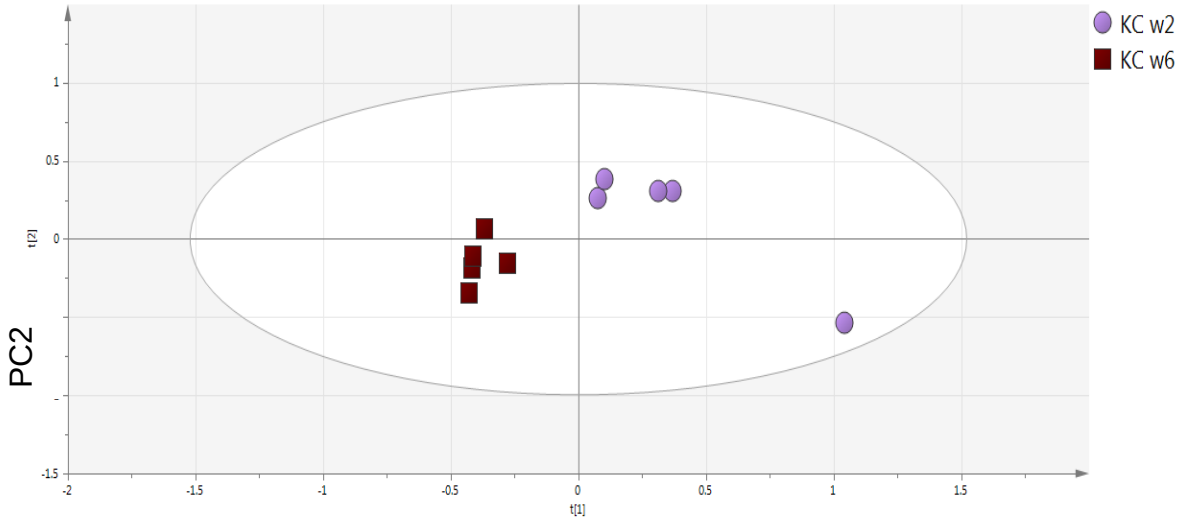

Figure 45: PCA Score plot showing Changes in Metabolomic profiles with progression of pancreatic cancer in animals of KC group from week 2 to 6.
(p value < 0.05)

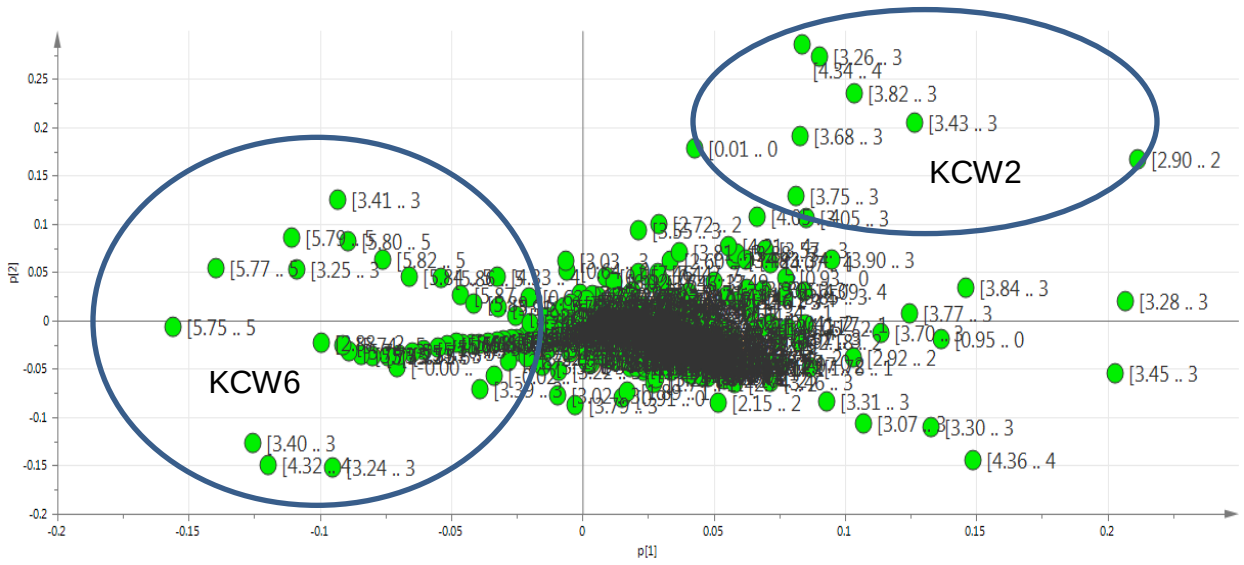

Figure 46: Potential biomarkers for Pancreatic cancer progression.
Loading plot showing regions of NMR spectra (ppm) responsible for separation in score plot of Metabolomic profiles of KC mice at week 2 and week 6.

4.2.4 To investigate the diffrences in MP due to dietary intervention with Garcinol:

In order to study the effects of Dietary Gacinol on urinary Metabolomic profiles we compared ^{1}H-NMR spectra from KC and KGr (Garcinol treated) mice at week6 of the study. Score plot of this model showed seperation between the two groups compared indicating differences in ^{1}H-NMR spectra from KC and KGr groups (Figure 47). Loading plot explains the variables (ppm) responsible for seperation Figure 48.

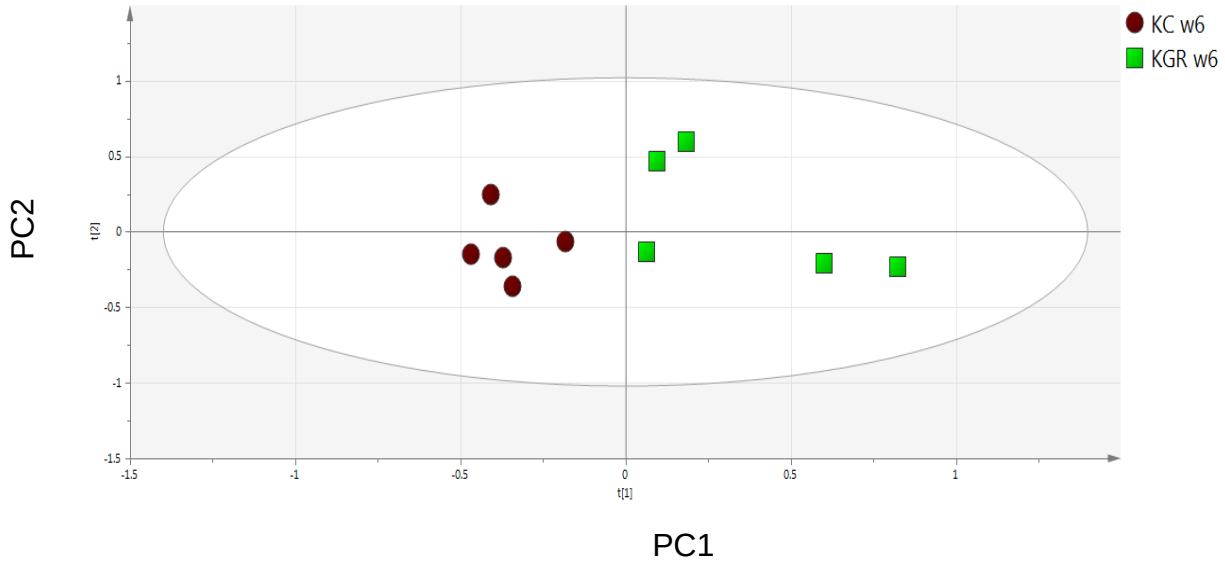

Figure 47: PCA score plot showing changes in Urinary metabolomic profiles of KPC mice with dietary Garcinol.
KC and KGr groups at week 6 were seperated on principle component1 and 2(p value < 0.05).

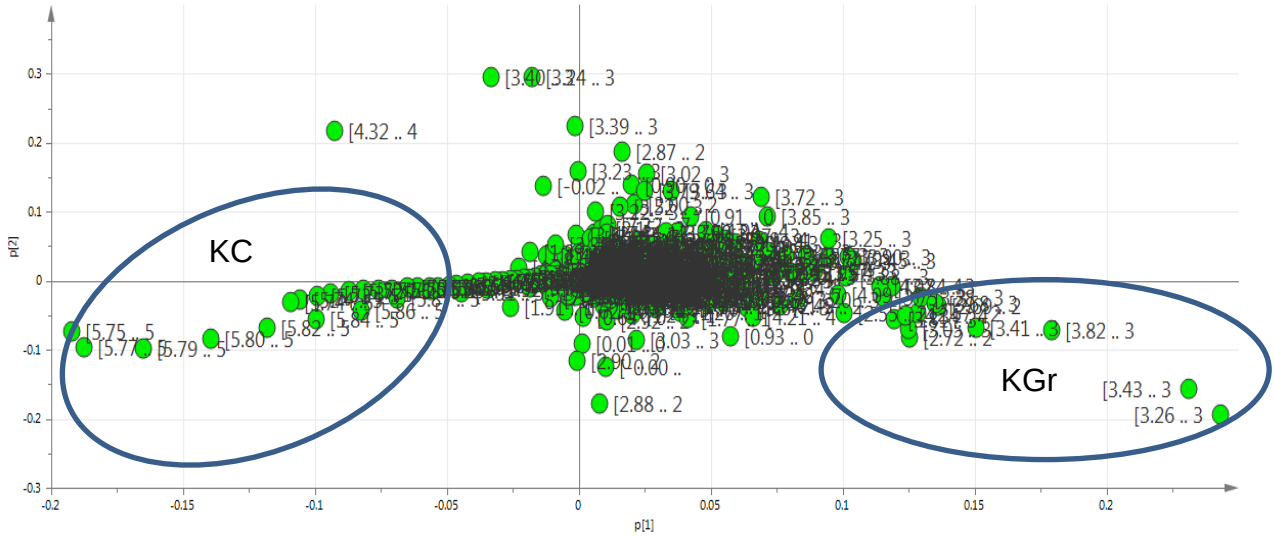

Figure 48: PCA Loading plot KCand KGr at week 6.
PCA Loading plot showing spectral regions responsible for seperation of KC and KGr groups at week 6.

4.2.5 Investigation of MP from KC, KGr and KGm groups at week 6 :

As we have noticed differences in Urinary metabolomics profiles of KC and KGr at week 6, we wanted to investigate whether these differences have any similarities with Gemcitabine treated mice (KGm), our chemotherapy group in the study. The score plot of the model with KC, KGr and KGm week 6 showed that KGr group's separation was in the same direction of KGm group. Differences between Gemcitabine responders and non-responders can also be predicted from this plot based on the distance between the individual KGm score and KC Group. Some of the KGr scores were further away, different from the separation of KGm responders Figure 49. The loading plot of this model pointed toward the variables (metabolites) present in different concentration in KGm, KGr and KC group. Some of the variables (ppm) were common to the CC and KC week2 in treatment group indicating their consistent role in Pancreatic cancer progression and treatment (ppm 5.79. 5.8 related to KC and 3.26-3.43, 4.3 related to CC, KGr and KGm etc.) Figure 50.

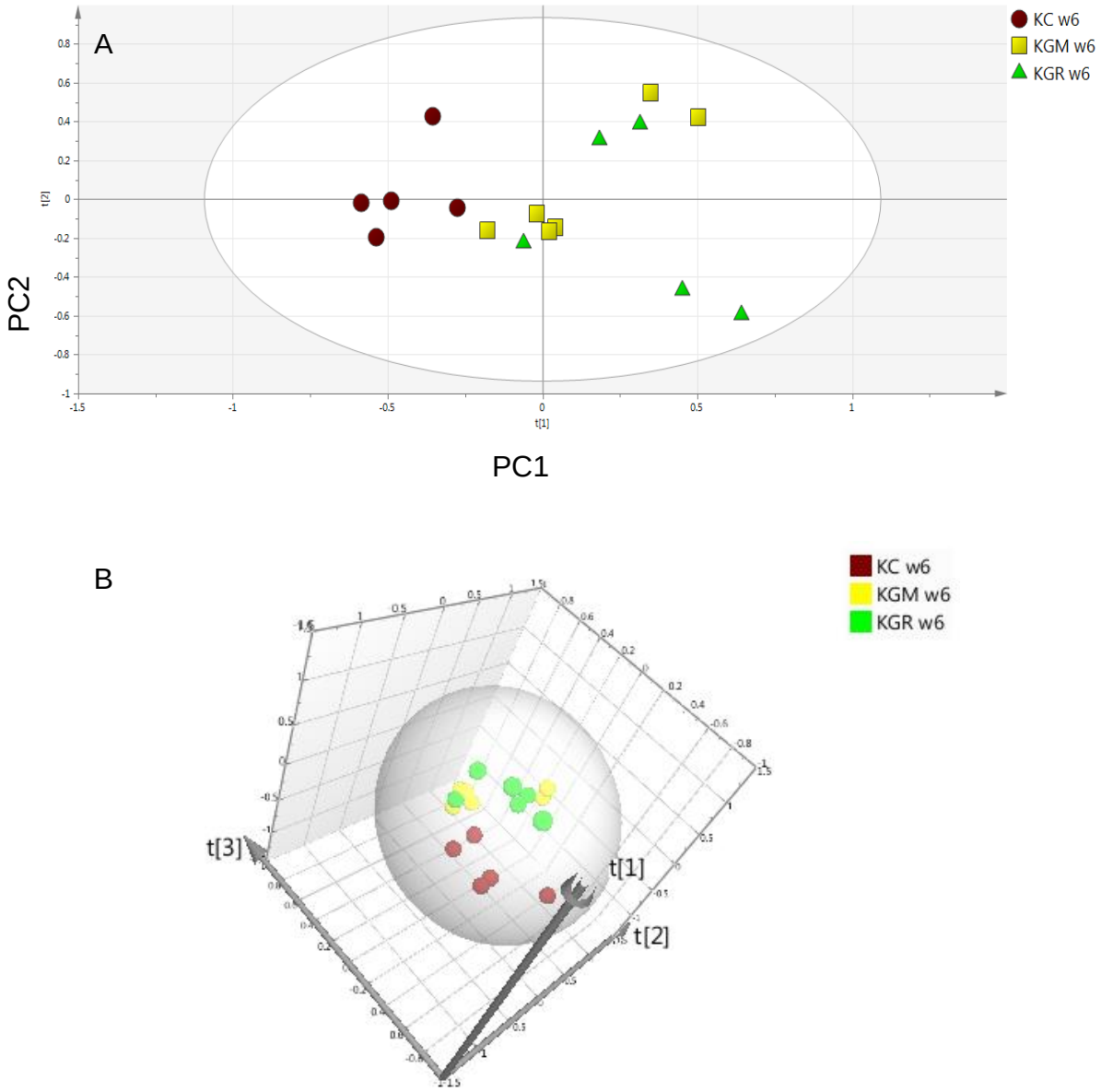

Figure 49: PCA score plot of groups KGr, KGm and KC week 6.
A, Showing KGr are separated from KC in the same direction of KGm (p value < 0.05) . KGr scores were closer to KGm on Principal component 3 as shown in 3D score plot.

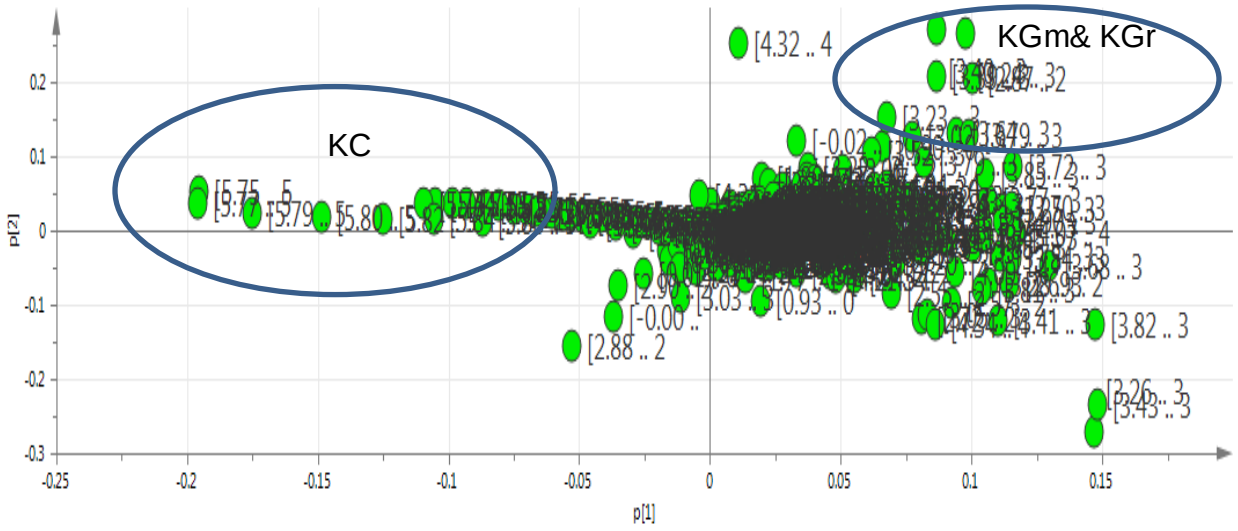

Figure 50: Loading plot explaining metabolites present in different concentrations in urine of KPC mice after treatment with Gemcitabine and Garcinol.

4.2.6 Investigation of MP from KC, KGr, CC week 6 and KC

Week 2 groups:

In order to investigate the seperation of KGr score points which were further away not in the direction of KGm reponders we made a model adding CC and KC week 2 along with KC and KGr week 6. Surprinsingly the score plot explains the seperation of KGr from KC week 6 in a new way. Some of the KGr week 6 scores were among CC (no cancer control) and some of the KGr scores were among KC week 2 scores Figure 51. This Urinary H-NMR data indicate that treatment with Garcinol has either treated KPC mice or have retarded the progression of Pancreatic cancer. Both ways the burden of the disease has been lessened, reflected by the differences in metabolomic profiles of KGr week6 from KC week 6. Corresponding Loading plot of this model explains the variables responsible for seperation after treatment Figure 52. The ppm associated with KC week 6 seperation with progresssion of disease compared to KC week 2 include 3.26-3.45 region along with 7.79- 7.8 region these ppm were also found to be different from KGr and CC groups in previous models.

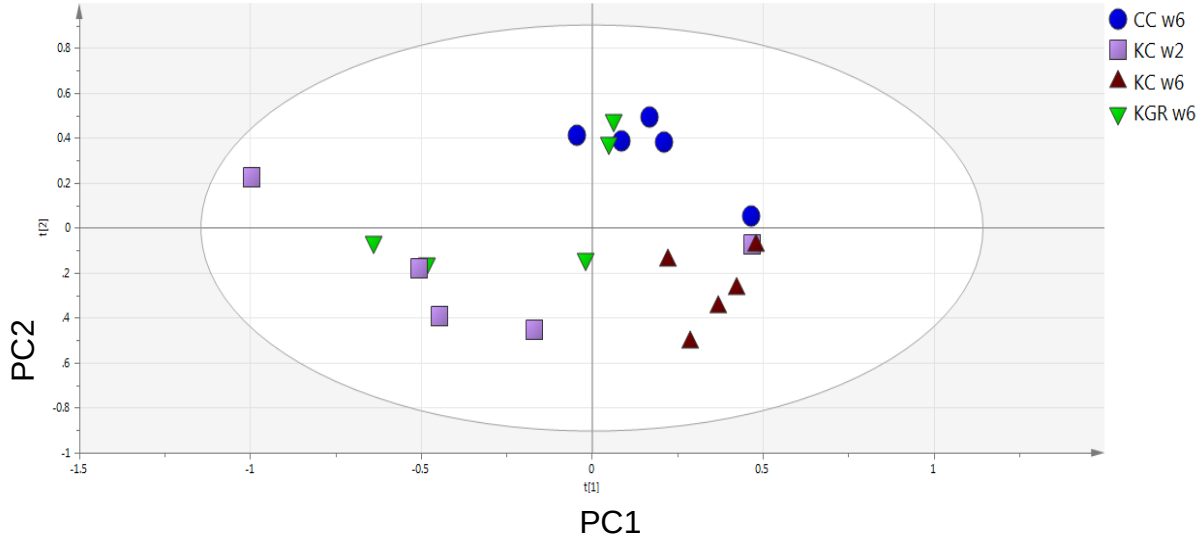

Figure 51: PCA score plot showing changes in Urinary metabolomic profiles of KC, KGr, CC week 6 and KC week2.
KGr score are positioned near CC and KC week 2 indicating retardation of pancreatic cancer growth with dietary Garcinol intervention (p value < 0.05).

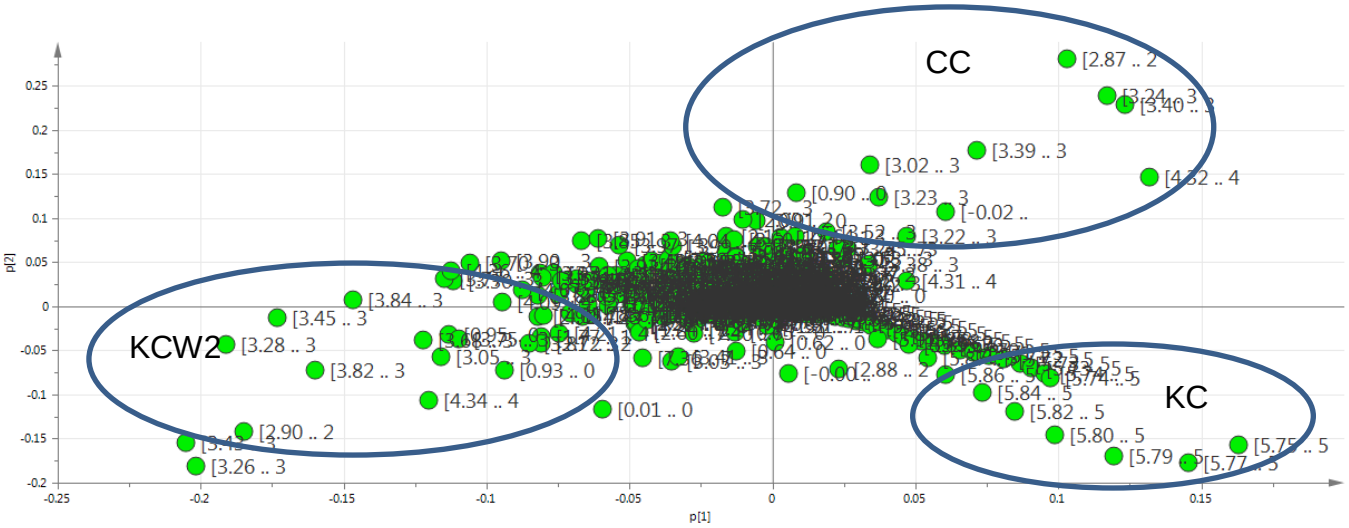

Figure 52: Loading plot of PCA KGr week 6, CC week 6, KC week 2 and 6.

4.2.7 CHENOMX, Metabolites identification and quantification:

Each spectrum was imported to CHENOMX NMR suite as fid file and processed in the processor module of the software. Processed spectrum was imported to profiler module of the software. Each peak was matched with metabolites present in that area and spectrum was fitted to identify and quantify the metabolites present in the urinary H-NMR spectra from KPC mice groups. Five spectra from each group were fitted in the profiler interface with metabolite directory containing more than 300 compounds. The profiled compounds were exported to Excel files and compounds found to be different among groups were analyzed by ANOVA (SPSS software) and t-test for statistical significance. Metabolites found to be different among KC, KGr, KGG and KGM groups week6 along with ppm for peaks identified, are listed in Table 6. Metabolites found to be significantly different in groups are listed in Table 7.

Additionally it was observed that concentration of urea was higher in KC (untreated KPC) group compared to CC, KGr and KGm groups (p value> 0.05, not significant). The ppm 5.79- 5.8 representing Urea peak were strongly related to KC group in all the PCA loading plots.

Metabolite profiled	PPM
2-Methylglutarate	2.2, 2.1, 1.7, 1.6,1.1
2-Oxoglutarate	3.0, 2.4
3-Methylglutarate	2.2, 2.0 , 0.9
Allantoin	8.0, 7.3, 6.0, 5.4,
Anserine	8.3, 7.1, 4.5, 3.8, 3.2,3.0,2.7, 2.6
Arginine	7.2, 6.7, 3.8, 3.2, 1.9, 1.7, 1.6
Cadaverine	3.0, 1.8, 1.5
Cholate	4.1, 3.9, 3.5, 2.2, 2.1, 2, 1.9, 1.8, 1.7, 1.6, 1.5,1.4,1.3,1.2,1,0.9, 0.7
Citrate	2.7, 2.5
Creatine	3.9, 3.0
Creatine phosphate	3.9, 3.0
Creatinine	4.0, 3.0
Cystathionine	3.9, 3.1, 2.7, 2.2, 2.1
Cystine	4.1, 3.4, 3.2
Dimethylamine	2.7
Ethylene glycol	3.7
Glycerate	4.1, 3.8, 3.7,
Indole-3-acetate	10,7.6, 7.5, 7.2, 3.6
Indole-3-lactate	10, 7.7, 7.5, 7.3, 7.2, 4.3, 3.2,3.1
Isovalerate	2.0, 1.9, 0.9
Lysine	3.7, 3.0, 1.9, 1.7, 1.5, 1.4
Methionine	3.9, 2.6, 2.2, 2.1
N,N-Dimethylglycine	3.7, 2.9
N-Isovaleroylglycine	8.0, 3.7, 2.2, 2.0, 0.9
N-Phenylacetylglycine	8.0, 7.4, 7.3, 3.7
Phenylacetate	7.4, 7.3, 3.5
Sarcosine	3.6, 2.7
Succinate	2.4
Sucrose	5.4, 4.2, 4.0, 3.9, 3.8, 3.7, 3.6 3.5
Tartrate	4.3
Taurine	3.4, 3.3
Trimethylamine	2.9
Tropate	7.4, 7.3, 4.1, 3.9, 3.7
Tryptophan	10.2, 7.7, 7.5, 7.3, 7.2, 4.1, 3.5, 3.3

Table 6: Metabolites found to be in different concentrations in Urinary spectra of KPC mice .

Compound	Concentration	PPM	Sig
Allantoin	Decreased	8.0, 7.3, 6.0, 5.4,	.006
Dimethylamine	Increased	2.7	.020
Ethylene glycol	Increased	3.7	.028
Indole-3-acetate	Increased	7.4, 7.2, 7, 6.8, 3.6	.019
Taurine	Increased	3.4, 3.3	.008
Tryptophan	Increased	10.2, 7.7, 7.5, 7.3, 7.2, 4.1, 3.5, 3.3	.036
Phenylacetate	increased	7.4, 7.3, 3.5	.336
Tartrate	Increased	4.3	.168

Table 7: Compounds found to be significantly different in KC, KGr, KGG and KGm groups. Tartrate and phenylacetate were only significantly different in KGr from KC group($p < 0.05$) not in KGm group.

4.2.8 Allantoin:

Allantoin is oxidative product of Urate which is an end product of purine metabolism. As urate has anti-oxidative properties, it oxidation can lead to allantoin production and which can be a marker of oxidative stress [82]. Several studies have shown correlation of allantoin excretion in urine with oxidative stress. Recently urinary allantoin is considered as a known marker of oxidative stress and several studies have reported it along with isoprostanes and other oxidative markers [83, 84]. In one of the study they compared to TBARs and have concluded that Allantoin is better and stable marker of oxidative stress than TBARS. Allantoin levels were stable indicating it represents the internal oxidative stress not by urate just produced during temporary exercise [85].

In Urinary H-NMR spectra peaks from allantoin comes around 8.0, 7.3, 6.0 and 5.4 ppm. One of the peak in NMR spectrum is shown in Figure 53. Although the peak comes near urea, it can be fitted and quantified. The levels of allantoin were significantly decreased in urinary NMR spectra from Garcinol treated KGr group and KGm group as compared to KC group (Figure 54).

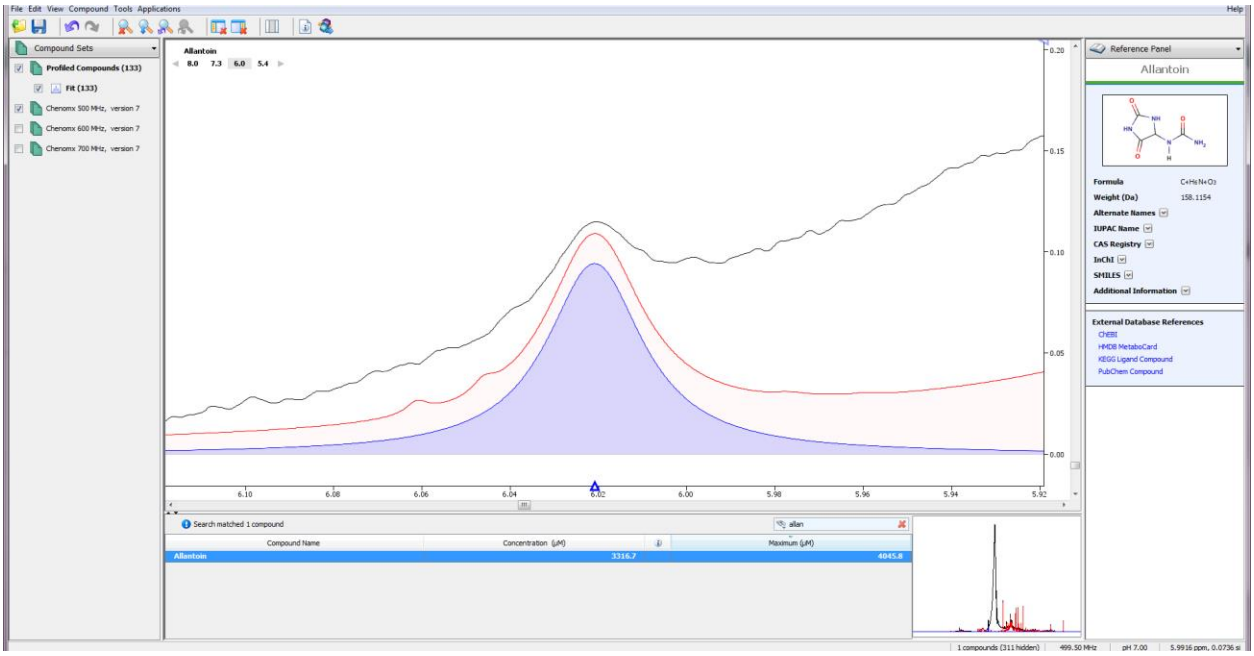

Figure 53: Allantoin peak around 6 ppm.

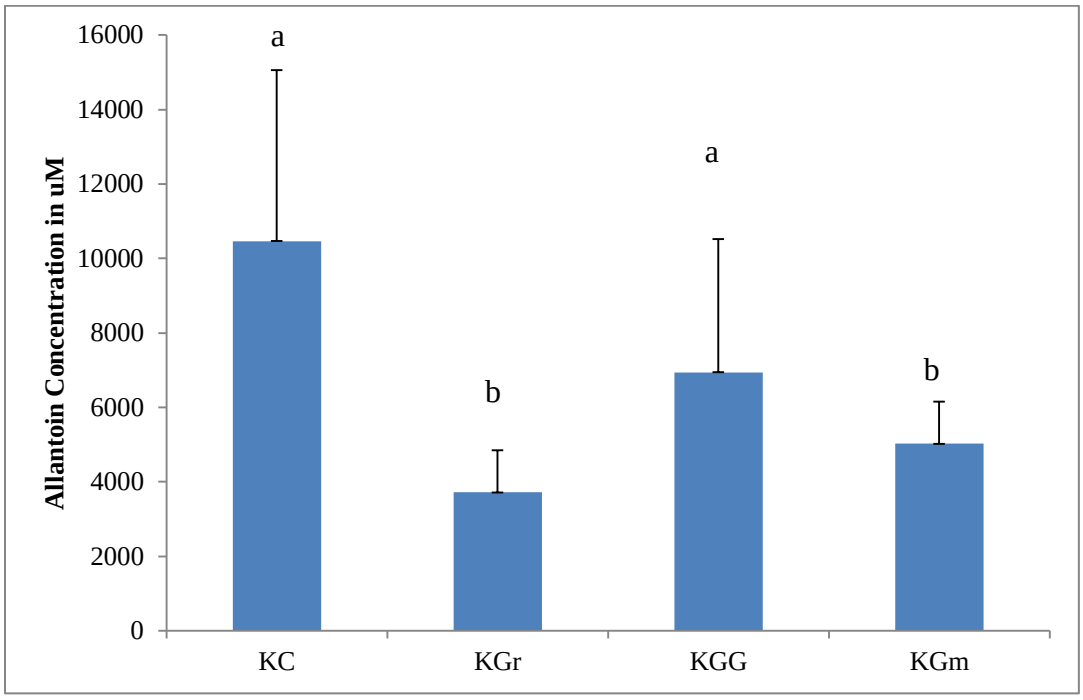

Figure 54: Urinary Allantoin concentrations in KC, KGr, KGG and KGm week 6. KGr and KGm are statistically significantly different compared to KC ('a' is significantly different to 'b' p value <0.05). Error bars represents standard deviation.

4.2.9 Phenylacetate:

Phenylacetate is a terminal product of Phenylalanine and Phenylethylamine metabolism [86]. Can be a mood indicator , and has antidepressant effect of exercise due to amphetamine like action of Phenylethylamine [87]. Its levels are very high in patients with phenylketone urea patients. Our mice were severely ill mice and we observed mostly lower phenylacetate levels in KC (week 6) mice compared to KCW2 and CC mice Figure 55. Phenylacetate levels were increased with treatment with Garcinol in KGr group Figure 56. Although Gemcitabine (KGm) and combination group (KGG) showed increasing trend but were not significant due to high standard deviation(responder and non-responders).

Phenylacetate has been reported to have anti-cancer effects also. In a study conducted on renal cancer cell lines phenylacetate treatment have inhibited growth. Main target of phenylacetate was p21CIP1 but it also caused inactivation of CDK2, hypophosphorylation of pRb. leading to G1 cell cycle arrest[88]. It has also shown to improve sensitivity of multidrug resistant breast, ovarian and colon tumor cell lines when treated along with phenylbutyrate [89]. Phenylacetate is also reported in clinical trial conducted on 17 advanced solid tumor patients where it has been reported to stabilize 3 prostate cancer patients and decreased bone pain in one patient. One of six glioblastoma patient showed improvement over nine month [90].

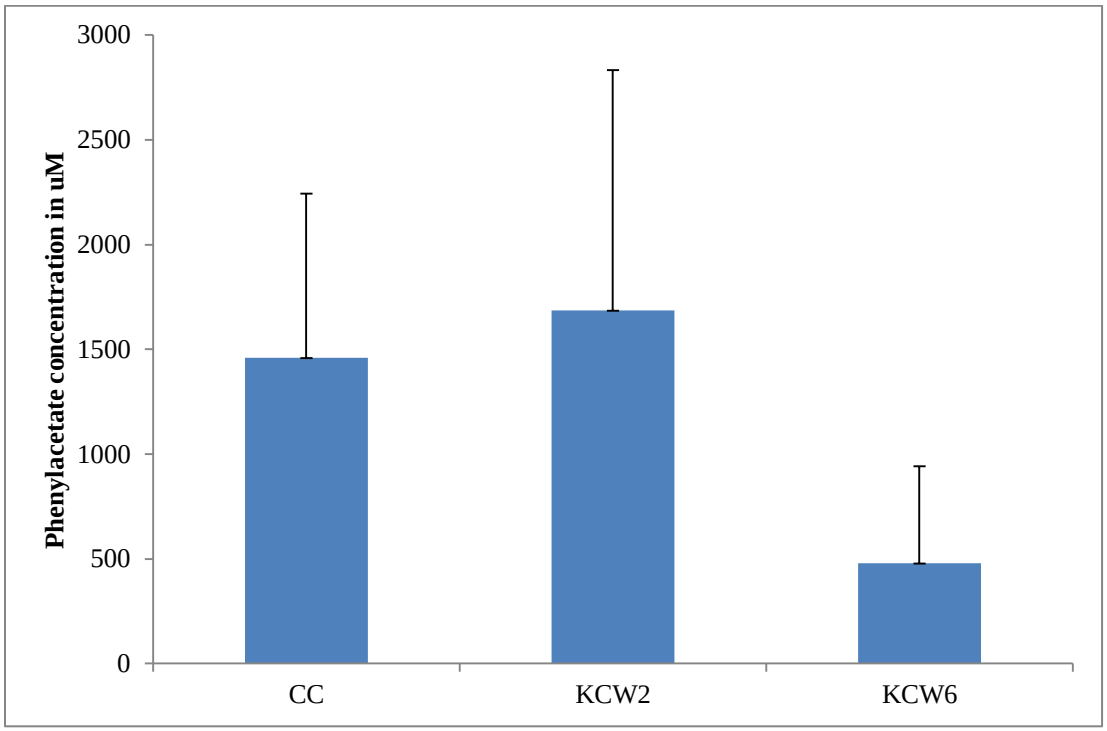

Figure 55: Urinary Phenylacetate levels decrease with progression of pancreatic cancer and in KC compared to CC mice.
Although not significant (p value KCW2=0.068 and CC= 0.082) but showed trend. Error bars represent standard deviation.

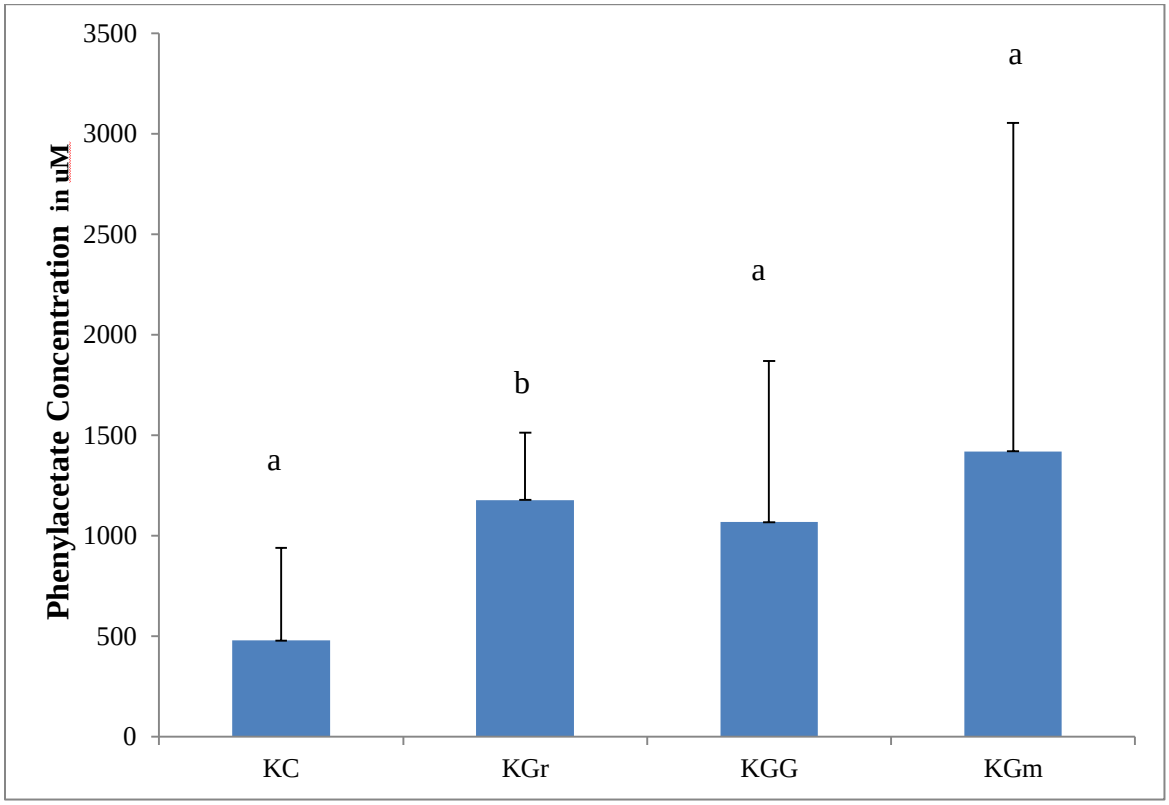

Figure 56: Phenylacetate levels in KCW6, KGrW6, KGGW6 and KGmW6.
KGr is significantly different from KCW6 (‘a‘ is significantly different from ‘b’ p value < 0.05).Error bars represents one standard deviation.

4.2.10 Tartrate:

Tartrate excreted in urine is mainly from diet and about 15 to 20 percent of tartrate ingested is excreted without change. Tartrate is mostly metabolized by intestinal bacteria and tissue metabolism is very slow [91]. Urinary tartrate excretion is high in males and vegetarian people have lower tartrate in urine. It poses antioxidant activity and is powerful chelating agent. Urinary tartrate is a reported to be protective against kidney stone formation, as it can form stable soluble complexes with calcium. Tartrate is also investigated for it effects as an inhibitor of surface controlled crystallization similar to the effects of citrate on this process[91].

In H-NMR spectra Tartrate peak comes around 4.3ppm as shown in Figure 57.

Figure 58 illustrate Tartrate metabolic role in Glyoxylate and Dicarboxylate pathway.

Urinary tartrate excretion was lower in KC mice at week 6 compared to CC (p value < 0.05) and showed a decreasing trend from KC week 2 to week 6 Figure 59. Indicating that Pancreatic cancer and its progression can have lowering effect on urinary Tartrate levels. Tartrate was found to be increased in concentration in Garcinol treated KGr group compared to KC mice Figure 60.

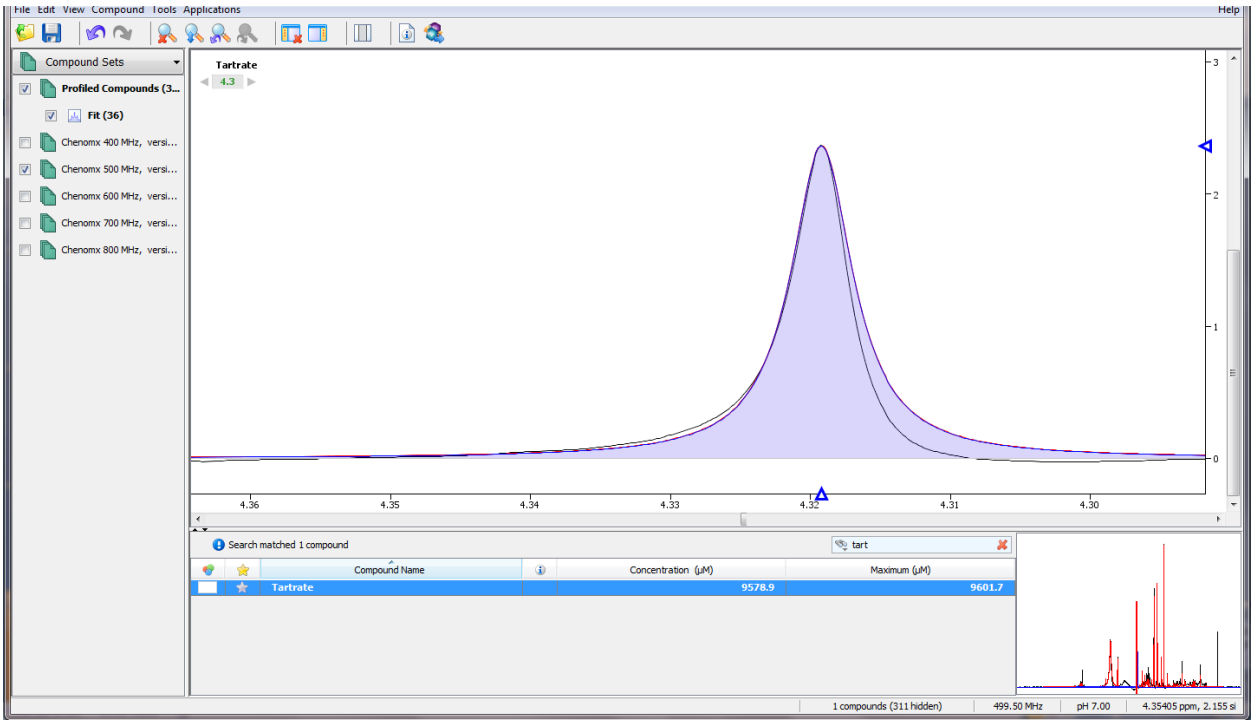

Figure 57: Tartrate peak at 4.3 ppm.

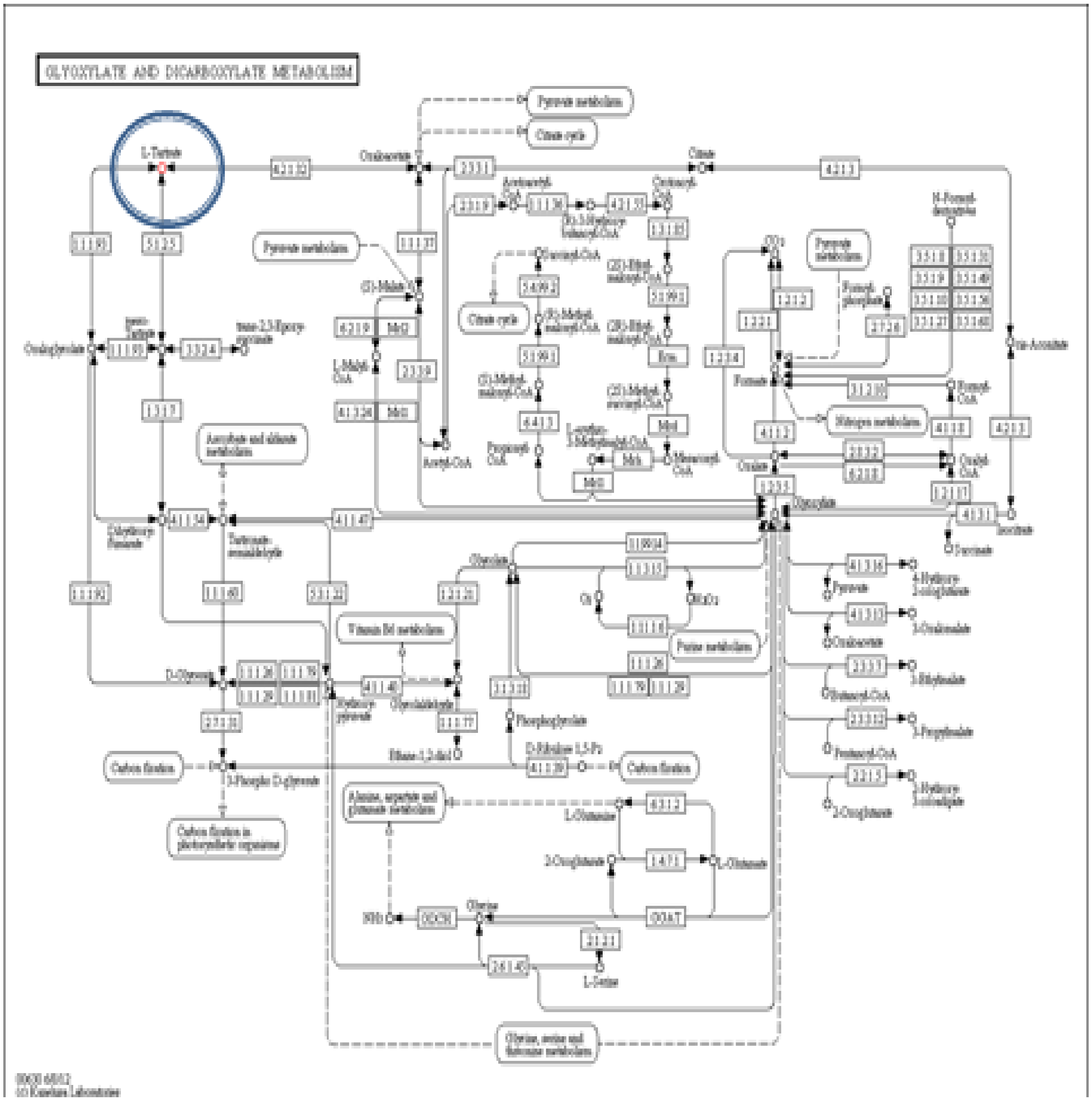

Figure 58: Role of Tartrate in Glyoxylate and Dicarboxylate metabolism.

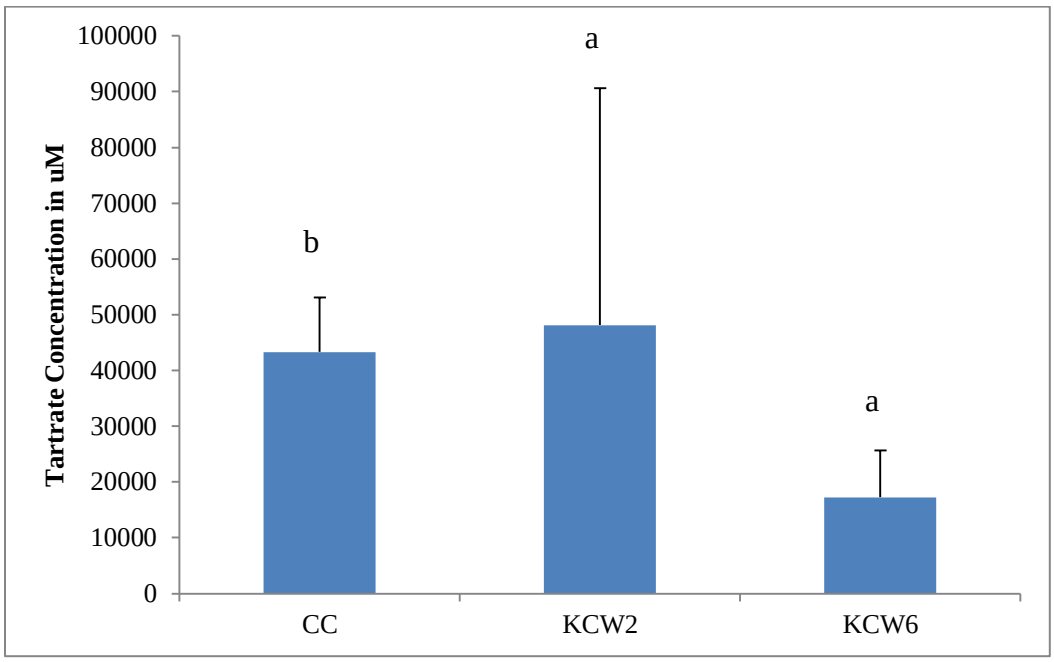

Figure 59: Urinary Tartrate levels decrease with progression of pancreatic cancer. Tartrate is significantly higher in CC compared to KCW6. ('a' is significantly different from 'b' p value < 0.05). Error bars represents one standard deviation.

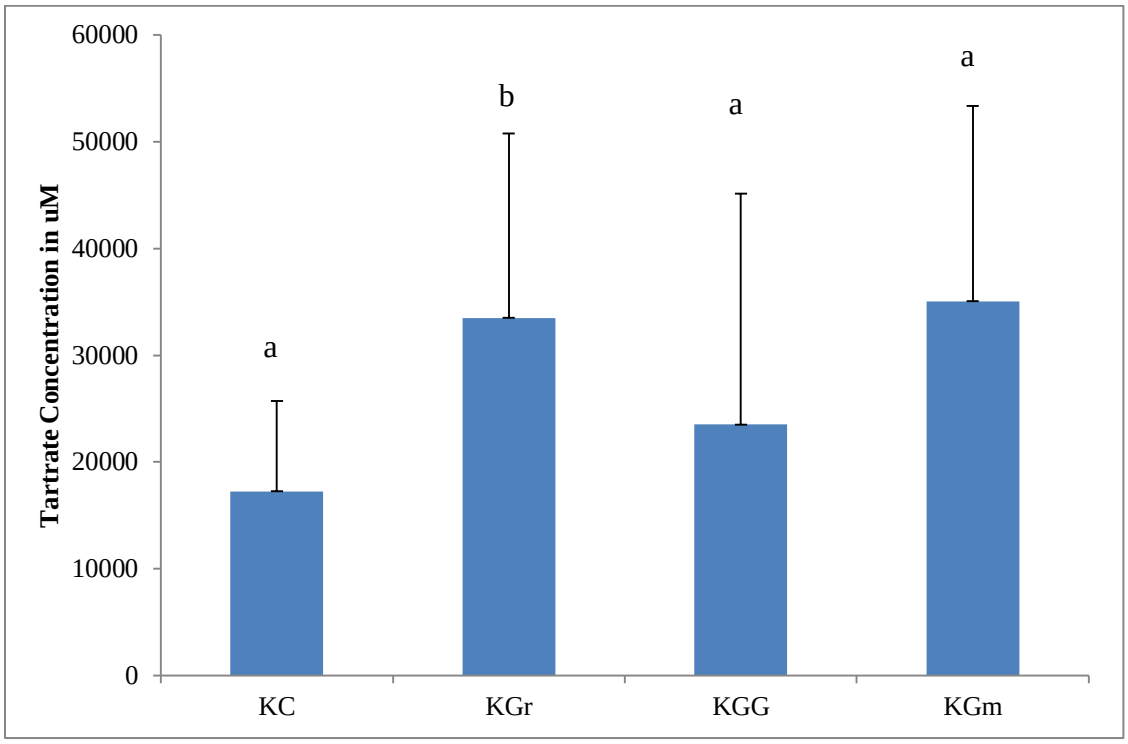

Figure 60: Urinary Tartrate concentrations in KC, KGr, KGG and KGm week 6. KGr is statistically significantly different to KC ('a' is significantly different from 'b' p value <0.05). Error bars represents ± standard deviation.

4.2.11 Taurine:

Taurine is an amino and sulphur group containing organic acid commonly present in most tissues of the body, including heart brain and liver. A very little is known about its involvement in major metabolic pathways, It is involved in methionine and cysteine metabolism.[92]. Its role in bile has been elucidated by several studies, bile acids are conjugated with taurine and these conjugates works as detergents in bile [93]. Multiple other roles of taurine have been reported. It helps maintaining osmotic balance and membrane potential of cells and mitochondria. Helps lowering superoxide synthesis in mitochondria [94]. It has shown to improve cardiovascular health and anti-hypertensive, anti-diabetic effects [94]. It is also known to have Hypoglycemic action, anti-oxidation, and detoxification [92]. Taurine is also found to be effective in pancreatic islets remodeling against cytokine-induced apoptosis [92].

Serum taurine levels are reported to be lower in many cancer types including breast, ovarian, endometrial and colon cancer. In a clinical study, serum taurine levels were found to be very low in female breast cancer patients (p value 0.001), possible reason to taurine depletion, as discussed by researchers, is that the tumor cells produce a very large number of sulphate polysaccharides utilizing and depleting sulphur containing taurine in the surrounding. As the detection was 100 percent with no false positives, they proposed taurine as a biomarker for breast cancer diagnosis [95].

Taurine peaks are very distinct peaks around 3.2-3.45 ppm in Urinary H-NMR spectrum. Figure 61 shows taurine peaks fitted on CHENOMX software. Metabolic pathway of Taurine and hypotaurine metabolism is illustrated in Figure 62.

KPC mice showed a trend in reduction of taurine urinary levels with progression of cancer (P value >0.05) Figure 63. KC mice had very low concentration of taurine at week 6 which is improved after Garcinol and Gemcitabine treatments as observed in Figure 64. Urinary Taurine levels were higher in KGr and KGM group after 6 weeks treatment.

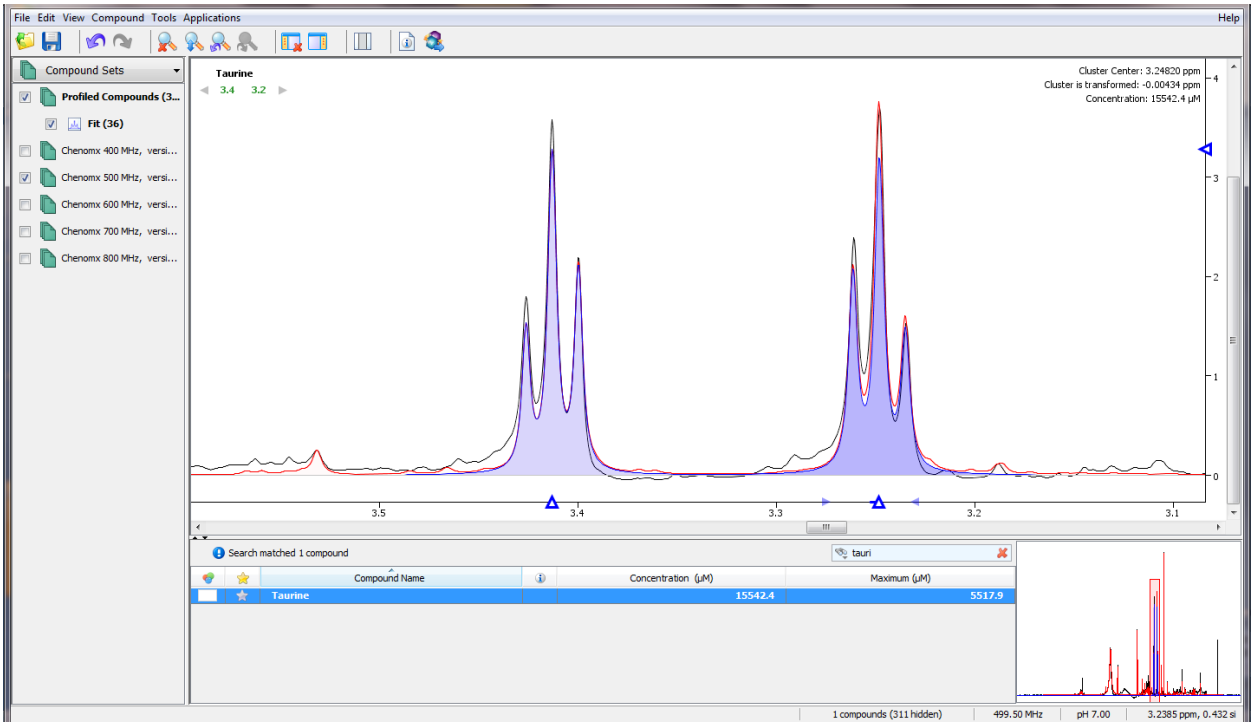

Figure 61: Fitted Taurine peaks near 3.2- 3.45 ppm.

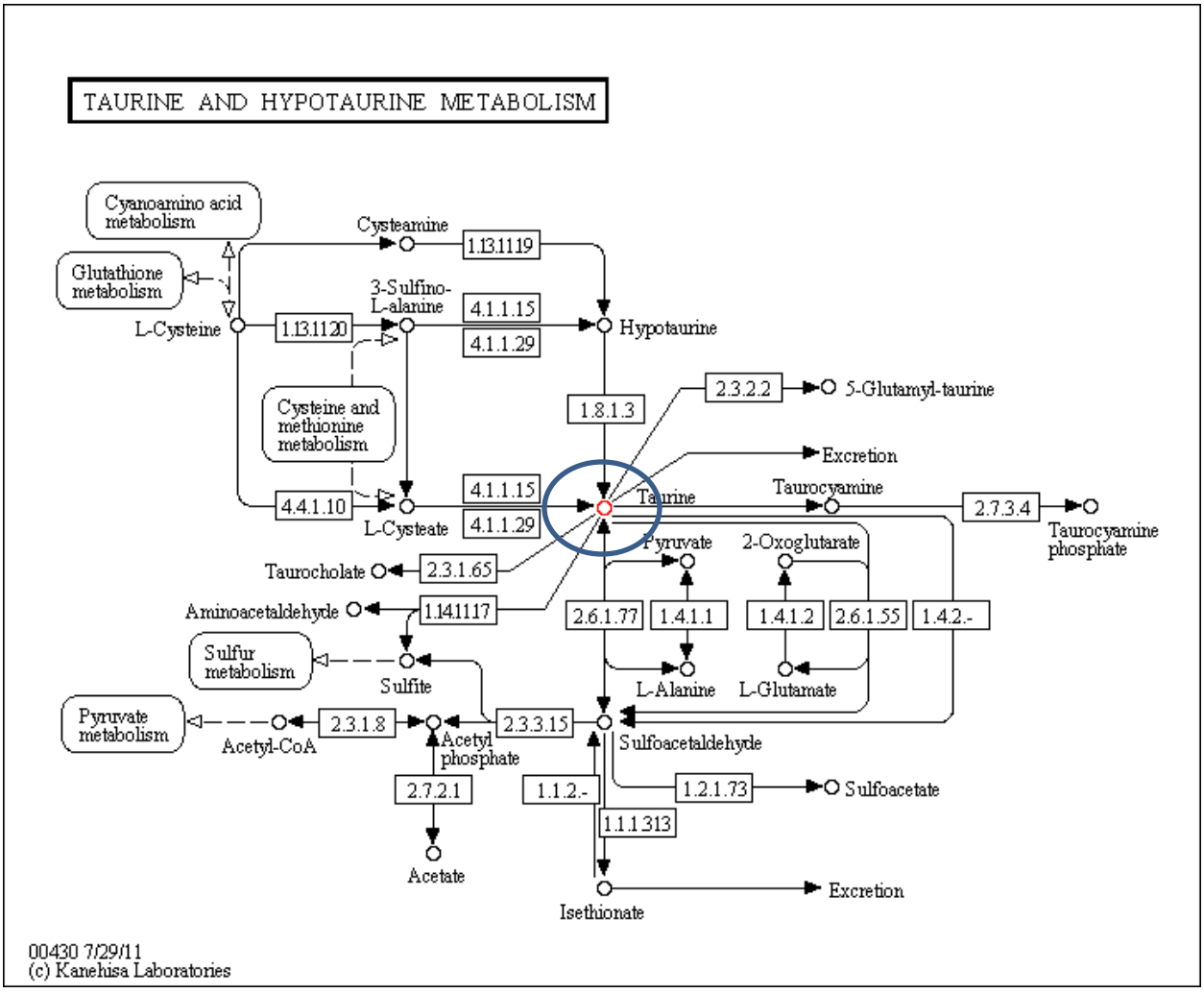

Figure 62: Taurine and Hypotaurine metabolism (KEGG Ligand database).

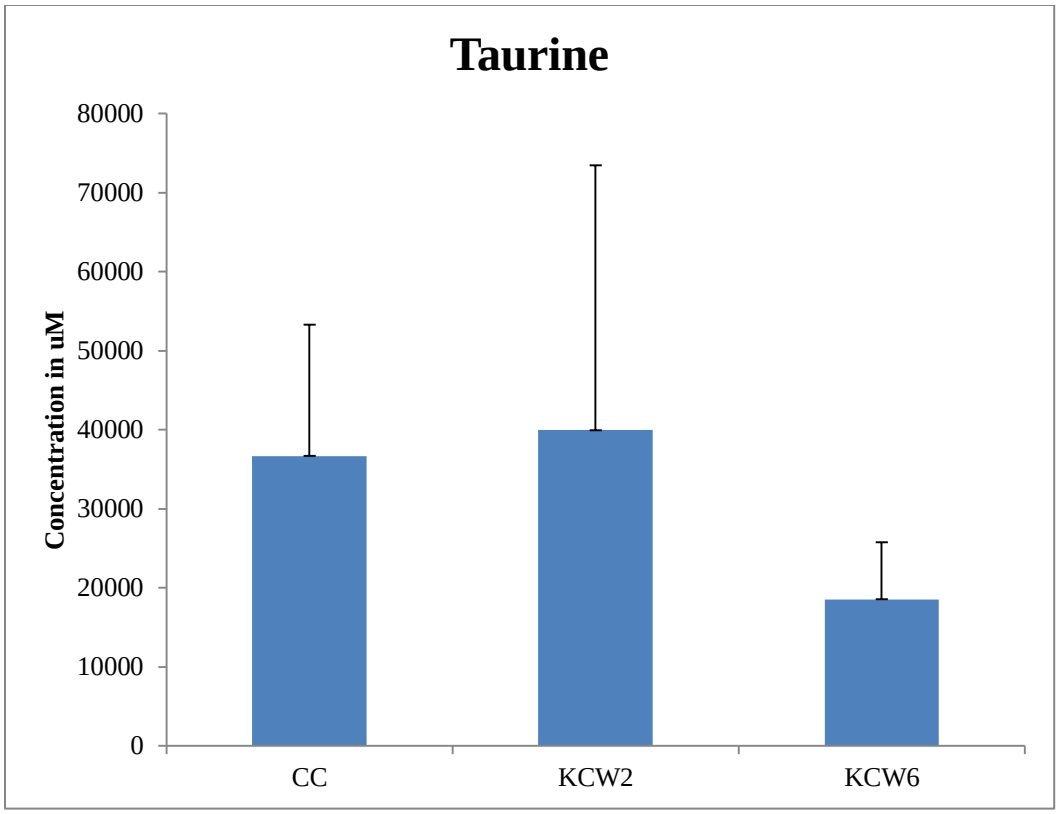

Figure 63: Urinary Taurine levels showed a decreasing trend with progression of pancreatic cancer in KC compared to CC mice (p value > 0.05).

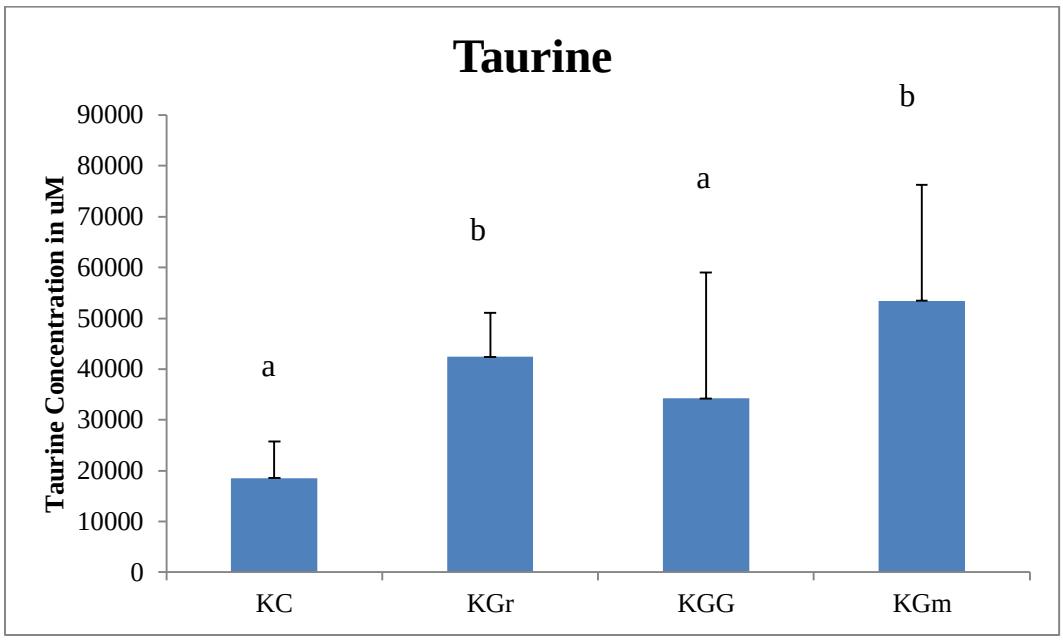

Figure 64:Urinary Taurine concentrations in KC, KGr, KGG and KGm week 6. KGr and KGm are statistically significantly different to KC ('a' is significantly different from 'b' p value <0.05). Error bars represents standard deviation.

CHAPTER 5: Conclusions

We investigated the response of KPC mice with k-ras and Trp53 mutations in pancreas to dietary Garcinol. This pancreatic mouse model reflects a close picture of the human disease with the full array of lesions including early PanINs developing into aggressive PDA and metastasis to lymph nodes and other organs. Dietary Garcinol improved survival of KPC mice, with all the mice within the group surviving 6 weeks of study. Garcinol alone was able to halt the progression and reduction in size of some of the tumors monitored by MRI and ultrasound. In combination with Gemcitabine the response to drug increase from 10-15% to 25%, Indicating the potential of Garcinol in adjuvant therapy

No adverse changes to red blood cells, white blood cells and overall blood morphology were noted after the Garcinol diet. NK&NKT cell ratio was found to be increased in Garcinol treated group, upon investigation of blood smears from these mice. This is a very interesting finding and warrants detailed investigation. KPC mice develop lower esophageal and fore-stomach papillomas [32]. These papillomas may be due to its pdx component in the genetic background related to gut development [32], or else can be due to genetic instability including SMAD expressions[37], leading to complications and death in many cases of these mice due to intestinal obstruction. Garcinol ingestion reduced these papilloma formations in treated mice improving overall inflammation and patency of the foregut, vital for nutrition of these severely ill mice.

Histological investigation of pancreatic tissue correlated with the MRI Ultrasound findings. Minimum number of mouse pancreatic intraepithelial neoplasia was found in Gemcitabine plus Garcinol combination group. Progression of mPanIN 1 to mPanIN 3

was observed to be retarded in Garcinol treatment group with lower number of mPanINs in mPanIN3 grade. Further exploration of Paraffin embedded pancreatic tissue with S100P antibody, a protein overexpressed in pancreatic cancer tissue but not in normal pancreas, opened up new doors for studying KPC mice pathology. S100P expression very well correlated with mPanIN grading and advancement to aggressive pancreatic ductal adenocarcinoma in KPC mice. Labeling of S100P validated the H&E findings in different groups. Although mutation in DPC4 and other tumor suppressor genes were not found to be signature of this model[32], exploration of DPC 4 expression in the pancreatic tissue with immunohistochemistry revealed that there was considerable loss of DPC4 expression in advanced mPanIN, Pancreatic ductal adenocarcinoma and surrounded tissue compared to healthier acinar and ductal tissue. Garcinol treated mice showed improvement in the architecture of lobular structure and preservation of acinar and ductal organization confirmed with normal expression of DPC4. Coherent with findings on invitro effects of Garcinol on Pancreatic cancer cell lines from our lab, invivo anti-cancer effects of Garcinol has been elucidated in this study.

Dietary Garcinol has modulated the microRNA microarray profiles in favorable manner, many of the tumor promotor miRNA were observed to be down regulated after treatment. Additionally multiple tumor suppressor miRNA have shown higher expressions after Garcinol ingestion for just 6 weeks. We investigated some of the target gene pathways of these altered microRNA, to Study the gene regulations by microRNA and regulation of microRNA by some genes like Notch1 have been reported by earlier studies to regulate miR451 expression. CCND1, MMP9, and notch1 showed reduced expression in Garcinol treated group in pancreatic tissue. One of the first

metastatic site, liver also showed reduction of CCND1 and MMP9. These results necessitate further investigation of pathways and molecular mechanism involved in down regulation of these genes, based on our miRNA data and mRNA data we propose that miRNA 451a, miRNA 23a and other microRNAs statically differently expressed, could be involved in epigenetic modulation of gene expressions in P53 and kras mutated pancreatic cancer mouse model.

Urinary metabolomics profiles of the Garcinol treated mice showed differences from KC mice after 6 weeks of treatment as observed by the separation in PCA score plots. After further investigation, using models with different treatment and control groups, it was explained that the separation of Garcinol treated mice were in the direction of Control mice without cancer and KPC mice at the beginning of the study. These results suggest that Garcinol has improved the urinary metabolomic profiles of KPC mice indicating slowed progression of the disease. Loading plots directed toward some of the peaks in the spectra responsible for this improvement. These peaks were later identified and quantified in the CHENOMX. Compounds which were observed to be differently expressed included reduction of Allantoin, a known oxidative stress marker. Increased levels of Phenylacetate and Tartrate. Taurine levels were also increased as compared to KC. Serum Taurine levels are reported to be decreased with progression different cancer types [95] and its increase can reflect improvement in the disease. Excretion of urea was found to be higher in KC group compared to other groups this could be indicative of cachexia and muscle protein loss in KC mice.

Results from this study can be investigated in a larger scale animal study involving larger animals and more number of animals. Further investigation of molecular

pathways identified can lead to its incorporation as a chemotherapeutic agent in clinical trial. Beneficial results may lead into a pilot human study. Garcinol showed synergistic effects with Gemcitabine in some of the investigated pathways, further exploration of dose and response can be done to optimize this beneficial combination.

REFERENCES

1. Freelove R, Walling AD: **Pancreatic cancer: diagnosis and management.** *Am Fam Physician* 2006, **73:**485-492.
2. Pliarchopoulou K, Pectasides D: **Pancreatic cancer: current and future treatment strategies.** *Cancer Treat Rev* 2009, **35:**431-436.
3. Tripathi YB, Tripathi P, Arjmandi BH: **Nutraceuticals and cancer management.** *Front Biosci* 2005, **10:**1607-1618.
4. Woutersen RA, Appel MJ, Van Garderen-Hoetmer A: **Modulation of pancreatic carcinogenesis by antioxidants.** *Food Chem Toxicol* 1999, **37:**981-984.
5. Dhillon N, Aggarwal BB, Newman RA, Wolff RA, Kunnumakkara AB, Abbruzzese JL, Ng CS, Badmaev V, Kurzrock R: **Phase II trial of curcumin in patients with advanced pancreatic cancer.** *Clin Cancer Res* 2008, **14:**4491-4499.
6. Jatoi A, Burch P, Hillman D, Vanyo JM, Dakhil S, Nikcevich D, Rowland K, Morton R, Flynn PJ, Young C, Tan W: **A tomato-based, lycopene-containing intervention for androgen-independent prostate cancer: results of a Phase II study from the North Central Cancer Treatment Group.** *Urology* 2007, **69:**289-294.
7. Wang Z, Desmoulin S, Banerjee S, Kong D, Li Y, Deraniyagala RL, Abbruzzese J, Sarkar FH: **Synergistic effects of multiple natural products in pancreatic cancer cells.** *Life Sci* 2008, **83:**293-300.
8. Kunnumakkara AB, Guha S, Krishnan S, Diagaradjane P, Gelovani J, Aggarwal BB: **Curcumin potentiates antitumor activity of gemcitabine in an orthotopic model of pancreatic cancer through suppression of proliferation, angiogenesis, and inhibition of nuclear factor-kappaB-regulated gene products.** *Cancer Res* 2007, **67:**3853-3861.

9. Harikumar KB, Kunnumakkara AB, Sethi G, Diagaradjane P, Anand P, Pandey MK, Gelovani J, Krishnan S, Guha S, Aggarwal BB: **Resveratrol, a multitargeted agent, can enhance antitumor activity of gemcitabine in vitro and in orthotopic mouse model of human pancreatic cancer.** *Int J Cancer* 2009.

10. Parasramka MA, Gupta SV: **Synergistic effect of garcinol and curcumin on antiproliferative and apoptotic activity in pancreatic cancer cells.** *J Oncol* 2012, **2012:**709739.

11. Parasramka MA, Ali S, Banerjee S, Deryavoush T, Sarkar FH, Gupta S: **Garcinol sensitizes human pancreatic adenocarcinoma cells to gemcitabine in association with microRNA signatures.** *Mol Nutr Food Res* 2013.

12. Padhye S, Ahmad A, Oswal N, Sarkar FH: **Emerging role of Garcinol, the antioxidant chalcone from Garcinia indica Choisy and its synthetic analogs.** *Journal of hematology & oncology* 2009, **2:**38.

13. Rao AVR, Venkatswamy G, Pendse AD: **Camboginol and Cambogin.** *Tetrahedron Letters* 1980, **21:**1975-1978.

14. Sahu A, Das B, Chatterjee A: **Polyisoprenylated Benzophenones from Garcinia-Pedunculata.** *Phytochemistry* 1989, **28:**1233-1235.

15. Sang S, Cheng X, Stark RE, Rosen RT, Yang CS, Ho CT: **Chemical studies on antioxidant mechanism of tea catechins: analysis of radical reaction products of catechin and epicatechin with 2,2-diphenyl-1-picrylhydrazyl.** *Bioorganic & medicinal chemistry* 2002, **10:**2233-2237.

16. Hamed W, Brajeul S, Mahuteau-Betzer F, Thoison O, Mons S, Delpech B, Van Hung N, Sevenet T, Marazano C: **Oblongifolins A-D, polyprenylated benzoylphloroglucinol derivatives from Garcinia oblongifolia.** *Journal of Natural Products* 2006, **69:**774-777.

17. Fuller RW, Blunt JW, Boswell JL, Cardellina JH, 2nd, Boyd MR: **Guttiferone F, the first prenylated benzophenone from Allanblackia stuhlmannii.** *Journal of Natural Products* 1999, **62:**130-132.

18. Bakana P, Claeys M, Totte J, Pieters LA, Van Hoof L, Tamba V, Van den Berghe DA, Vlietinck AJ: **Structure and chemotherapeutical activity of a polyisoprenylated benzophenone from the stem bark of Garcinia huillensis.** *Journal of ethnopharmacology* 1987, **21:**75-84.

19. Yamaguchi F, Ariga T, Yoshimura Y, Nakazawa H: **Antioxidative and anti-glycation activity of garcinol from Garcinia indica fruit rind.** *Journal of agricultural and food chemistry* 2000, **48:**180-185.

20. Liao CH, Ho CT, Lin JK: **Effects of garcinol on free radical generation and NO production in embryonic rat cortical neurons and astrocytes.** *Biochemical and biophysical research communications* 2005, **329:**1306-1314.

21. Tanaka T, Kohno H, Shimada R, Kagami S, Yamaguchi F, Kataoka S, Ariga T, Murakami A, Koshimizu K, Ohigashi H: **Prevention of colonic aberrant crypt foci by dietary feeding of garcinol in male F344 rats.** *Carcinogenesis* 2000, **21:**1183-1189.

22. Wattenberg LW: **Chemoprevention of cancer.** *Cancer research* 1985, **45:**1-8.

23. Yoshida K, Tanaka T, Hirose Y, Yamaguchi F, Kohno H, Toida M, Hara A, Sugie S, Shibata T, Mori H: **Dietary garcinol inhibits 4-nitroquinoline 1-oxide-induced tongue carcinogenesis in rats.** *Cancer letters* 2005, **221:**29-39.

24. Hong J, Sang S, Park HJ, Kwon SJ, Suh N, Huang MT, Ho CT, Yang CS: **Modulation of arachidonic acid metabolism and nitric oxide synthesis by garcinol and its derivatives.** *Carcinogenesis* 2006, **27:**278-286.

25. Pan MH, Chang WL, Lin-Shiau SY, Ho CT, Lin JK: **Induction of apoptosis by garcinol and curcumin through cytochrome c release and activation of caspases in human leukemia HL-60 cells.** *Journal of agricultural and food chemistry* 2001, **49:**1464-1474.

26. Hong J, Kwon SJ, Sang S, Ju J, Zhou JN, Ho CT, Huang MT, Yang CS: **Effects of garcinol and its derivatives on intestinal cell growth: Inhibitory effects and autoxidation-dependent growth-stimulatory effects.** *Free radical biology & medicine* 2007, **42:**1211-1221.

27. Ahmad A, Wang Z, Ali R, Maitah MY, Kong D, Banerjee S, Padhye S, Sarkar FH: **Apoptosis-inducing effect of garcinol is mediated by NF-kappaB signaling in breast cancer cells.** *Journal of cellular biochemistry* 2010, **109:**1134-1141.

28. Prasad S, Ravindran J, Sung B, Pandey MK, Aggarwal BB: **Garcinol potentiates TRAIL-induced apoptosis through modulation of death receptors and antiapoptotic proteins.** *Molecular cancer therapeutics* 2010, **9:**856-868.

29. Balasubramanyam K, Altaf M, Varier RA, Swaminathan V, Ravindran A, Sadhale PP, Kundu TK: **Polyisoprenylated benzophenone, garcinol, a natural histone acetyltransferase inhibitor, represses chromatin transcription and alters global gene expression.** *The Journal of biological chemistry* 2004, **279:**33716-33726.

30. Saadat N, Gupta SV: **Potential role of garcinol as an anticancer agent.** *J Oncol* 2012, **2012:**647206.

31. Hruban RH, Adsay NV, Albores-Saavedra J, Anver MR, Biankin AV, Boivin GP, Furth EE, Furukawa T, Klein A, Klimstra DS, et al: **Pathology of genetically engineered mouse models of pancreatic exocrine cancer: consensus report and recommendations.** *Cancer Res* 2006, **66:**95-106.

32. Hingorani SR, Wang L, Multani AS, Combs C, Deramaudt TB, Hruban RH, Rustgi AK, Chang S, Tuveson DA: **Trp53R172H and KrasG12D cooperate to promote chromosomal instability and widely metastatic pancreatic ductal adenocarcinoma in mice.** *Cancer Cell* 2005, **7:**469-483.

33. Olive KP, Jacobetz MA, Davidson CJ, Gopinathan A, McIntyre D, Honess D, Madhu B, Goldgraben MA, Caldwell ME, Allard D, et al: **Inhibition of Hedgehog signaling enhances delivery of chemotherapy in a mouse model of pancreatic cancer.** *Science* 2009, **324:**1457-1461.

34. Syder AJ, Oh JD, Guruge JL, O'Donnell D, Karlsson M, Mills JC, Bjorkholm BM, Gordon JI: **The impact of parietal cells on Helicobacter pylori tropism and host pathology: an analysis using gnotobiotic normal and transgenic mice.** *Proc Natl Acad Sci U S A* 2003, **100:**3467-3472.

35. McKee JS, Gass JH: **Acetaminophen-induced forestomach lesion in normal rats following intravenous exposure.** *Toxicol Pathol* 2011, **39:**861-866.

36. Hirose M, Masuda A, Imaida K, Kagawa M, Tsuda H, Ito N: **Induction of forestomach lesions in rats by oral administrations of naturally occurring antioxidants for 4 weeks.** *Jpn J Cancer Res* 1987, **78:**317-321.

37. Nam KT, O'Neal R, Lee YS, Lee YC, Coffey RJ, Goldenring JR: **Gastric tumor development in Smad3-deficient mice initiates from forestomach/glandular transition zone along the lesser curvature.** *Lab Invest* 2012, **92:**883-895.

38. Fong LY, Ishii H, Nguyen VT, Vecchione A, Farber JL, Croce CM, Huebner K: **p53 deficiency accelerates induction and progression of esophageal and forestomach tumors in zinc-deficient mice.** *Cancer Res* 2003, **63:**186-195.

39. Vivier E, Raulet DH, Moretta A, Caligiuri MA, Zitvogel L, Lanier LL, Yokoyama WM, Ugolini S: **Innate or adaptive immunity? The example of natural killer cells.** *Science* 2011, **331:**44-49.

40. Vivier E, Ugolini S, Blaise D, Chabannon C, Brossay L: **Targeting natural killer cells and natural killer T cells in cancer.** *Nat Rev Immunol* 2012, **12:**239-252.

41. Smyth MJ, Hayakawa Y, Takeda K, Yagita H: **New aspects of natural-killer-cell surveillance and therapy of cancer.** *Nat Rev Cancer* 2002, **2:**850-861.

42. Herberman RB: **Cancer immunotherapy with natural killer cells.** *Semin Oncol* 2002, **29:**27-30.

43. Arumugam T, Simeone DM, Van Golen K, Logsdon CD: **S100P promotes pancreatic cancer growth, survival, and invasion.** *Clin Cancer Res* 2005, **11:**5356-5364.

44. Dowen SE, Crnogorac-Jurcevic T, Gangeswaran R, Hansen M, Eloranta JJ, Bhakta V, Brentnall TA, Luttges J, Kloppel G, Lemoine NR: **Expression of S100P and its novel binding partner S100PBPR in early pancreatic cancer.** *Am J Pathol* 2005, **166:**81-92.

45. Deng H, Shi J, Wilkerson M, Meschter S, Dupree W, Lin F: **Usefulness of S100P in diagnosis of adenocarcinoma of pancreas on fine-needle aspiration biopsy specimens.** *Am J Clin Pathol* 2008, **129:**81-88.

46. Liu H, Shi J, Anandan V, Wang HL, Diehl D, Blansfield J, Gerhard G, Lin F: **Reevaluation and identification of the best immunohistochemical panel (pVHL, Maspin, S100P, IMP-3) for ductal adenocarcinoma of the pancreas.** *Arch Pathol Lab Med* 2012, **136:**601-609.

47. Wilentz RE, Su GH, Dai JL, Sparks AB, Argani P, Sohn TA, Yeo CJ, Kern SE, Hruban RH: **Immunohistochemical labeling for dpc4 mirrors genetic status in pancreatic adenocarcinomas : a new marker of DPC4 inactivation.** *Am J Pathol* 2000, **156:**37-43.

48. Wilentz RE, Iacobuzio-Donahue CA, Argani P, McCarthy DM, Parsons JL, Yeo CJ, Kern SE, Hruban RH: **Loss of expression of Dpc4 in pancreatic intraepithelial neoplasia: evidence that DPC4 inactivation occurs late in neoplastic progression.** *Cancer Res* 2000, **60:**2002-2006.

49. Doench JG, Sharp PA: **Specificity of microRNA target selection in translational repression.** *Genes Dev* 2004, **18:**504-511.

50. Ouellet DL, Perron MP, Gobeil LA, Plante P, Provost P: **MicroRNAs in gene regulation: when the smallest governs it all.** *J Biomed Biotechnol* 2006, **2006:**69616.

51. John B, Enright AJ, Aravin A, Tuschl T, Sander C, Marks DS: **Human MicroRNA targets.** *PLoS Biol* 2004, **2:**e363.

52. Singh PK, Brand RE, Mehla K: **MicroRNAs in pancreatic cancer metabolism.** *Nat Rev Gastroenterol Hepatol* 2012, **9:**334-344.

53. Bloomston M, Frankel WL, Petrocca F, Volinia S, Alder H, Hagan JP, Liu CG, Bhatt D, Taccioli C, Croce CM: **MicroRNA expression patterns to differentiate pancreatic adenocarcinoma from normal pancreas and chronic pancreatitis.** *JAMA* 2007, **297:**1901-1908.

54. Parasramka MA, Ho E, Williams DE, Dashwood RH: **MicroRNAs, diet, and cancer: new mechanistic insights on the epigenetic actions of phytochemicals.** *Mol Carcinog* 2012, **51:**213-230.

55. Xie B, Ding Q, Han H, Wu D: **miRCancer: a microRNA-cancer association database constructed by text mining on literature.** *Bioinformatics* 2013, **29:**638-644.

56. Jiang Q, Wang Y, Hao Y, Juan L, Teng M, Zhang X, Li M, Wang G, Liu Y: **miR2Disease: a manually curated database for microRNA deregulation in human disease.** *Nucleic Acids Res* 2009, **37:**D98-104.

57. Kozomara A, Griffiths-Jones S: **miRBase: integrating microRNA annotation and deep-sequencing data.** *Nucleic Acids Res* 2011, **39:**D152-157.

58. Alexiou P, Maragkakis M, Papadopoulos GL, Simmosis VA, Zhang L, Hatzigeorgiou AG: **The DIANA-mirExTra web server: from gene expression data to microRNA function.** *PLoS One* 2010, **5:**e9171.

59. Chhabra R, Dubey R, Saini N: **Cooperative and individualistic functions of the microRNAs in the miR-23a~27a~24-2 cluster and its implication in human diseases.** *Mol Cancer* 2010, **9:**232.

60. Jahid S, Sun J, Edwards RA, Dizon D, Panarelli NC, Milsom JW, Sikandar SS, Gumus ZH, Lipkin SM: **miR-23a promotes the transition from indolent to invasive colorectal cancer.** *Cancer Discov* 2012, **2:**540-553.

61. Pan X, Wang R, Wang ZX: **The potential role of miR-451 in cancer diagnosis, prognosis, and therapy.** *Mol Cancer Ther* 2013, **12:**1153-1162.

62. Hannafon BN, Ding WQ: **Intercellular Communication by Exosome-Derived microRNAs in Cancer.** *Int J Mol Sci* 2013, **14:**14240-14269.

63. Li X, Sanda T, Look AT, Novina CD, von Boehmer H: **Repression of tumor suppressor miR-451 is essential for NOTCH1-induced oncogenesis in T-ALL.** *J Exp Med* 2011, **208:**663-675.

64. Bitarte N, Bandres E, Boni V, Zarate R, Rodriguez J, Gonzalez-Huarriz M, Lopez I, Javier Sola J, Alonso MM, Fortes P, Garcia-Foncillas J: **MicroRNA-451 is involved in the self-renewal, tumorigenicity, and chemoresistance of colorectal cancer stem cells.** *Stem Cells* 2011, **29:**1661-1671.

65. Ali S, Saleh H, Sethi S, Sarkar FH, Philip PA: **MicroRNA profiling of diagnostic needle aspirates from patients with pancreatic cancer.** *Br J Cancer* 2012, **107:**1354-1360.

66. Deryugina EI, Quigley JP: **Matrix metalloproteinases and tumor metastasis.** *Cancer Metastasis Rev* 2006, **25:**9-34.

67. Rybakowski JK: **Matrix Metalloproteinase-9 (MMP9)-A Mediating Enzyme in Cardiovascular Disease, Cancer, and Neuropsychiatric Disorders.** *Cardiovasc Psychiatry Neurol* 2009, **2009:**904836.

68. Fu M, Wang C, Li Z, Sakamaki T, Pestell RG: **Minireview: Cyclin D1: normal and abnormal functions.** *Endocrinology* 2004, **145:**5439-5447.

69. Alao JP: **The regulation of cyclin D1 degradation: roles in cancer development and the potential for therapeutic invention.** *Mol Cancer* 2007, **6:**24.

70. Youle RJ, Strasser A: **The BCL-2 protein family: opposing activities that mediate cell death.** *Nat Rev Mol Cell Biol* 2008, **9:**47-59.

71. Gutierrez-Puente Y, Zapata-Benavides P, Tari AM, Lopez-Berestein G: **Bcl-2 related antisense therapy.** *Semin Oncol* 2002, **29:**71-76.

72. Green DR, Reed JC: **Mitochondria and apoptosis.** *Science* 1998, **281:**1309-1312.

73. Hemann MT, Lowe SW: **The p53-Bcl-2 connection.** *Cell Death Differ* 2006, **13:**1256-1259.

74. Mumm JS, Kopan R: **Notch signaling: from the outside in.** *Dev Biol* 2000, **228:**151-165.

75. Wang Z, Zhang Y, Li Y, Banerjee S, Liao J, Sarkar FH: **Down-regulation of Notch-1 contributes to cell growth inhibition and apoptosis in pancreatic cancer cells.** *Mol Cancer Ther* 2006, **5:**483-493.

76. Monteiro MS, Carvalho M, Bastos ML, Guedes de Pinho P: **Metabolomics analysis for biomarker discovery: advances and challenges.** *Curr Med Chem* 2013, **20:**257-271.

77. Ganti S, Weiss RH: **Urine metabolomics for kidney cancer detection and biomarker discovery.** *Urol Oncol* 2011, **29:**551-557.

78. Lauridsen M, Hansen SH, Jaroszewski JW, Cornett C: **Human urine as test material in 1H NMR-based metabonomics: recommendations for sample preparation and storage.** *Anal Chem* 2007, **79:**1181-1186.

79. Saadat N, IglayReger HB, Myers MG, Jr., Bodary P, Gupta SV: **Differences in metabolomic profiles of male db/db and s/s, leptin receptor mutant mice.** *Physiol Genomics* 2012, **44:**374-381.

80. Pan Z, Raftery D: **Comparing and combining NMR spectroscopy and mass spectrometry in metabolomics.** *Anal Bioanal Chem* 2007, **387:**525-527.

81. Baryshnikova OK, Williams TC, Sykes BD: **Internal pH indicators for biomolecular NMR.** *J Biomol NMR* 2008, **41:**5-7.

82. Gruber J, Tang SY, Jenner AM, Mudway I, Blomberg A, Behndig A, Kasiman K, Lee CY, Seet RC, Zhang W, et al: **Allantoin in human plasma, serum, and nasal-lining fluids as a biomarker of oxidative stress: avoiding artifacts and establishing real in vivo concentrations.** *Antioxid Redox Signal* 2009, **11:**1767-1776.

83. Tolun AA, Scarbrough PM, Zhang H, McKillop JA, Wang F, Kishnani PS, Millington DS, Young SP, Il'yasova D: **Systemic oxidative stress, as measured by urinary allantoin and F(2)-isoprostanes, is not increased in Down syndrome.** *Ann Epidemiol* 2012, **22:**892-894.

84. Yardim-Akaydin S, Sepici A, Ozkan Y, Simsek B, Sepici V: **Evaluation of allantoin levels as a new marker of oxidative stress in Behcet's disease.** *Scand J Rheumatol* 2006, **35:**61-64.

85. Mikami T, Kita K, Tomita S, Qu GJ, Tasaki Y, Ito A: **Is allantoin in serum and urine a useful indicator of exercise-induced oxidative stress in humans?** *Free Radic Res* 2000, **32:**235-244.

86. Baxter LR, Jr., Kelly RC, Peter JB, Liston EH, Touserkani S: **Urinary phenylacetate and response to methylphenidate.** *J Psychiatr Res* 1988, **22:**131-139.

87. Sabelli HC, Fawcett J, Gusovsky F, Javaid J, Edwards J, Jeffriess H: **Urinary phenyl acetate: a diagnostic test for depression?** *Science* 1983, **220:**1187-1188.

88. Franco OE, Onishi T, Umeda Y, Soga N, Wakita T, Arima K, Yanagawa M, Sugimura Y: **Phenylacetate inhibits growth and modulates cell cycle gene expression in renal cancer cell lines.** *Anticancer Res* 2003, **23:**1637-1642.

89. Shack S, Miller A, Liu L, Prasanna P, Thibault A, Samid D: **Vulnerability of multidrug-resistant tumor cells to the aromatic fatty acids phenylacetate and phenylbutyrate.** *Clin Cancer Res* 1996, **2:**865-872.

90. Thibault A, Cooper MR, Figg WD, Venzon DJ, Sartor AO, Tompkins AC, Weinberger MS, Headlee DJ, McCall NA, Samid D, et al.: **A phase I and pharmacokinetic study of intravenous phenylacetate in patients with cancer.** *Cancer Res* 1994, **54:**1690-1694.

91. Petrarulo M, Marangella M, Bianco O, Linari F: **Ion-chromatographic determination of L-tartrate in urine samples.** *Clin Chem* 1991, **37:**90-93.

92. El Idrissi A, Boukarrou L, L'Amoreaux W: **Taurine supplementation and pancreatic remodeling.** *Adv Exp Med Biol* 2009, **643:**353-358.

93. Sturman JA, Hepner GW, Hofmann AF, Thomas PJ: **Metabolism of [35S]taurine in man.** *J Nutr* 1975, **105:**1206-1214.

94. Wesseling S, Koeners MP, Joles JA: **Taurine: red bull or red herring?** *Hypertension* 2009, **53:**909-911.

95. El Agouza IM, Eissa SS, El Houseini MM, El-Nashar DE, Abd El Hameed OM: **Taurine: a novel tumor marker for enhanced detection of breast cancer among female patients.** *Angiogenesis* 2011, **14:**321-330.

ABSTRACT

ANTI-CANCER EFFECTS OF GARCINOL IN PANCREATIC CANCER TRANSGENIC MOUSE MODEL

by

NADIA SAADAT

December 2013

Advisor: Dr. Smiti Gupta

Major: Nutrition and Food Science

Degree: Doctor of Philosophy

Adenocarcinoma of pancreas is recognized for its poor prognosis, as it progresses asymptomatically and is rarely diagnosed at early stage. According to American cancer society pancreatic cancer, it has lowest survival rate in all cancer types, with less than 6% five year survival rate. Surgical resection is only possible for 20% of diagnosed cases and current chemotherapy has only 15% response rate. Even the most favored drug, Gemcitabine, increases survival time only by a few months, depending on the stage at diagnosis. Some bioactive food components or nutraceuticals have shown chemopreventive and chemotherapeutic effects without added side effects. Garcinol is a polyisoprenylated benzophenone derivative from Garcinia Indica fruit extract. Garcinol has shown dose dependent favorable response in pancreatic cancer cell lines, alone and in combination with Gemcitabine. In this study, we investigated the *invivo* effects of dietary Garcinol in a transgenic mouse model of Pancreatic Cancer (PaCa). This model is considered to be the animal model which best mimics development of human PaCa. Based on *invitro* data from our lab we

hypothesized that Dietary Garcinol treatment will slow down the progression of Pancreatic Cancer in Kras and p53 transgenic Pancreatic Cancer mouse model. We had three specific aims. **Specific aim 1)** To investigate the *invivo* response of dietary Garcinol on PaCa animal models and to monitor the tumor progression with MRI. We also ruled out the possibility of toxicity of dietary Garcinol by blood smears and fore stomach H& E slides. Additionally we did detailed histological investigation of Intraepithelial neoplasia lesions in the pancreatic tissue collected at sacrifice. **Specific aim 2,** To investigate the mouse pancreatic and liver tissue, for response to the dietary Garcinol at molecular level. We studied changes in the micro RNA profile of Garcinol treated vs. non-treated animals and investigated the response of dietary Garcinol on tumor promoter target genes of miRNAs from different molecular pathways, in pancreas and a common metastatic liver tissue. **Specific aim 3,** To investigate the differences in Urinary Metabolomic profiles of Garcinol treated mice compared to non-treated mice and Target analysis to identify metabolites responsible for differences. **Methods**, Six to eight week old male KPC mice (kras and P53 conditional mutant) were divided into 4 groups(KC- cancer control; KGr- 0.05% Garcinol diet; KGm-Gemcitabine injected; KGG- Garcinol+Gemcitabine), littermates without mutation served as non- cancer controls were divided into 2 groups(CC- isocaloric diet, CG- Garcinol diet) . Mice were fed 0.05% Garcinol added diet or isocaloric diet (Dyets- Bethlehem, PA). Mice were individually housed. Body weight were measured twice/week from week 1 to week 6. Two groups received Gemcitabine weekly injections (100mg/kg- intraperitoneal injections) up to 5 week. MRI T2 weighted image scans were conducted on 7T scanner (ClinScan, Bruker, Karlsruhe, Germany) in week 1 and week 5 of the study. Urine

samples were collected in week 2, 4 and 6 for metabolomic analysis. Mice were euthanized in week six of the study and tissues were collected. Blood smear slides were prepared at the time of sacrifice and after drying were fixed in 95% Ethanol. The smears were stained with Wright Giemsa Stain and observed under the microscope (Nikon Eclipse 80i). Pancreatic tissues was fixed in 10% neutral buffered formalin and then transferred to 70 % ethanol before staining. H&E stained slides were prepared and observed under microscope (Nikon Eclipse 80i). Specific immuno histostaining (IHC) with S100P and DPC4/SMAD4 was performed to confirm the findings. MicroRNA array analysis was conducted and some miRNA were validated by RTPCR. Some of the target genes of miRNA identified to be differently expressed were investigated by RTPCR. Nuclear Magnetic resonance spectroscopy was performed on Varian-500S. Simca P+ and CHENOMX NMR suite were used for Metabolomic analysis of urinary spectra. **Results**, Dietary Garcinol arrests the Progression of Pancreatic Cancer *invivo* in KRAS and p53 pancreas- specific mutant mouse model. All the mice in Garcinol group survived the 6 week study, with 75% survival in KGm and KGG. We observed tumor reduction in KGr, KGm and KGG groups. There was no toxicity observed to the blood in blood smears with Garcinol treatment, NK and NKT cell were found to be in higher percentage in KGr group compared to KC group. No toxicity to Garcinol was observed in fore stomach H&E slides, additionally we observed reduced papilloma formations in KGr group compared to KC group. Reduction in total number of Pancreatic intraepithelial neoplasia (mPanIN) was observed in both Garcinol treated groups with lowest number of mPanIN 3 in KGG group indicating slowed progression of mPanIN 1 to mPanIN 3. Histology findings were confirmed with specific immuno-

histostaining with S100P and DPC4/SMAD4 antibodies. MicroRNA microarray data showed down regulation of multiple tumor promotor miRNA and up regulation of several tumor suppressor miRNA with Garcinol treatment. Lower expression levels of miRNA 23a and higher expression levels miRNA 451a after Garcinol treatment were validated by RTPCR. Relative mRNA expressions levels of MMP9, CCND1 and Notch1 were found to be decreased in KGr and KGG groups compared to KC group in pancreatic tissue samples. Relative expression levels of CCND1 were decreased in KGr and KGG groups in Liver tissue samples. MMP9 relative expression levels showed reduction in Garcinol treated groups KGr group. Relative expression levels of Bcl2 were found to be decreased in KGr, KGm and KGG groups. Urinary metabolomics profiles from week 6 Garcinol treated group were closer to non- cancer and week 2 of non-treated KC group. Target analysis with CHENOMX identified Taurine, Tartrate and Phenylacetate to be in higher concentrations in Garcinol treated group compared to non-treated group and Allantoin was found to be lower in Garcinol treated group compared to KC non-treated group. This *invivo* dietary Garcinol study has highlighted anti-cancer potential of this bioactive food component. Our data indicates that dietary Garcinol retarded pancreatic cancer progression in transgenic pancreatic cancer mice. Garcinol has shown pleotropic effects, targeting multiple tumor related pathways. Further investigation of molecular pathways identified can lead to its incorporation as a chemotherapeutic agent in a clinical trial.

AUTOBIOGRAPHICAL STATEMENT

Nadia Saadat was born in Karachi, Pakistan and received her early education from Habib Girls School, Karachi. She was awarded with the President's Talent Award (awarded to only 50 student by the President of Pakistan for their outstanding Academic achievements and provided full scholarship, books and stipend) during her high school and college education. She finished her F.Sc from St Joseph's College Karachi. Later she went to Dow Medical College, Karachi, for her Medical and Surgery education and received her M.B.B.S degree from there. She moved to USA after her marriage and joined Master's program at Wayne State University. During her masters studies she received Graduate Professional Scholarship. Her Masters project was finding differences in Metabolomic profiles of leptin receptor mutant mice in Dr. Smiti Gupta's lab. She received her M.S degree from Department of Nutrition and Food science, Wayne State University and joined the PhD program in Dr. Smiti Gupta's lab, Department of Nutrition and Food Science at Wayne State University. She was awarded with the Parent Family Endowed Fellowship and the Golden Key research scholarship during her PhD studies.

Her interest in bioactive food components and their medicinal properties kept her motivated to continue her research in this field. She worked on different animal studies during her PhD program, including some studies on Lung Cancer, Cardiovascular disease and Pancreatic Cancer. She plans to continue in the medical research field: especially biomarker discovery of disease processes and treatment options.